



Universidade do Minho
Escola de Engenharia

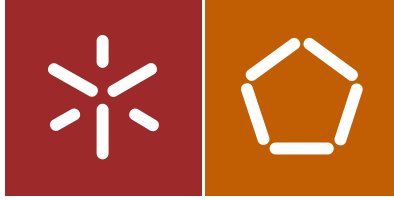
José Miguel Gomes Costa

Numerical Simulation of the
Reflow Soldering Process

José Miguel Gomes Costa Numerical Simulation of the Reflow Soldering Process

UMinho | 2015

December of 2015



Universidade do Minho
Escola de Engenharia

José Miguel Gomes Costa

Numerical Simulation of the
Reflow Soldering Process

Master Thesis
Integrated Master in Mechanical Engineering

Work accomplished under orientation of
José Carlos Fernandes Teixeira
Delfim Fernandes Soares
José Ricardo Barros Alves (Bosch Car Multimedia)

December of 2015

DECLARAÇÃO

Nome:

José Miguel Gomes Costa

Endereço eletrónico: jose.m.costa44@gmail.com Telefone: 914372138 / _____

Número do Bilhete de Identidade: 14162705

Título da dissertação:

Numerical Simulation of the Reflow Soldering Process

Orientador(es):

José Carlos Fernandes Teixeira; Delfim Fernandes Soares; José Ricardo Barros Alves

Ano de conclusão: 2015

Designação do Mestrado:

Integrated Master in Mechanical Engineering

Nos exemplares das teses de doutoramento ou de mestrado ou de outros trabalhos entregues para prestação de provas públicas nas universidades ou outros estabelecimentos de ensino, e dos quais é obrigatoriamente enviado um exemplar para depósito legal na Biblioteca Nacional e, pelo menos outro para a biblioteca da universidade respetiva, deve constar uma das seguintes declarações:

1. É AUTORIZADA A REPRODUÇÃO INTEGRAL DESTA DISSERTAÇÃO APENAS PARA EFEITOS DE INVESTIGAÇÃO, MEDIANTE DECLARAÇÃO ESCRITA DO INTERESSADO, QUE A TAL SE COMPROMETE;
2. É AUTORIZADA A REPRODUÇÃO PARCIAL DESTA DISSERTAÇÃO (indicar, caso tal seja necessário, nº máximo de páginas, ilustrações, gráficos, etc.), APENAS PARA EFEITOS DE INVESTIGAÇÃO, MEDIANTE DECLARAÇÃO ESCRITA DO INTERESSADO, QUE A TAL SE COMPROMETE;
3. DE ACORDO COM A LEGISLAÇÃO EM VIGOR, NÃO É PERMITIDA A REPRODUÇÃO DE QUALQUER PARTE DESTA TESE/TRABALHO

Universidade do Minho, ___/___/_____

Assinatura: _____

Acknowledgments

In first place I would like to thank to all people that help me in a way or another in the development of this thesis.

A special thanks to my mentors, Prof. Doctor José Carlos Fernandes Teixeira, Prof. Doctor Delfim Fernandes Soares and Dr. José Ricardo Barros Alves, for their personal effort in the attribution of this theme and particularly in make possible my internship at Bosch Car Multimedia. Thank you also by the help, orientation, and time dispensed during the entire project.

Thanks to Mr. Nelson Rodrigues for the help with familiarization with the ANSYS Fluent software. Also thank for the advices related to the simulations and for the clarification of some doubts.

I also thank to all people at Bosch Car Multimedia that helped me in this thesis. Especially to Dr. Ricardo Alves that was my mentor during the internship at Bosch, for all dedication, patience and time spent in the work done at Bosch. Thank to Ms. Lais Oliveira and to Mr. Miguel Peixoto for the help in the realization of the Reflow thermal simulation of a real electronic product at Bosch. Also thank to some friends done during the internship, as Vera Vilas Boas, Sofia Mouta, and Roberto Magalhães for all the help, advices and good disposition.

I would like to also thank to my friends and colleagues of internship at Bosch Car Multimedia, Daniel Barros, Andreia Oliveira, and Susana Rodrigues for all the work realized together, for the support, for the motivation, and for the good disposition.

Finally, I address my greatest thank to my parents and brother for all the support demonstrated along my academic journey and by the effort made so I could finish my master's degree.

Abstract

The work developed in this thesis is inserted in a large project involving the University of Minho and the Bosch Car Multimedia, in which it is intended to create a numerical model capable of simulate the Reflow soldering process. Thus, during this thesis will be given a small contribution to the creation of this model by continuing the work already developed by Costa (2014), student who initiated this project in his master's thesis.

Before starting the development of the simulation model, it is performed a brief description of the electronic products manufacturing process and its composition, such as PCBs, electronic components and solders used. Being even discussed in greater detail the Reflow soldering process. To carry out this simulation model it is used the computational program ANSYS Fluent being analyzed its way of functioning and the main models used during the simulations, as the VOF model (Volume of Fluid) and the Solidification/Melting model.

Regarding the development of the simulation model, the first step passed by the analysis of the work carried out by Costa (2014), which it resulted in detection of a problem in his last model, related to the deformation of solder paste at room temperature. In an attempt to prevent this deformation several variables were analyzed such, as density, viscosity and surface tension of solder paste, as well as the presence of gravity and the Mushy-zone parameter in order to understand their impact on the solder paste deformation at room temperature. Through this analysis, it was found a solution which involves the alteration of Mushy-zone parameter and the use of a surface tension of solder paste function of temperature. With this solution it was possible to create a model for the fusion of solder paste, with the objective to validate the solution found and to analyze the deformation of solder paste. Finally, it developed a simulation model that allows to simulate any Reflow thermal cycle and to analyze the deformation of solder paste during the entire thermal cycle, including its melting and solidification.

In parallel with this project, it was accomplished at Bosch the thermal simulation of the Reflow soldering process of a real product and compared the values obtained with the actual data from the production line.

Keywords

Numerical simulation – Reflow – Solder paste deformation – Thermal cycle – PCBAs

Resumo

O trabalho desenvolvido nesta tese está inserido num projeto de grande dimensão, envolvendo a Universidade do Minho e a Bosch Car Multimedia, no qual se pretende criar um modelo numérico capaz de simular o processo de soldadura por Reflow. Desta forma, durante esta tese será dado um pequeno contributo para a criação deste modelo, através da continuação do trabalho já desenvolvido pelo Costa (2014), aluno que iniciou este projeto na sua tese de mestrado.

Antes de iniciar o desenvolvimento do modelo de simulação é realizada uma pequena descrição do processo de produção de produtos eletrónicos e da sua composição, como os PCBs, os componentes eletrónicos e das soldas utilizadas. Sendo ainda abordado com maior detalhe o processo de soldadura por Reflow. Para a realização deste modelo de simulação é utilizado o programa computacional ANSYS Fluent, sendo analisada a sua forma de funcionamento e os principais modelos utilizados durante as simulações, como o modelo VOF (Volume of Fluid) e o modelo Solidification/Melting.

Quanto ao desenvolvimento do modelo de simulação, o primeiro passo passou pela análise do trabalho desenvolvido pelo Costa (2014), o que resultou de deteção de um problema no seu último modelo, relacionado com a deformação da pasta de solda à temperatura ambiente. Numa tentativa de impedir esta deformação várias variáveis foram analisadas, tais como densidade, viscosidade e tensão superficial da pasta de solda, bem como a presença da gravidade e o Mushy-zone parameter, por forma a perceber o seu impacto na deformação da pasta de solda à temperatura ambiente. Através desta análise foi encontrada uma solução que passa pela alteração do Mushy-zone parameter e pela utilização de uma tensão superficial da pasta de solda função da temperatura. Com esta solução foi possível criar um modelo para a fusão da pasta de solda com o objetivo de validar a solução encontrada e analisar a deformação da pasta de solda. Por último, é desenvolvido um modelo de simulação que permite simular qualquer ciclo térmico de Reflow e analisar a deformação da pasta de solda durante todo esse ciclo térmico, incluindo a sua fusão e solidificação.

Paralelamente a este projeto foi realizada na Bosch a simulação térmica do processo de Reflow de um produto real e a comparação os valores obtidos com os dados reais da linha de produção.

Palavras-Chave

Simulação numérica – Reflow – Deformação da pasta de solda – Ciclo térmico – PCBAs

Index

Acknowledgments.....	iii
Abstract.....	v
Resumo.....	vii
Index of Figures	xiii
Index of Tables	xvii
List of Symbols	xix
List of Abbreviations, Initials and Acronyms	xxi
Chapter 1 Introduction	1
1.1 Motivation.....	1
1.2 Objectives of the Work	2
1.3 Thesis Structure	3
Chapter 2 Physical Problem Definition	5
2.1 State of the Arte.....	5
2.2 Definition and Fabrication of PCBAs	8
2.2.1 Reflow Line	8
2.2.2 Radial Line.....	9
2.2.3 Wave Line	10
2.3 PCBs.....	11
2.3.1 Immersion Tin.....	12
2.3.2 ENIG (Electroless Nickel/Immersion Gold).....	13
2.3.3 OSP (Organic Solderability Preservative)	13
2.3.4 HASL (Hot Air Solder Leveling)	14
2.4 Solder	14
2.4.1 Solder Types	15
2.5 Electronic Components	16
2.5.1 THT (Through Hole Technology)	16
2.5.2 SMT (Surface Mount Technology)	17

2.5.3	Components Metallization	18
2.6	Reflow Soldering Process	19
Chapter 3	Numerical Models and Methodology	23
3.1	Multiphase Flows	23
3.1.1	Approaches to Multiphase Modeling	24
3.1.2	Volume of Fluid (VOF) Model	25
3.2	Solidification/Melting Model	30
3.3	Finite Volume	33
3.4	Finite Volume Notation	33
3.5	6SigmaET Overview	35
3.6	Experimental Work Procedure	36
Chapter 4	Test Cases	37
4.1	Reference Model	38
4.2	Reference Model Test and Problem Found	41
4.3	Influence of some Variables in the Solder Paste Deformation	43
4.4	Influence of Mushy-zone Parameter in the Solder Paste Deformation	44
4.5	Solution and Validation	45
4.6	Thermal Cycle	46
4.7	Study Case at Bosch	47
Chapter 5	Results and Discussion	53
5.1	Reference Model	54
5.2	Reference Model Test and Problem Found	56
5.3	Influence of some Variables in the Solder Paste Deformation	59
5.3.1	Problem Correction First Attempt	62
5.4	Influence of Mushy-zone Parameter in the Solder Paste Deformation	64
5.4.1	Problem Correction Second Attempt	65
5.5	Solution and Validation	66
5.6	Thermal Cycle of Solder Paste	68

5.7 Study Case at Bosch.....	72
Chapter 6 Conclusions and Future Work.....	83
6.1 Conclusions.....	83
6.2 Future Work.....	85
References	87

Index of Figures

Figure 2.1 - Reflow line (Adapted from [16]).	9
Figure 2.2 - Radial line (Adapted from [16]).	9
Figure 2.3 - SMD components fixed with an adhesive on the face B of the PCB.	10
Figure 2.4 - Wave line (Adapted from [16]).	11
Figure 2.5 - Constitution of a multilayer PCB (Adapted from [20]).	12
Figure 2.6 – THT (Through Hole Technology).	17
Figure 2.7 - SMT (Surface Mount Technology).	18
Figure 2.8 - Different layers of components metallization.	18
Figure 2.9 - Operation principle of a Reflow oven [34].	20
Figure 2.10 – Typical Reflow thermal cycle for lead-free solder pastes (Adapted from [36]).	20
Figure 3.1 - Notation for simulation domain division (Adapted from [46]).	34
Figure 3.2 - Notation of the nodes and control volume faces (Adapted from [46]).	34
Figure 4.1 – Reference model simulation domain.	39
Figure 4.2 – Simulation domain with a small copper pad and a normal quantity of solder paste (a) and with a high quantity of solder paste (b). Simulation domain with a big copper pad and a normal quantity of solder paste (c) and with a high quantity of solder paste (d).	42
Figure 4.3 – Surface tension variation function of temperature.	45
Figure 4.4 – Simplified Reflow thermal cycle, used in the simulation.	46
Figure 4.5 – Average of AOI pseudo-errors per component, in the Reflow soldering process with and without N ₂ .	48
Figure 4.6 – Product to be simulated with the 6SigmaET.	49
Figure 4.7 – Simulation domain of the program 6SigmaET.	50
Figure 4.8 – Thermal cycle of the Reflow oven used to produce the product in analysis and perform the simulation.	50
Figure 4.9 – Real product with thermocouples installed.	51
Figure 4.10 – Thermal cycle of the Reflow oven used to test the product in analysis.	52
Figure 5.1 – Initial state of simulation.	54
Figure 5.2 – Liquid solder paste deformation in the presence of a component (Adapted from [34]).	55

Figure 5.3 – Temperature variation in the simulation domain (Adapted from [34]).	56
Figure 5.4 – Solder paste deformation at room temperature.	56
Figure 5.5 – Solder paste deformation with a shorter copper pad.	57
Figure 5.6 - Solder paste deformation with a shorter copper pad and with more solder paste. ..	58
Figure 5.7 - Solder paste deformation with a bigger copper pad.	58
Figure 5.8 – Solder paste deformation with a bigger copper pad and with more solder paste. ..	59
Figure 5.9 – Density increase of 10 times (a) and 100 times (b), relatively to the reference model.	60
Figure 5.10 - Viscosity increase of 10 times (a) and 100 times (b), relatively to the reference model.	60
Figure 5.11 – Surface tension increase of 10 times (a) and 100 times (b), relatively to the reference model.	61
Figure 5.12 – Gravity absence.	62
Figure 5.13 – Surface tension equal to 0 N/m and contact angles equal to 90°.	63
Figure 5.14 - Surface tension equal to 0 N/m, contact angles equal to 90° and gravity absence.	63
Figure 5.15 - Mushy-zone parameter of 10 ⁷ (a) and 10 ⁸ (b).	64
Figure 5.16 – Mushy-zone parameter of 10 ⁷ (a) and 10 ⁸ (b), and surface tension of 0 N/m.	65
Figure 5.17 – Solder paste deformation and temperature after 0.5 s of simulation.	66
Figure 5.18 – Solder paste deformation and temperature after 0.76 s of simulation.	67
Figure 5.19 - Solder paste deformation and temperature after 1.2 s of simulation.	68
Figure 5.20 – Simplified Reflow thermal cycle, initial state.	68
Figure 5.21 - Simplified Reflow thermal cycle, at 1.4 s of simulation.	69
Figure 5.22 - Simplified Reflow thermal cycle, at 1.5 s of simulation.	69
Figure 5.23 - Simplified Reflow thermal cycle, at 1.73 s of simulation.	70
Figure 5.24 - Simplified Reflow thermal cycle, at 2.16 s of simulation.	71
Figure 5.25 - Simplified Reflow thermal cycle, at 3 s of simulation.	72
Figure 5.26 – Product 5106, Reflow thermal simulation, after 100 s of simulation.	73
Figure 5.27 - Product 5106, Reflow thermal simulation, after 200 s of simulation.	73
Figure 5.28 - Product 5106, Reflow thermal simulation, after 250 s of simulation.	74

Figure 5.29 - Product 5106, Reflow thermal simulation, after 350 s of simulation.	75
Figure 5.30 – QFP components thermal cycle.	75
Figure 5.31 – Temperature difference between the QFP components (C2 - C1).	76
Figure 5.32 – Real Reflow thermal cycle of the QFP components and solder joints.	78
Figure 5.33 – Real temperature difference between the QFP components and solder joints.	78
Figure 5.34 – Sectional cuts of the QFP component's pins, in a product produced with N ₂ in the Reflow soldering process (a), and in a product produced without N ₂ in the Reflow soldering process (b).	80

Index of Tables

Table 2.1 – Solder alloy classification in function of particle size (Adapted from [14]).	16
Table 2.2 - Constitutions most used for components metallization (Adapted from [14]).	19
Table 4.1 – Material properties (Adapted from [34]).	39

List of Symbols

Symbol	Designation	Unities
A_{mush}	Constant of mushy-zone	
c_p	Specific heat at constant pressure	[J/(kg.K)]
E	Node at right of the point P	
E	Total energy	[J]
EE	Point two nodes to the right of P	
E_q	Energy of the phase q^{th}	[J]
\vec{F}	Force vector	[N]
\vec{g}	Gravitational acceleration	[m/s ²]
H	Enthalpy	[J/kg]
h	Sensible enthalpy	[J/kg]
h_{ref}	Reference enthalpy	[J/kg]
K	Thermal conductivity	[W/(m.K)]
K_{eff}	Effective thermal conductivity	[W/(m.K)]
L	Latent heat of the material	[J/kg]
\dot{m}_{pq}	Mass transferred from the phase p to the phase q	[kg/s]
\dot{m}_{qp}	Mass transferred from the phase q to the phase p	[kg/s]
N	Node at top of the point P	
n	Previous time-step	
$n + 1$	Current time-step	
P	Central node	
P	Pressure	[Pa]
q^{th}	Phase q^{th}	
S	Node at bottom of the point P	
S	Source term	
S_h	Source term	[J]
S_{α_q}	Source term	
T	Temperature	[K]

$T_{liquidus}$	Temperature of <i>Liquidus</i>	[K]
T_{ref}	Reference temperature	[K]
$T_{solidus}$	Temperature of <i>Solidus</i>	[K]
u, v, w	Velocity magnitude	[m/s]
U_f	Volume fraction through the face, based in normal velocity	
V	Cell volume	[m ³]
\vec{v}	Overall velocity vector	[m/s]
\vec{v}_p	Pull velocity	[m/s]
W	Node at left of the point P	
WW	Point two nodes to the left of P	
α_q	Volume fraction of the phase q th	
$\alpha_{q,f}$	Volume fraction value in the face of the phase q th	
β	Volume liquid fraction	
ΔH	Latent heat content	[J/kg]
Δt	Time change	[s]
Δx	Volume control length	[m]
Δy	Volume control height	[m]
σ	Surface tension	[N/m]
ε	Emissivity	
μ	Viscosity	[kg/(m.s)]
ρ	Density	[kg/m ³]
ρ_q	Density of the phase q th	[kg/m ³]

List of Abbreviations, Initials and Acronyms

Abbreviations, Initials Designation

and Acronyms

AOI	Automatic Optical Inspection
BGA	Ball Grid Array
CFD	Computational Fluid Dynamics
CICSAM	Compressive Interface Capturing Scheme for Arbitrary Meshes
CM	Car Multimedia
ENIG	Electroless Nickel/Immersion Gold
Face B	Bottom side of the PCB
FVM	Finite Volume Method
GUI	Graphical User Interface
HASL	Hot Air Solder Leveling
HRIC	High Resolution Interface Capturing
OSP	Organic Solderability Preservative
PCB	Printed Circuit Board
PCBA	Printed Circuit Board Assembly
QFP	Quad Flat Package
QUICK	Quadratic Upstream Interpolation for Convective Kinematics
SAC	Sn-Ag-Cu
SMD	Surface Mount Device
SMT	Surface Mount Technology
SPI	Solder Paste Inspection
TAL	Time Above <i>Liquidus</i>
TH	Through-hole
THT	Through-hole Technology
UDF	User Defined Function
VOF	Volume of Fluid

Chapter 1

Introduction

1.1 Motivation

The electronic products are present in our lives all days, even without we realize. They are present in all electronic devices that we use like the computer, the cell phone, the domestic machines, and so on.

Due this fast increase of electronic devices in our lives, the electronic industry is today a business sector with a high growth and very competitive. The constant technological development is other fact that requires a constant innovation and optimization of products and fabrication processes used by these corporations.

Electronic products are known in the electronic industry as PCBAs (Printed Circuit Boards Assembly). These are constituted essentially by three parts, as the PCBs, the electronic components, and the solder. The PCBs (Printed Circuit Boards) are the structural support for the components and at same time they provide the electrical connection between them. The solder is used to connect permanently the components to the PCB and this way establishes an electrical connection between both. The soldering processes most used in the industry are the Reflow and the Wave soldering processes.

In the recent past, the solder paste most used was the alloy Sn-Pb. However, this alloy has in its constitution lead, which was prohibited by specific legislation [1], due its harmful effects for the environment and for the human health.

The prohibition of use lead based solder alloys led the industry to use other solder alloys, which forced the introduction of changes in the production processes, due to its inferior properties. The higher melting point of the new solder alloys is clearly an example of a property of solder paste that decreases the production process window. The soldering temperatures are now higher, which means that the components are closer to their temperature limits and that the soldering process is longer than in the past. All this combined with the increased complexity of PCBAs, which have more and more components, due the increase of its functions coupled with its miniaturization, results is a higher risk of occurring production defects and decrease of products reliability.

To avoid these problems it is now more important than never, the correct layout of components in the PCB, and the prediction of temperatures in the product during the soldering process, before its real production, in order to avoid the problems referred. It is in this point where a new area of study has been growing in the industry, with the objective of simulate the soldering process.

The numerical simulation of the electronic products soldering process, although it is something relatively recent, has already showed great potential to provide in a precise, simple, fast and economical way, the thermal profile of a product during the soldering process. With the simulations results, it is then possible to predict the temperature of each component, the temperature differences in the product and its hottest and coolest points, allowing the redesign of the product to avoid problems during the production.

1.2 Objectives of the Work

With the objective of understanding the different variables that may influence the Reflow soldering process and predict what happens during this process, there are several computational programs available in the market to simulate this soldering process. However, most of them, only do the thermal simulation of the PCB and components and do not allow for the simulation of solder paste and its change of physical phase.

The simulation of solder paste is now the next step in the simulation of Reflow soldering process, since it will allow to predict the solder paste phase, deformation and wetting, during the entire process of soldering. This simulation will thus help in the prediction of soldering errors, such as bridging, in the correct definition of the copper pad dimension and form, as well as in the correct definition of the solder

paste amount that need to be printed in the copper pad. In this way, the simulation of solder paste will allow a higher control level of the soldering process and avoid errors in the production.

The objectives of this work are specifically the following:

- Study the deformation of solder paste during its melting, in the presence of a component.
- Study the effect of the copper pad dimension and of the solder paste amount in the deformation of solder paste, in the presence of a component.
- Analysis and definition of variables that have influence in the deformation of solder paste.
- Creation of a Reflow thermal cycle simulation model.
- Analysis the deformation of solder paste during a simplified Reflow thermal cycle, specifically in its melting and solidification, in the presence of a component.
- Identification the reasons for the difference in the Reflow AOI pseudo-errors found between two equal components placed in equal products of the same *nutzen*.

1.3 Thesis Structure

In chapter 2, the fabrication process of a PCBA is analyzed and defined. It is even specified the different types of PCBs, solders, and electronic components normally used in the industry. At the end of the chapter the Reflow soldering process is presented and analyzed with more detail.

Chapter 3 explores the ANSYS Fluent, specifically the discretization model of finite volumes, and the solver models. Two other important models used by ANSYS Fluent are even defined, since they are used in the simulations present in this work: the volume of fluid (VOF) and the Solidification/Melting model.

In chapter 4, the study cases are presented. It is also explained the reasons for its selection, the objectives, the methodology, and the expected results. The results of all cases of study are presented in chapter 5, where they are also analyzed along with the principal conclusions extracted from them.

In chapter 6, the main conclusions this thesis are finally presented and suggested some future work.

Physical Problem Definition

The present chapter presents the state of the arte related with the simulation of the Reflow soldering process and the basics about the production of Printed Circuit Board Assembly (PCBA) and all the necessary components to produce it.

First, an analysis to the bibliography showing the studies carried out on the simulation of the Reflow soldering process is presented. Second, the production process and constitution of the lines which may be necessary to manufacture a PCBA era presented, as well as the PCBs, the solder, and the electronic components, which may compose the PCBA. Finally, the process of soldering by Reflow is presented in a more extensive way, since this will be used as a reference to do the numerical model.

2.1 State of the Arte

With the objective of upgrading the components layout in the PCBAs, it is currently increasingly the use of CFD software that they allow to predict the temperatures of the PCB and electronic components during its pass by the Reflow oven. In this way, it is possible to reduce temperature differences in the PCB that may cause its distortion or hot points that may cause damages in the electronic components, before the production. However, the numerical simulation of the Reflow soldering process is even a recent technology that it needs to be improved.

Lau, Abdullah and Ani [2] simulated the Reflow soldering process using two software (Multi-physics Code Coupling Interface), where the ANSYS Fluent 6.3.26 is used to simulate the Reflow oven

by forced convection and the ABAQUS 6.9 is used to simulate the thermal profile of the PCB and electronic components, with the objective of to observe the thermal answer of the PCB during the pre-heating phase of Reflow.

In this study, five PCBs were used with different levels of complexity (changing the number of components in the PCB) with the objective of identify the differences in the thermal profile of the products. Through the CFD software (ANSYS Fluent 6.3.26) was simulated the flow of hot air inside the oven and it was obtained the heat transfer coefficient along the PCB. The heat transfer coefficient is used than in the finite differences software (ABAQUS 6.9) with the objective of determine the temperature of the PCB along the time.

With this study, it was concluded that the temperature of the PCB decreases with its increase of complexity. It was even possible to conclude that the decrease of temperature happens in two places, around the components, due the difference the heights between the components and the PCB, and between the components, where the air flow is interrupted resulting in a decrease of its velocity and as consequence in a decrease of heat transferred by forced convection. Finally, it was concluded that the increase of complexity of the PCBs also increases the difference of temperature between the hottest component and the coldest solder joint on the PCB.

However, it is possible to change the velocity of the Reflow line in order to minimize the difference of temperature in the PCB. Lau, Abdullah and Ani [2] verified that the velocity decrease of 35 % results in a decrease of the highest temperature difference in the PCB of 2.5 °C.

Balázs and István [3] performed a study to understand the air flow inside the Reflow oven. In this study was concluded that there are two zones of laminar flow in the direction of the Reflow oven ends. This it results in a big variation of the heat transfer coefficient in this direction, which may cause problems in the solder joint quality.

One of the main objectives in the numerical simulation of the Reflow soldering process it is the simulation of the solder paste geometry. The Surface Evolver software, developed by Brakke [4], it has been used to simulate the solder paste geometry and it achieved good results. However, this software has the limitation of not simulate cases where the solder paste flows out of the copper pad [5].

In order to overtake this limitation and to take into account the solder mask, it was developed an algorithm by Ya-Yun, Hung-Ju, Jer-Haur and Weng-Sing [6] based in fluid dynamics. With this new model it was possible to achieve all the results of the Surface Evolver software and correct its limitations, and also to analyze the wetting and thickness of solder paste.

Hao, Mattila and Kivilahti [7] used two thermal models, one for the components and other for the solder joints, with the objective of to simulate the solidification of lead-free solder paste, in the presence of a component. The heat transfer coefficient used it was obtained in a previous study [8]. The results for the components model show that the components cool faster than the PCB, and the solder joints model shows that the difference of temperature has no meaning until its solidification.

In order to simplify the simulation of the Reflow soldering process, Whalley [9] instead simulating the entire Reflow oven to obtain the heat transfer coefficients, sensors were placed in a PCB in order to obtain these values directly from the Reflow oven. The PCB was simplified also using a 2D model. As consequence, it is considered that there is not difference of temperature between the components and the PCB area below the components. This assumption it has into account the results achieved by Sarvar and Conway [10] however, it cannot be used in problems with high thermal mass components and where the connection to the PCB do not allow a good conduction of heat. With the model presented by Whalley [9] it was possible to achieve accurate results even with all simplifications, which it allowed to reduce the simulation time.

Srivalli, Abdullah and Khor [11] investigated the effect of different cooling periods in the Reflow soldering process of a BGA IC package. The domain of a lead-free Reflow oven was built in GAMBIT 2.3.16 and the model was exported to Fluent 6.3.26 for further parametric study. Simulation results were validated by experimental data according to the American Society of Mechanical Engineers standard for computational fluid dynamics and heat transfer. The simulations results show that a very high radiation heat flux (122.760 W/m^2) in a short cooling duration result in unmelted solder powders, which it has a consequence of poor wetting. On the other hand, a reduced heat flux (9.262 W/m^2) affects the mechanical properties of solder balls with its continued cooling. As a conclusion the results show that 111 s was the optimum cooling period to avoid soldering defects.

Costa, Soares, S. Teixeira, Cerqueira, Macedo, Rodrigues, Ribas and J. Teixeira [12] modeled two study cases in ANSYS Fluent. In the first case is analyzed the melting process and the dropping behavior of different materials in a presence of a thermal source. The model is validated using a study case found in the literature and using water as the melting material due its well-known behavior. Finally, tin and SAC 405 were used as melting materials and some variables as surface tension and latent heat of fusion were analyzed also. In the second study case is analyzed the deformation of solder paste (SAC 405) during its melting in a presence of a component and of a copper pad on top of a PCB. The heat source is the copper pad that it has a constant temperature.

2.2 Definition and Fabrication of PCBAs

As the name suggests, the PCBA is a product formed by the PCB, the electronic components and the soldering process that attaches the components to the PCB.

In this way, to produce a PCBA it is necessary first produce the different parts that are necessary for assembly the PCBA, know the product, and the required fabrication processes, because different products with different electronic components require different soldering processes.

Normally the companies that produce the PCBA, like the Bosch Car Multimedia, buy all the necessary components and only do the assembly of the electronic components in the PCB and then the soldering process. This assembly process can be more complex than it may seem at first sight. Depending on the complexity of the products the fabrication process may need to pass by three lines (the Reflow line, the radial line, and the Wave line) [13].

In the following sections it is explained in a simple way the different steps needed to produce a PCBA in the different lines.

2.2.1 Reflow Line

In a typical Reflow line, like that at Bosch Car Multimedia as depicted in figure 2.1, PCBs are loaded on the line and marked with an individual barcode by laser. After, the solder paste is printed above the pads and it is inspected, to confirm that it is correctly printed in all pads and in the right quantities. The next step is the insertion of SMD components in the correct position of PCB. Note that, in this line only SMD components are inserted. The product is subsequently mounted, and ready for the soldering process that occurs in a Reflow oven, where the solder paste melts and solidifies becoming a strong connection between the SMD components and the PCB. When the products leave the Reflow oven they are unloaded in a special container that can load several products, and unload for the AOI (Automatic Optical Inspection) one PCB each time, only when the operator in the visual inspection removes a PCB of the line.

The AOI is the final automatic inspection done in this line, and the objective is to inspect the solder and the SMD components to confirm or not the quality of the product. The operator at the end of the line sees the results of the AOI, if the AOI do not detect any defect the product is considered good. However, if the AOI detects only pseudo-errors, the operator needs to check visually if these pseudo-errors are real errors, occurred in the soldering process or in the insertion of the SMD

components, or if these pseudo-errors in reality do not represent any real error. In the first case the product must be rejected and in the second one the product is considered good. When the AOI detects an error the product must be rejected. After the final inspection, it is the operator who takes manually the products out the line and places them in containers [14] [15].

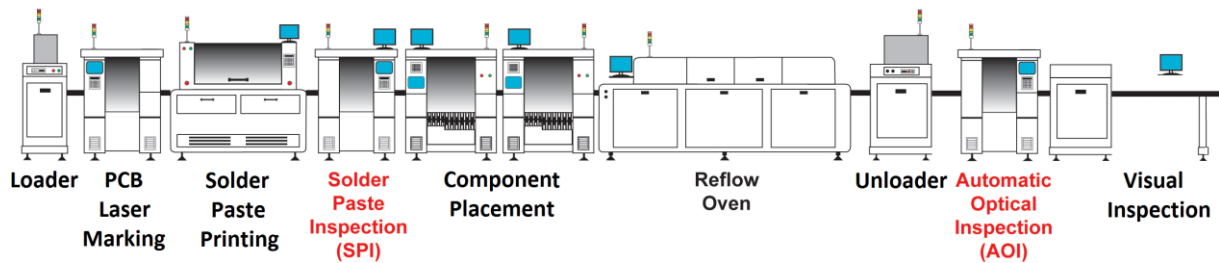


Figure 2.1 - Reflow line (Adapted from [16]).

At Bosch Car Multimedia a product can have a maximum of three soldering processes, taking into account the Reflow and Wave soldering processes. In this way, an ordinary product can have a single Reflow soldering process, or two Reflow soldering processes, or one Reflow and one Wave soldering processes, or two Reflow and one Wave soldering processes [14].

The products that have only a single reflow have SMD components in only one side of the PCB. However, when necessary do two Reflow soldering processes, the PCB needs two passes in the Reflow line. In the first pass are inserted SMD components in one side of the PCB. Then the PCB is placed upside down and the second pass begins at the Reflow line to insert SMD components in the other side of the PCB [14].

2.2.2 Radial Line

The products that leave the Reflow line may need to come to the radial line, figure 2.2, to do the automatic insertion of radial components and, if necessary, the placement of SMD components on the face B of the PCB [14].

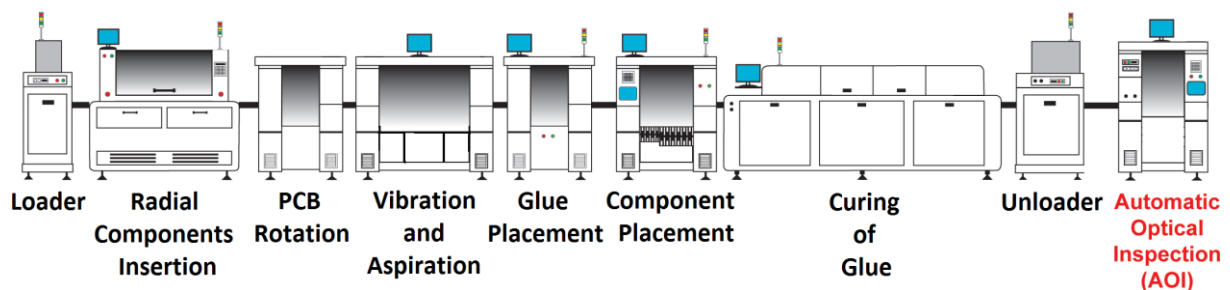


Figure 2.2 - Radial line (Adapted from [16]).

Once the products coming from the Reflow process enter the radial line from the loader, the components are inserted, and the length excess of metallic pins of the components is cut. Subsequently, the PCBs are rotated and pass by a process of vibration and suction to clean the product, of metal filings that may be in the PCB that result of cutting metallic pins. In the case of the product having SMD components in the face B to be soldered by Wave soldering process, it is necessary to apply an adhesive to the PCB, between the pads where the component sits, and then place the SMD components above the adhesive, as presented in figure 2.3 [14].

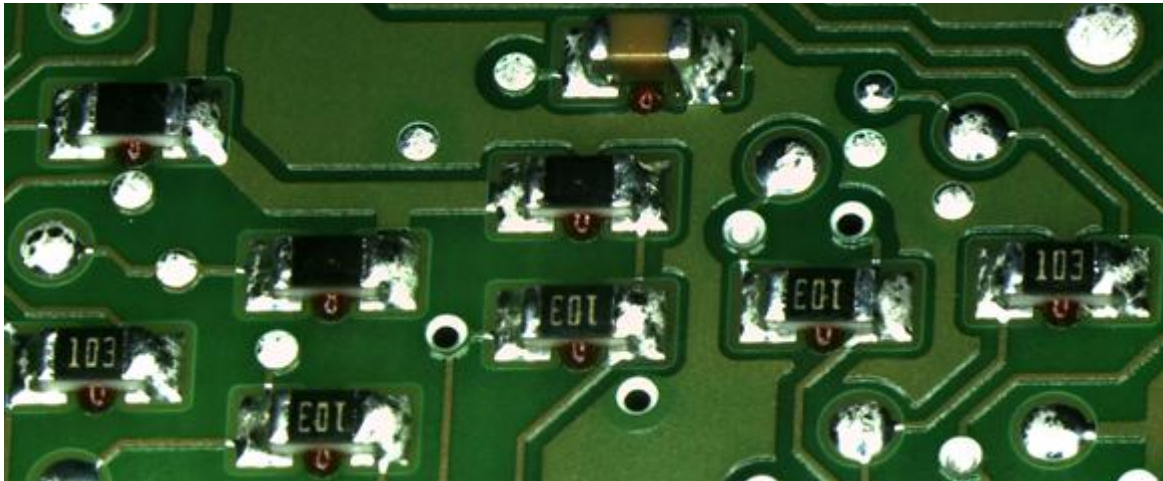


Figure 2.3 - SMD components fixed with an adhesive on the face B of the PCB.

In the next step the adhesive is cured in an oven at 150 °C, hardens and holds the component to the PCB. This process is necessary because during the Wave soldering process the components are upside down, so, an adhesive is necessary to hold the components in place during the process. After the curing of adhesive, the products are unloaded in a container, and at the end of the line is done the AOI, where the operator puts the product in the machine, evaluates the results, and removes the product out the line [14]. All products that need Radial components, or SMD components in its face B, arrive to this line to be soldered by Wave soldering process [14].

2.2.3 Wave Line

The Wave line is the last line in the process of fabrication the one PCBA. The products coming from the Reflow line or Radial line enter this line from the loader, through an operator who picks the product and puts them into the line. The next step is the manual insertion of TH components, if necessary. Then the products pass in the AOI to check if the product contains all the components in the right position. When the products arrive to the Wave oven, three distinct processes occur: a) the flux is

applied to the surface of the product that needs to be soldered; b) this surface is pre-heated and c) the Wave soldering occurs.

After the Wave oven, the products are cooled by fans, to allow the operator handle them out the line, and place them in the AOI. In the AOI the operator verifies if the product is free of soldering defects or bad component alignment. If the product presents some defect, and depending on the defect, this maybe has reparation, which is performed by an operator. However, if the product is free of defects, the operator removes it from the line, and the product is completed [14] [17]. The Wave line is presented in the figure 2.4.

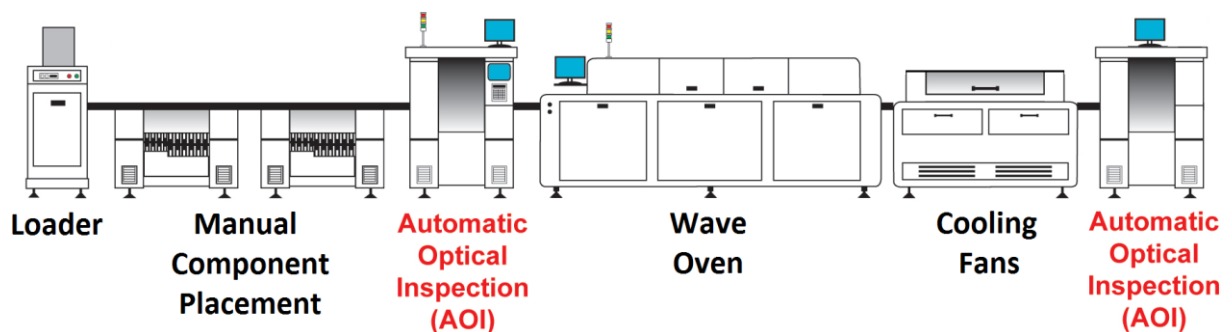


Figure 2.4 - Wave line (Adapted from [16]).

2.3 PCBs

The PCBs have in the PCBAs two main functions: a) provide to the electronic components the structural resistance to maintain them in the right position, and b) the electrical connections between the different electronic components in the PCB.

The PCBs are produced from FR-4 as a base material, which is a substrate of fiberglass impregnated in epoxy resin. In addition to the base material the PCBs have in your constitution printed electrical copper circuits (tracks) that provide the necessary electrical connections. Depending of complexity of the PCBs, these copper circuits may be printed only in one face, in both faces, or in multilayer. In the last case, presented in figure 2.5, in addition to the printed copper circuits in the faces of PCBs, these are also printed inside of the PCB. This method is used when the density of electrical connections is high for only two superficial layers in the faces of the PCBs.

The connection between the printed copper circuits and the electronic components is done by copper pads. To connect different copper layers it is used metalized copper holes (vias) that may pass through the entire thickness of the PCB [18] [19].

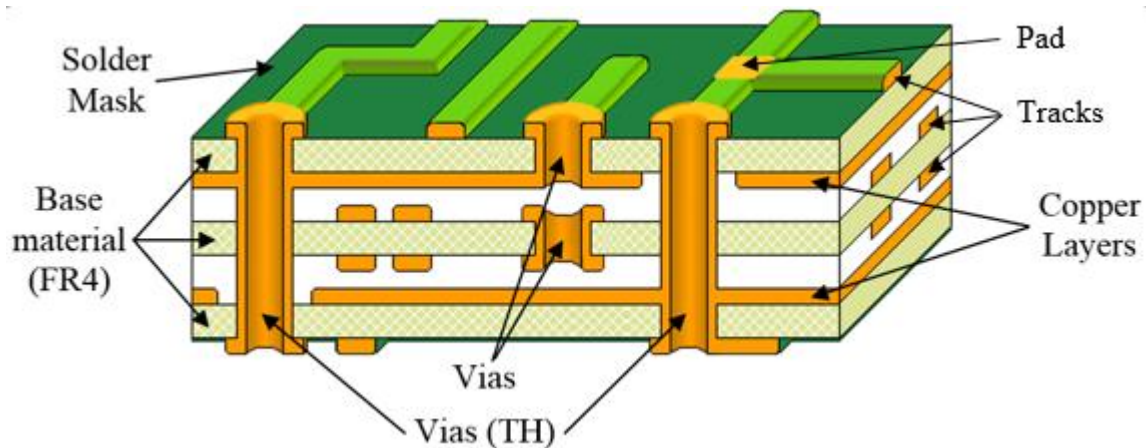


Figure 2.5 - Constitution of a multilayer PCB (Adapted from [20]).

After the PCBs production, it is necessary to protect the copper with a surface finish. This process is done mainly to avoid the oxidation of the copper pads. However, the surface finish is also used to improve the solderability, and to minimize the copper diffusion during the soldering process.

In the market there are several types of surface finish being the most used the Immersion Tin, the Ni/Au, the OSP, and the HASL. The choice of the surface finish depends of several factors as solderability, cost, and product quality. So, different surface finishes yield different intermetallic compounds, which affects the microstructure and mechanical properties of solder joints. The intermetallic compound created during the soldering process, between the solder and the copper pad, has an extreme importance in the quality and reliability of the solder joints. So, it is important to achieve a good formation of the intermetallic compound, which depends of the solder alloy and the surface finish used [21]. At Bosh Car Multimedia all surface finish need to have a metallization that resists for three soldering processes (Reflow and Wave) as requirement, due its degradation during the soldering processes.

2.3.1 Immersion Tin

The Immersion Tin is a surface finish created from the deposition of tin over the copper on the surface of the PCB, through the immersion of the PCB in liquid tin. The resulting layer of tin has a thickness normally between 0.8 and 1.2 μm , which depends of intermetallic thickness. It is important that the intermetallic do not arrive at the surface, of surface finish, to avoid problems with the solderability and wetting. So, the thickness of surface finish needs to be high enough to have a pure tin layer in its surface. In proper conditions of storage this surface finish protects the copper pads for up to one year. After this period the PCBs need to be analyzed, and if they are still in good condition the

expiration date is extended. This method is the same for every surface finish at Bosch Car Multimedia [22].

2.3.2 ENIG (Electroless Nickel/Immersion Gold)

The Ni/Au surface finish it is in reality two surface finish layers, first the nickel is deposited over the copper pads and after the gold is deposited over the nickel.

In this process the PCB is submersed in a nickel solution, and the deposition process occurs with the help of a reducing agent and without using an electrical current. After the nickel deposition, the PCB is immersed again, now in a solution of gold, where the gold is deposited over the nickel. The thickness of the nickel layer it is comprehended between 3 and 6 μm , and the thickness of the layer of gold between 0.05 and 0.1 μm . The use of the layer of gold it has the principal objective of to protect the nickel from oxidation. During the soldering process the gold layer is dissolved in the solder, exposing the nickel layer that will promote connection with the solder. This surface finish presents normally the best results of all surfaces in terms of soldering quality. Due to the good anti-oxidation protection that it is provided by the gold, resulting in a good solder paste wetting. And due to the presence of nickel that it stops the diffusion of copper. However, the quality increase provided by this surface finish it has a price, since this surface finish is the most expensive [22].

2.3.3 OSP (Organic Solderability Preservative)

The OSP is an organic surface finish with 0.2 to 0.5 μm of thickness that it prevents the oxidation of the PCB copper pads.

Since the OSP is not a solderable surface finish, the copper needs to have an excellent solderability, because it is this surface that will determine the wetting and spreading of molten solder during the soldering process.

The OSP layer is dissipated during the soldering process at high temperatures (120 $^{\circ}\text{C}$ to 150 $^{\circ}\text{C}$) exposing the copper pads to the flux and environment. With the temperature increase, the solder starts to melt and to wet the copper pads on the PCB. The principal disadvantage of the OSP surface finish is the difficulty in providing a good protection to the copper pads in multiple soldering processes. Since the OSP layer is degraded continuously in each thermal cycle, the last pads to being soldered, after one

or two soldering processes, will have a high probability of being oxidized due the degradation of all OSP layer. This it is currently one of the challenges for the PCBs manufacturers with OSP surface finish.

The use of an atmosphere of N_2 during the soldering process it is in this surface finish particularly important, since this atmosphere prevents the copper pads oxidation when the OSP surface is degraded.

The main advantage of OSP surface finish it is the low cost. This it is also suitable for fine-pitch products, when compared with the HASL, due the more uniform layer of OSP that will not interfere with the placement of the fine-pitch components [22] [23].

2.3.4 HASL (Hot Air Solder Leveling)

The HASL surface finish it is accomplished by immersing the PCB into molten solder. The solder alloy used may be a Sn-Pb or a lead-free alloy, depending of required product.

The thickness and texture of the HASL layer, which depends of the surface tension of molten solder, can vary from 2 to 20 μm or more.

HASL advantages can be enumerated as excellent solderability, since the HASL layer it is normally produced using the same alloy that will be used in the soldering process, and as good oxidation protection that it is provided to copper pads by the HASL layer. However, this technology has also some disadvantages, such as the loss of copper due the formation of an intermetallic layer between the copper pad and the HASL layer. Other important disadvantage, it is the not flat HASL layer, making assembling fine-pitch technology difficult or impossible [22].

2.4 Solder

In respect to solders used in electronic industry, it is possible to divide them in two groups, the Sn-Pb and the lead-free solder alloys.

The solder alloys with lead were in the past very often used by the electronic industry, due to their superior properties such as low melting point (183 $^{\circ}\text{C}$), superior manufacturability and process compatibility. However, the Pb as a toxic substance it was prohibited in the production of electronic components, by specific legislation [1]. This fact created a big change in the electronic industry, and the appearance of a high number of new lead-free solder alloys as substitutes of Sn-Pb alloys [24].

The first studied alloys were binary eutectic alloys of Sn and other elements, including Sn-Ag, Sn-Cu, Sn-Sb, Sn-Zn, Sn-In and Sn-Bi. The Sn-Cu alloy was implemented in the production of low cost products by Nortel [25] and it was achieved good results. The reasons for their choice were the cost and availability in comparison with Sn-Ag alloy. However, Sn-Cu presents inferior mechanical properties and wettability than Sn-Ag alloys [26].

However, the remaining binary alloys have a higher melting point than Sn-Pb, including Sn-Ag. To reduce the melting point, ternary alloys are desirable. Ternary alloys of copper with Sn-Ag were tested in BGA packages and the results obtained present superior performance than Sn-Pb alloys. Quaternary alloys were also tested, where the Sn_{3.5}Ag₁Zn_{0.5}Cu was reported as having good properties by McCormack and Jin in 1994. But, problems may be found in the production with this type of alloys, because the difficulties of reproducibility in the composition, result of quaternary alloys complexity [27].

Due the reasons presented above and due the good wetting, resistance to fatigue and plasticity, comparing to others lead free alloys, the SAC (Sn-Ag-Cu) alloys became the main alternative to Sn-Pb alloys. However, the SAC presents a higher melting point than Sn-Pb, between 217 °C and 221 °C, and due its composition, different intermetallic compounds may be formed during the soldering process, and this can change the properties of solder joints [24].

2.4.1 Solder Types

In the electronic industry is normal find two types of solders as uniquely solder, and solder paste. At Bosch Car Multimedia is used solder paste (SAC 405 + flux) in the Reflow soldering process, and uniquely solder (SAC 305) in the Wave soldering process [14].

The solder paste is composed by two mixed products, solder particles and flux. The solder particles used in solder paste they are classified in terms of size according to the table 2.1.

In high-temperature soldering processes, the primary purpose of flux it is to prevent oxidation of the materials to be soldered. Flux is inert at room temperature but became a stronger reducer at soldering temperatures, protecting and cleaning the surfaces that will be soldered. The flux is made by solvents, activators, vehicles, and additives. The solvents provide to the solder paste a pasty consistency, which it facilitates processing and deposition of solder paste. In the soldering process, the solvents are evaporated during the preheating. The activators have the function of to remove the oxides of surfaces to be soldered. The vehicles are liquid at soldering temperature, and their functions are actuate as barrier against oxidation, dissolve the reaction products of activators and carry them away

from the metal surface. At least, the additives are chemical products that may be added to the flux to change its properties, as corrosion inhibitors and antioxidants [28] [29].

Table 2.1 – Solder alloy classification in function of particle size (Adapted from [14]).

Solder alloy type	Particle Size Range (μm)
I	150 - 75
II	75 - 45
III	45 - 25
IV	38 - 20
V	25 - 15
VI	15 - 5

As mentioned above, in the Wave soldering process, it is used uniquely solder in the soldering process, however a flux is used separately of solder and before the soldering process to clean the surfaces to be soldered of any contamination or oxidation.

2.5 Electronic Components

Relatively to the components placed in the PCBs, it is important note that there is one important difference between the components. This difference it is related with the placement technology that can be SMT using SMD components or THT using TH components. In a PCBA may exist uniquely one or both technologies, depending of its complexity [14].

2.5.1 THT (Through Hole Technology)

The through hole technology uses through hole components. These components have pins and they are inserted in holes that pass through the PCB. In this kind of technology, the entire hole exposed surface it is the pad, which will be the connection point between the PCB electric circuit and the component's pins. The connection between the pads and the pins it is done by the solder, which it is placed in most of cases by Wave soldering process, but sometimes for specific components, can be done by Reflow soldering process. In the case of a component TH soldered by Reflow soldering process it is necessary take into account, during the design of electrical circuit of the PCB, the excess of solder paste which it needs to be printed to fill the holes during the reflow. This may be a problem in

components with a large number of pins or in PCBs with a high density of components. In this cases, may does not exist space enough to print the solder paste needed for fill all holes.

Figure 2.6 presents two through hole components to be soldered by Wave, and three to be soldered by Reflow. In the last ones, it is possible to observe the location specified for the overprint of solder paste near to the pins of the components [30].

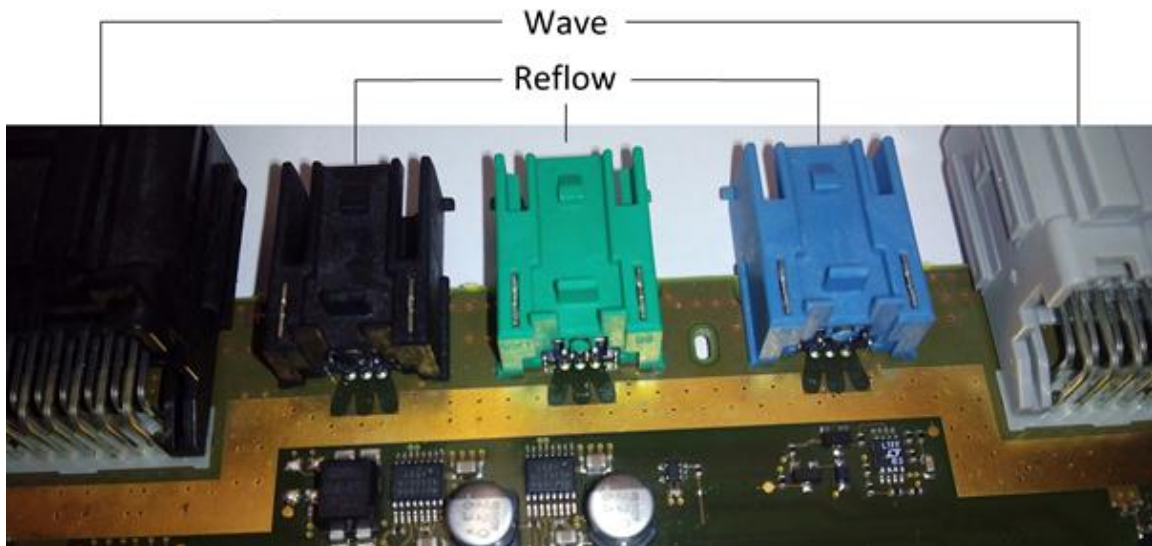


Figure 2.6 – THT (Through Hole Technology).

The main disadvantage is that this technology is associated with the use of large components. In this way, the PCB cannot have a high density of components, which it limits the functions or the miniaturization of a PCBA. However, this technology allows for some applications to reduce the production cost, due the lowest cost associated to the machines and process used in the Wave, comparing to the Reflow soldering process [30].

2.5.2 SMT (Surface Mount Technology)

The SMT is a technology more recent than THT and it is totally automated, contrarily to the THT where most of the components are placed by hand.

In the SMT technology, the components are soldered to the pads placed on PCB surface. In this way, it is possible to place components on top and bottom of the PCB.

The use of a fully automated production process is fundamental in this kind of technology, since it uses smaller components and more sensitive than THT. In this process it is also necessary a high precision and control of all production line, to achieve good products.

As it is possible to observe in figure 2.7, this technology allows to achieve smaller products or with more functions for the same PCB size, and a production rate higher than THT [30].

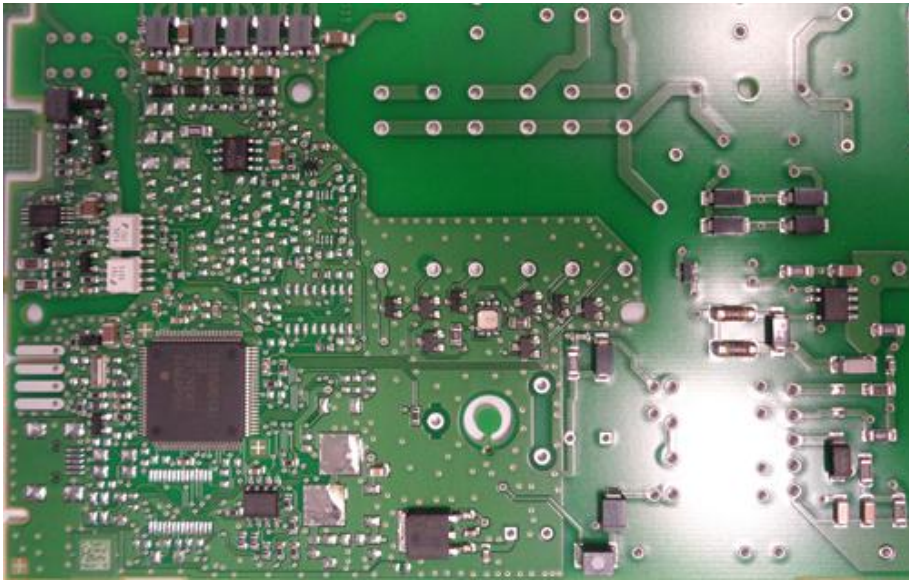


Figure 2.7 - SMT (Surface Mount Technology).

2.5.3 Components Metallization

The selection of the components metallization it is an important step on the PCBAs production, because this has the function of protecting the base metal of oxidation and it increases the solderability.

At Bosch Car Multimedia, the surfaces or the pins of the components to be soldered are formed essentially by copper, nearly 80%, or formed by Fe-Ni. The last one, it is used principally for components that need to resist to the mechanical stress [14].

The metallization finish layer most used in electronic industry it is the Tin (Sn). This layer may be applied by different techniques and with different thicknesses, depending of its application. In some components or applications in order to avoid defects, as whiskers, it is used a top underlayer of Ni or Cu between the base metal and the finish layer of Sn. In figure 2.8, it is possible to observe the distribution of the layers in a normal component metallization [14] [31].

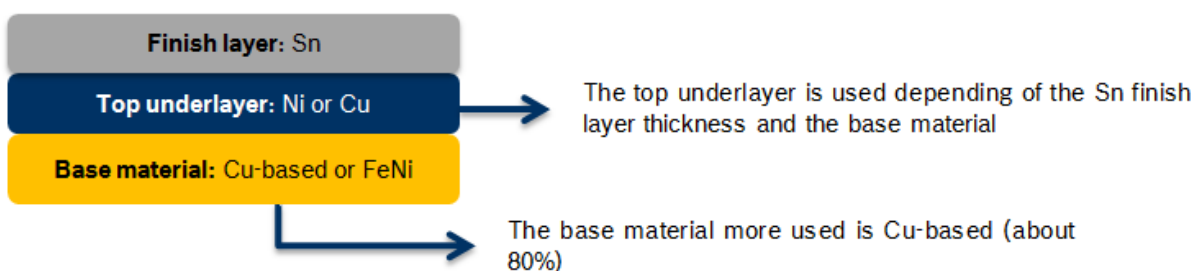


Figure 2.8 - Different layers of components metallization.

The finish layer and the top underlayer have different thicknesses, depending on the process of production and the application. It is necessary to take into account the degradation of the metallization during the soldering process, and in this way to produce a metallization that resists to the entire soldering process. Table 2.2 shows the metallizations most used at Bosch Car Multimedia [14].

Table 2.2 - Constitutions most used for components metallization (Adapted from [14]).

Metal Lead (Pin) Finish for CM												
Base Material			Cu-based				FeNi (not recommended)					
Sn finish layer	Galvanic matt	min. 2 μm	x	x					x	x		
		min. 7 μm			x			x			x	
	Hot dip plating	min. 2 μm				x	x					x
Top underlayer												
Galvanic Ni (min. 0.5 μm)			x				x	x	x			
Galvanic Cu (min. 2 μm)										x	x	x

2.6 Reflow Soldering Process

Reflow is a soldering process that occurs in an oven and where the solder paste is melted and solidified with the objective of attaching the components to the PCBs.

There are different methods to do the Reflow as through forced convection, in-line-conduction, infrared, and vapor phase [32]. However, at Bosch Car Multimedia it is only used the Reflow oven with forced convection, so this will be the focus of this thesis [14].

The forced convection oven, used in the Reflow soldering process, works through movement of hot gas heated by heat exchangers. This gas is normally N_2 , which it is a non-oxidant gas, contributing for a better solderability than air [14]. The gas is in this way the transporter of the heat from the heat exchanger to the PCB. The PCB is heated from top and bottom, and between the inlet, of the oven, and the exit it passes through four phases of heating well defined in terms of temperature and time. Figure 2.9 presents the operation principle of a Reflow oven [33].

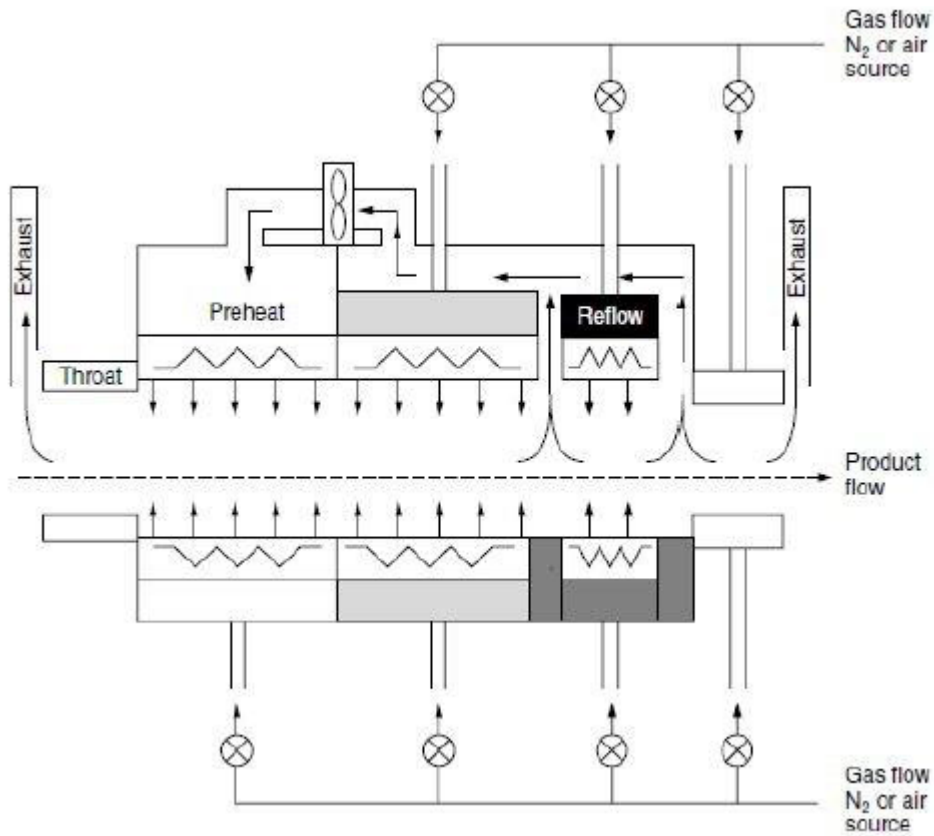


Figure 2.9 - Operation principle of a Reflow oven [34].

As presented in figure 2.10 the four phases of the Reflow soldering process are: a) the preheating, b) the activation of flux or Soak, c) the Reflow, and d) the cooling [35].

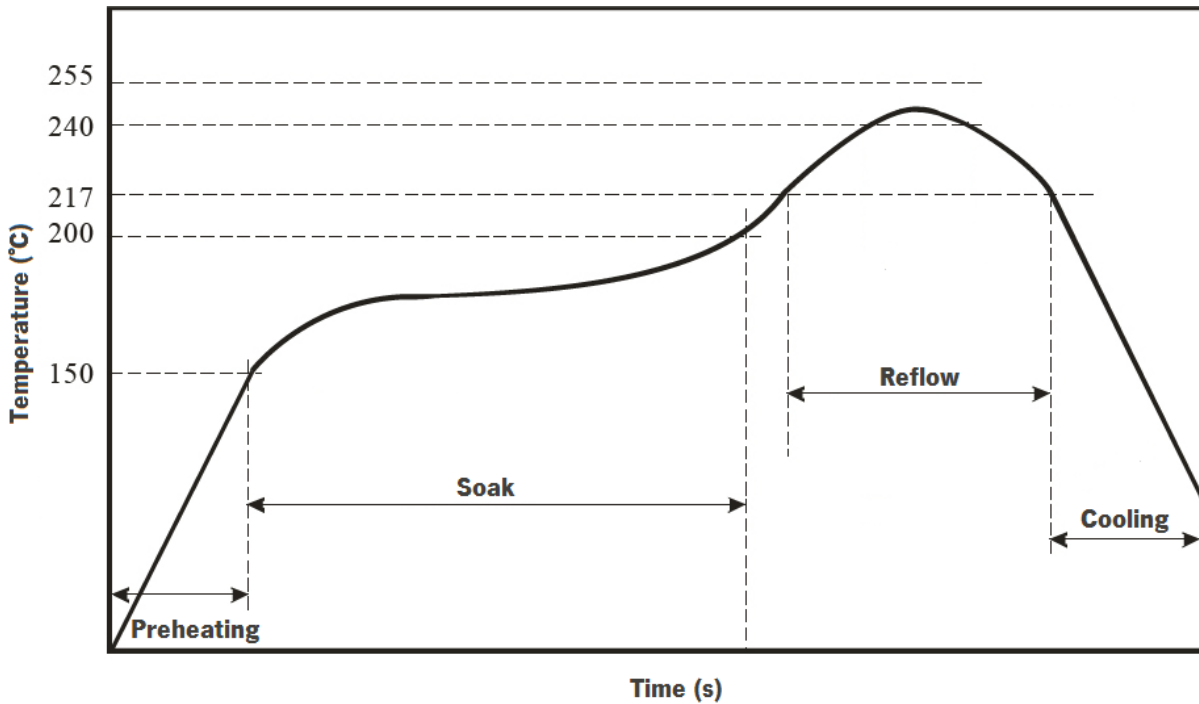


Figure 2.10 – Typical Reflow thermal cycle for lead-free solder pastes (Adapted from [36]).

In the preheating phase the PCB and the components are heated at low rate from the room temperature to 150 °C [14]. The main objective this phase is to evaporate the solvents of solder paste, and to do this, it is important make sure that the temperature and time of this phase they are the correct to evaporate all solvents. The low rate of heating is also important, because it avoids the thermal shock of the components and PCB, which could damage the components, distort the PCB, or provoke delamination due the different thermal expansion coefficient of the different materials [33].

The second phase named activation of flux or Soak occurs at near constant temperature during a well-defined period. During this phase, as the name suggests, the flux is activated and the oxidation-reduction reaction between the activators and the oxidized surfaces begins. In addition to removing the oxides, the activators also protect the surfaces to be soldered until the beginning of the third phase [14]. To achieve these objectives it is critical to have a perfect control of temperature and time. In fact, higher temperatures increase the oxidation and the activators may last less time that initially predicted, leaving later the solder and pads without protection anti-oxidant. Otherwise, with lower temperatures, the activators may not be entirely activated, not cleaning the surfaces to be soldered properly. The other main objective of this phase is the temperature homogenization around the PCB, this allows that all components are soldered at same time, avoiding hot points and distortions in the PCB and components [33].

The third phase is the Reflow. It is in this phase that the soldering process takes place. The temperature increase almost linearly up to the maximum temperature, between 245 °C and 260 °C [14], which is defined by taking into account the weakest component in terms of temperature resistance. Subsequently the temperature falls. Higher temperatures may cause damage in the components. However, the maximum temperature has to be high enough to ensure that all points of solder are melted in the PCB during the soldering process, due the temperature gradient around the PCB. Otherwise, low temperatures may not to melt all points of solder. In this way, it is possible understand that the definition of the maximum temperature has a critical importance in all process of Reflow [33].

Other variable extremely important in all soldering process it is the TAL (Time Above *Liquidus*), normally between 45 and 90 s [14]. This period of time needs to be as shorter as possible to avoid oxidation, but it is necessary to give enough time to melt the solder on all PCB, principally in the cold points. This period it is also important to achieve a good wetting of solder paste and consequently a good solder joint. However, if this period it is too long the intermetallic layer may grow more than desirable and make the solder joint more brittle [33].

The last phase is the cooling of the solder joints formed previously. In this phase the rate of cooling needs to be as higher as possible to obtain a solder with a fine granular structure, which it provides better mechanical properties [37]. But as in the preheating phase, it is necessary to be careful with the thermal shock and distortion of the components and PCBs respectively. However, the rate of cooling has influence on the intermetallic layer growth. Slow cooling rates may cause an excessive intermetallic layer growth, and formation of coarse granular structures that weaken the solder joints, resulting in poor stress resistance [33] [38].

Numerical Models and Methodology

This chapter presents a simple description of the most important models used in ANSYS Fluent, taking into account the objectives of the numerical simulations, an overview of the 6SigmaET software, and a description of the experimental procedure.

First, two models used by ANSYS Fluent are presented, due its importance in the simulations, as the Volume of Fluid (VOF) and the Solidification/Melting Model. Second, the discretization method, the Finite Volume Method, used by ANSYS Fluent to solve the integral systems of equations is described. Third, the thermal simulation software “6SigmaET” used in the work developed at Bosch Car Multimedia is presented. Finally, the experimental procedure used to validate the 6SigmaET simulations results is described.

3.1 Multiphase Flows

Normally the flows found in nature or in industry they are a mixture of phases. The physical phases of materials are three, gas, liquid and solid, but the concept of phase in multiphase flows it is applied in a more ample way. In multiphase flows one phase can be defined as a class of identified material that it has a particular answer of inertia and it interacts with the flow and with the potential field in which it is immersed. For example, solid particles with different dimensions of the same material can be defined as different phases, because each group of particles with the same dimension going to have a similar dynamic answer to the flow field.

Multiphase flows regimes can be divided in three categories as: a) flows gas-liquid or liquid-liquid, b) flows gas-solid and c) flows liquid-solid, and flows with three phases. Three-phase flows are combinations of others flow regimes listed above [39].

3.1.1 Approaches to Multiphase Modeling

There are currently two approaches for numerical calculations of multiphase fluids: the Euler-Lagrange approach and the Euler-Euler approach [39].

The Euler-Lagrange Approach

This model is appropriate to modulate spray dryers, combustion of liquid fuel and coal, flows with some particle-laden, but it is inappropriate to modulate flow regimes liquid-liquid, fluidized beds, or any application where the volume fraction of the second phase cannot be neglected [40].

The Euler-Euler Approach

In the Euler-Euler approach, the different phases are processed mathematically as interpenetrating. Once the volume of one phase cannot be occupied by other phases, the concept of volume fraction is introduced. These volume fractions are assumed as a continuous function of space and time and its sum is equal to 1.

In ANSYS Fluent, three different Euler-Euler multiphase models are available, the volume of fluid (VOF) model, the mixture model, and the Eulerian model [39].

- The VOF model

The VOF model is a technique of surface-tracking applied to a fixed Eulerian mesh. This model was developed for two or more immiscible fluids where the interface between the fluids has interest. In the VOF model, one unique set of momentum equations is shared by all fluids, and the volume fraction of each fluid in each cell is tracked across the domain.

The VOF model can be applied for stratified flows, free-surface flows, filling, sloshing, the movement of large bubbles in a liquid, the movement of liquid after a dam break, and the steady or transient tracking of any interface liquid-gas [39].

- The Mixture Model

The mixture model is developed for two or more phases (fluid or particles). As in Eulerian model, the phases are processed as immiscible. The mixture model solves the mixture momentum equation and it sets relative velocities to define the dispersed phases.

The mixture model is applied to particle-laden flows with low loading, bubbly flows, sedimentation, and cyclone separators. The mixture model can also be used without relative velocities for dispersed phases to model homogeneous multiphase flows [39].

- The Eulerian Model

The Eulerian model is the most complex multiphase model of ANSYS Fluent. This model solves a set of n momentum and continuity equations one for each phase. Coupling is obtained by the exchange of pressure and interphase coefficients. The way coupling is done depends of the phase types involved. Granular flows (fluid-solid) are processed in different way that non-granular flows. For granular flows, the necessary properties are obtained by the application of kinetic theory. The change of momentum between the phases depends also of the phase types to be modulated.

The Eulerian model is applied to bubble columns, risers (vertical pipe), particle suspension, and fluidized beds [39].

3.1.2 Volume of Fluid (VOF) Model

Since the VOF model will be used in the present numerical simulations, because it is suitable for steady or transient tracking of any interface liquid-gas, this will be analyzed more carefully.

In addition to the above mentioned, this model has some limitations as [39]:

- The VOF model is only available with the pressure-based solver.
- The entire domain of simulation has to be filled with a unique phase or a combination of phases. The VOF model does not allow empty regions where none fluid of any type is present.
- Only one phase can be defined as a compressible ideal gas. However, there is no limitation about the use of compressible liquids when a user defined function is used.
- The second-order implicit time-stepping cannot be used with the VOF explicit scheme.

Steady-State and Transient VOF Calculations

The VOF formulation is based on fact that two or more fluids or phases are not interpenetrating. For each additional phase, the volume fraction of this phase is introduced in some computational cells. In each cell, the volume fraction of all summed phases must be equal to the unity. The variables and properties are shared by the phases and they represent volume-averaged values, since the volume fraction of each phase is known in each local. In this way, the variables and properties are in each cell purely representative of a phase or of a mixture of phases, depending on the values of volume fraction. In other words, if the fluid, q^{th} has a volume fraction, α_q , in a given cell, then three conditions are possible [39]:

- $\alpha_q = 0$ The cell is empty (of the q^{th} fluid).
- $\alpha_q = 1$ The cell is full (of the q^{th} fluid)
- $0 < \alpha_q < 1$ The cell contains an interface between the q^{th} fluid and one or more other fluids.

Based on the local value of α_q , the properties and the appropriate variables for each control volume will be attributed and calculated, inside the domain.

Volume Fraction Equation

The tracking of interface or interfaces between the phases is done solving the continuity equation for the volume fraction the one or more phases. For the phase q^{th} , the continuity equation has the following form [39]:

$$\frac{1}{\rho_q} \left[\frac{\partial}{\partial t} (\alpha_q \rho_q) + \nabla (\alpha_q \rho_q \vec{v}_q) \right] = S_{\alpha_q} + \sum_{p=1}^n (\dot{m}_{pq} - \dot{m}_{qp}) \quad (1)$$

where \dot{m}_{qp} is the mass transferred from the phase q to the phase p , and \dot{m}_{pq} is the mass transferred from the phase p to the phase q .

As default, the source term S_{α_q} is 0, but can be defined as a constant or as a function defined by the user for the source mass of each phase. The volume fraction equation is not solved for the primary phase. Instead, the volume fraction is calculated based in the following restriction [39]:

$$\sum_{q=1}^n \alpha_q = 1 \quad (2)$$

The volume fraction equation can be solved through the implicit or explicit time discretization.

The Implicit Scheme

When the implicit scheme is used for time discretization, the following finite-difference interpolation schemes are used by ANSYS Fluent, QUICK, Second Order Upwind and First Order Upwind, and the Modified HRIC, to obtain the face fluxes for all cells, including the cells close to the interface [39].

$$\frac{\alpha_q^{n+1} \rho_q^{n+1} - \alpha_q^n \rho_q^n}{\Delta t} V + \sum_f (\rho_q^{n+1} U_f^{n+1} \alpha_{q,f}^{n+1}) = \left[S_{\alpha_q} + \sum_{p=1}^n (\dot{m}_{pq} - \dot{m}_{qp}) \right] V \quad (3)$$

This equation needs the volume fraction values in the current time-step, contrary to the explicit scheme which it needs only the volume fraction values in the previous time-step. In this way, a standard scalar transport equation is solved iteratively for each volume fraction of one secondary phase in each time-step. The implicit scheme can be used to solve stationary and transient problems [39].

The explicit Scheme

In the explicit scheme, the standard ANSYS Fluent finite-difference interpolation schemes are applied to the volume fraction values computed in the previous time-step [39].

$$\frac{\alpha_q^{n+1} \rho_q^{n+1} - \alpha_q^n \rho_q^n}{\Delta t} V + \sum_f (\rho_q U_f^n \alpha_{q,f}^n) = \left[\sum_{p=1}^n (\dot{m}_{pq} - \dot{m}_{qp}) + S_{\alpha_q} \right] V \quad (4)$$

where $n + 1$ is the current time-step, n is the previous time-step, $\alpha_{q,f}$ is the volume fraction value on the face of phase q^{th} , computed from the first- or second- order upwind, QUICK, modified HRIC, compressive, or CICSAM scheme, V is the cell volume, and U_f is the volume flux through the face, based in normal velocity.

Contrary to implicit scheme, the explicit method does not need to solve the transport equation iteratively for each time-step. When the explicit scheme is used, a time dependent solution must be computed [39], so, with the explicit scheme, only transient problems can be solved.

When an explicit scheme is used for time discretization, the face fluxes can be interpolated using an interface reconstruction or using a finite volume discretization scheme [39].

Material Properties

The properties present in the transport equations are determined taking into account the phases present in each control volume. In two phase systems, for example, if the phases are represented by the nomenclature 1 and 2, and if the volume fraction of the second phase is tracked, the density of each control volume is the following [39]:

$$\rho = \alpha_2 \rho_2 + (1 - \alpha_2) \rho_1 \quad (5)$$

In general, for systems with n phases, the average density takes the following form [39]:

$$\rho = \sum \alpha_q \rho_q \quad (6)$$

All the other properties, as the viscosity, are calculated in this way.

Momentum Equation

A single momentum equation is solved in the entire domain, and the resultant velocity field is shared by the phases. The momentum equation, below, is dependent of volume fraction of all phases through the properties ρ and μ [39].

$$\frac{\partial}{\partial t}(\rho \vec{v}) + \nabla(\rho \vec{v} \vec{v}) = -\nabla p + \nabla[\mu(\nabla \vec{v} + \nabla \vec{v}^T)] + \rho \vec{g} + \vec{F} \quad (7)$$

One limitation of shared velocity fields is found in cases where there is a big velocity difference between the phases. In these cases, the precision of computed velocities near the interface can be seriously affected [39].

Note that, if the viscosity ratio is higher than 1×10^3 , this can cause difficulties of convergence. To solve this problem the Compressive Interface Capturing Scheme for Arbitrary Meshes (CICSAM) is used, because it is suitable for fluxes with a high viscosity ratio between the phases, so this model can solve the poor convergence problem [39].

Energy Equation

The energy equation is also shared between the phases, and is the following [39].

$$\frac{\partial}{\partial t}(\rho E) + \nabla(\vec{v}(\rho E + p)) = \nabla(K_{eff} \nabla T) + S_h \quad (8)$$

The VOF model deals with the energy, E , and the temperature, T , as variables dependent of mass percentage or as variables dependent of average mass of each phase [39]:

$$E = \frac{\sum_{q=1}^n \alpha_q \rho_q E_q}{\sum_{q=1}^n \alpha_q \rho_q} \quad (9)$$

where E_q for each phase is based in the specific heat of phase and in the shared temperature.

The properties ρ and K_{eff} (effective thermal conductivity) are shared by phases. The source term, S_h , takes into account others contributions as radiation, as well as, any other source of volumetric heat [39].

As the velocity fields, the precision of temperature near the interface is limited in cases where there is a big temperature difference between the phases. These problems also appear in cases where the properties vary several orders of magnitude. For example, if a model includes liquid metal in combination with air, the materials conductivity can vary up to four orders of magnitude. High discrepancies in properties originate a group of equations with anisotropic coefficients, which in turn can lead to limitations of convergence and precision [39].

Additional Scalar Equations

Depending on the problem definition, additional scalar equations can be added to solution. In the case of problems involving turbulence, a unique group of scalar equations is solved, and the turbulence variables, for example, k and α or the Reynolds stresses are shared by phases across the domain [39].

Time Dependence

To solve transient problems using the VOF model, the equation 1 is solved using the explicit scheme. The ANSYS Fluent refines automatically the time-step for the integration of volume fraction equation, but the time-step can be influenced by the change of Courant Number. The user can also choose to actualize the volume fraction one single time in each time-step, or in every iteration inside of the same time-step [39].

Surface Tension and Adhesion

The VOF model can also take into account the effects of superficial tension along the interface between each pair of phases. The model can be expanded through the additional specification of contact angles between the phases and the walls, as well by defining a porosity variation. The surface tension can be specified as a constant, as a function of temperature through a polynomial, or as a function of any variable through a UDF. The calculation method, Solver, will take into account the

additional tangential stress terms (causing the named as Marangoni Convection) which appears due the variation of superficial tension. The effects of surface tension variation are normally important only when the gravity is zero or near zero [39].

3.2 Solidification/Melting Model

The ANSYS Fluent can be utilized to solve solidification and melting problems, at constant melting temperature for pure metals, or at a range of melting temperatures for metallic alloys. The ANSYS Fluent instead of tracking the liquid-solid front explicitly, it utilizes the enthalpy-porosity formulation, which it was suggested by Voller and Prakash [41]. In this formulation, the porosity is obtained through the liquid fraction, which it is the fraction of volume in one cell that it is in the liquid form. The liquid fraction is associated with each cell of domain and it is calculated in each iteration based in the enthalpy balance [42].

The Mushy-zone is a region with a mixing of solid and liquid material, which it is treated as a porous zone with porosity equal to the liquid fraction. In this way, the liquid fraction has a value between 0 and 1. The solid region has a liquid fraction of 0, so the porosity is also 0. In opposite way, in the liquid region, the liquid fraction is 1, so the porosity is also 1. When the material solidifies, the porosity decreases from 1 to 0, and when the porosity becomes 0, the velocity drops also for 0 m/s [42].

ANSYS Fluent has the following capabilities to modulate solidification and melting [42]:

- Calculation of liquid-solid solidification/melting for pure metals and binary alloys.
- Modulation of continuous casting processes (this is, “polling” the solid material to out of domain).
- Modulation of thermal contact resistance between the solid materials and the wall (for example, because the existence of an air gap).
- Modulation of species transport with the solidification/melting model.
- Post-processing of variables related to the solidification/melting model (this is, liquid fraction and pull velocities).

These capabilities allow the ANSYS Fluent to model a high range of problems involving the solidification/melting model, as melting, solidification or freezing, crystal growth and continuous casting [42].

Limitations

In ANSYS Fluent the solidification/melting model has the following limitations [42]:

- The solidification/melting model is available only with the pressure-based solver, so this model cannot be used with the density-based solver.
- The solidification/melting model cannot be used with compressible fluids.
- For the generality of multiphase models (VOF, mixture and Eulerian), only the VOF model can be utilized with the solidification/melting model.
- With the exception of species diffusion, it is impossible to specify different properties to the same material when it is liquid or solid through the GUI (Graphical User Interface). However, if necessary, different properties can be utilized to solid and liquid form of the same material with user-defined functions (UDF).
- When the solidification/melting model is used in conjunction with the species transport and its reactions, there is not any action that restricts the reaction only in the liquid region, so the reaction is solved in the entire domain of simulation.

Energy Equation

The enthalpy of a material it is computed as a sum of sensible enthalpy, h , and the latent heat, ΔH [42]:

$$H = h + \Delta H \quad (10)$$

where

$$h = h_{ref} + \int_{T_{ref}}^T c_p dT \quad (11)$$

and h_{ref} is the reference enthalpy, T_{ref} is the reference temperature, and c_p is the specific heat at constant pressure.

The liquid fraction, β , can be defined as [42]:

$$\begin{aligned} \beta &= 0 && \text{if } T < T_{solidus} \\ \beta &= 1 && \text{if } T > T_{liquidus} \\ \beta &= \frac{T - T_{solidus}}{T_{liquidus} - T_{solidus}} && \text{if } T_{solidus} < T < T_{liquidus} \end{aligned} \quad (12)$$

Now the latent heat content can be written with reference to the latent heat of the material (L) and the liquid fraction of one specific cell [42].

$$\Delta H = \beta L \quad (13)$$

The value of latent heat can in this way vary between 0 (for solids) and L (for liquids).

So the energy equation used in the solidification/melting model is [42]:

$$\frac{\partial}{\partial t}(\rho H) + \nabla(\rho \vec{v} H) = \nabla(k \nabla T) + S \quad (14)$$

where H is the enthalpy, ρ is the density, \vec{v} is the fluid velocity, and S is the source term.

The energy equation is used to find the temperature, but to do this it is necessary to do an iteration between the energy equation and the liquid fraction equation. Using directly the liquid fraction equation to update the value of liquid fraction, normally it results in bad convergence of solution of the energy equation. To solve this problem, in ANSYS Fluent, the model suggested by Voller and Swaminathan to update the liquid fraction is used [43]. For pure metals, where *Solidus* and *Liquidus* temperatures are equal, the method based on the specific heat, which was specified by Voller and Prakash [41], it is used instead the previous model [42].

Momentum Equation

The enthalpy-porosity technique processes the mushy region as a porous medium. In each cell, the porosity is obtained in the same way that liquid fraction. In regions completely solidified the porosity is equal to 0, and that it extinguishes the velocity in this region. The momentum equation, due the reduced porosity of mushy zone, it has the following form [42]:

$$S = \frac{(1 - \beta)^2}{(\beta^3 + \varepsilon)} A_{mush} (\vec{v} - \vec{v}_p) \quad (15)$$

where β is the volume liquid fraction, ε is a small number (0.001) to avoid the division by zero, A_{mush} is the constant of mushy zone, and \vec{v}_p is the velocity of the solidified material due the force exerted on it to out of domain (sometimes called pull velocity) [42].

The mushy zone constant defines the amplitude of velocity damping, as the higher the value, the faster is the decrease of material velocity while solidifies. Values of mushy zone constant too high can cause instability in the solution [42].

The pull velocity is needed to take into account the movement of solidified material while it is continually removed of domain in continuous casting processes. So this variable allows the solidified material to move at the pull velocity. If the solidified material is not pulled out of domain, then the pull velocity is 0 m/s [42].

3.3 Finite Volume

The Finite Volume Method (FVM) is one of the discretization methods more used in CFD to solve the partial differential equations. This technique is based on the concept of the control volume, in which the physical domain is divided in a finite number of control volumes. After this step the computational nodes are defined in the centroid of the control volume, where the variables of interest are calculated [44].

Next, it is necessary to integrate the differential form of the governing equations for each control volume, to obtain the discretized equations of the variable in study for each control volume. After that, the variable values at the control volume boundaries are interpolated from the centroid values of these variables. This process results in a discretized equation for each control volume, which expresses the conservation principle for the variable at the control volume [44].

The principal reason to use this method in the engineering problems is the resulting solution satisfies the conservation of variables like mass, momentum, energy, and species, for the entire domain and for any control volume. This method is also suitable for any geometry using structured meshes or not. However, this method has difficulty to solve high order schemes, without structured meshes [45].

3.4 Finite Volume Notation

The finite volume method starts by dividing the domain of simulation in a large number of small control volumes, using a grid to implement this division as represented in figure 3.1.

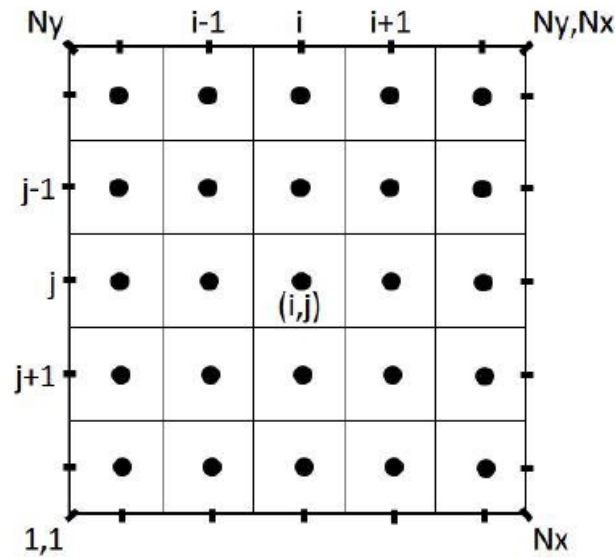


Figure 3.1 - Notation for simulation domain division (Adapted from [46]).

In Figure 3.1, it is possible to see that the nodes are located in the centroids of control volumes (the cell centered scheme). However the nodes can also be in the vertices of the control volumes (cell vertex scheme). However the first approach is the most used, because it allows better accuracy [46].

Other feature usually used in this method is the identification of the nodes by cardinal points, as depicted in figure 3.2. This allows easily identification of the nodes around the main node in analysis [46].

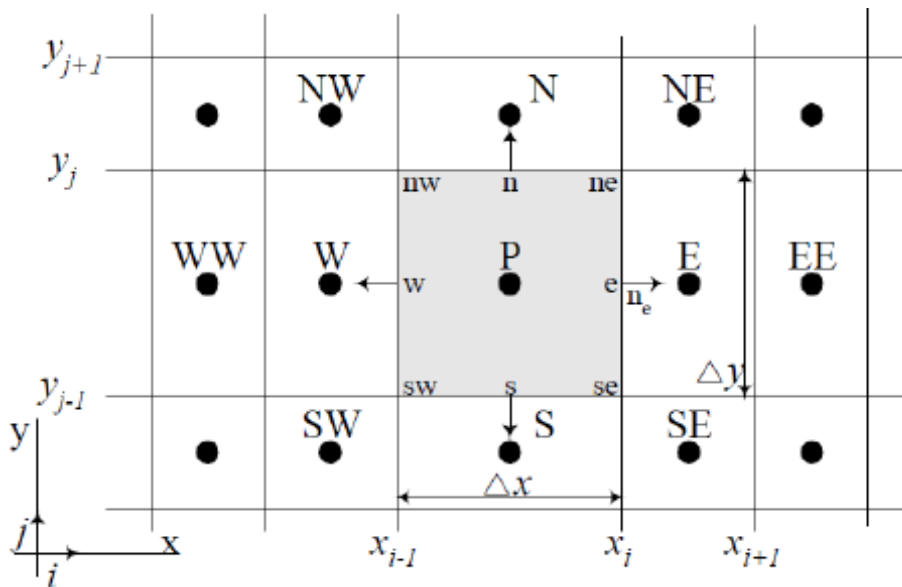


Figure 3.2 - Notation of the nodes and control volume faces (Adapted from [46]).

3.5 6SigmaET Overview

6SigmaET is a computational fluid dynamics (CFD) thermal simulation software launched by Future Facilities in 2009 that it was dedicated to the electronics industry [47]. This software makes available a broad range of intelligent modeling objects such as: PCBs, chip sockets, and electronic components such as resistors and capacitors, temperature controlled fans and blowers [48].

Since this software is dedicated to the industry and to the engineers without background in CFD modulation, 6SigmaET has a high level of intelligence and automation that it allows automatically to create rules to place, align, detect collisions and check error for different objects. The software creates also the grid automatically ensuring that the optimum grid is always used [48].

Simulation results are associated also with the objects, which it allows to initiate the display of critical temperatures and airflow patterns directly from the objects. The automatic report-generation ensures the results of the study can be easily and effectively communicated [48].

In 2014, a new solving methodology the Multi-Level Unstructured Staggered (MLUS) Solver was developed. The unstructured solver “employs a hierarchy of Cartesian grids and a face to cell connectivity graph to discretize the differential equations. The method uses a finite volume scheme with staggered variable arrangement and a pressure-based segregated iteration procedure to solve a discrete algebraic analogue of the Navier-Stokes equations” [49].

In terms of simulation capability, this program has the disadvantage of non-simulate the solder paste and its change of phase. In this way, this program does only a thermal simulation of the PCB and components. However, it has the advantage of having been produced specifically for this type of simulations, and this means that it is easier to work and more accurate.

In the industry, it is normal to do only the thermal simulation of the PCB and components, because the main objective is to ensure that no component in the product exceeds its temperature limit or that there is not any region of PCB with a difference of temperature too large, which may cause soldering problems. In other words, the main objective in the industry is predict the temperatures that the products will be exposed during the soldering process, and because the simulation of solder paste, and principally its change of phase, is a process that it needs much more time of simulation, they simply eliminate the solder paste of simulations. In this way, it is possible to simulate a real Reflow thermal cycle in one single day for a complete product.

3.6 Experimental Work Procedure

To confirm the results of a simulation, to validate a simulation model or to measure its accuracy, an experimental test is often realized. In this thesis, to confirm the results and measure the accuracy of the 6SigmaET thermal simulation model, an experimental test in the production line was realized.

To accomplish this test a real product is used where some thermocouples are installed at predetermined locations, in accordance to the test objective. The placement of the thermocouples must be carefully done to ensure that the thermocouple stays in contact with the object in analysis. Otherwise, the results recorded for a determined object do not will be precise. Other care to have taken in the placement of the thermocouples. They are the adhesive type used for fixing the thermocouples to the objects in analysis. The adhesive type used must be heat conductor to ensure that do not will interfere with the temperature read by the thermocouple.

After preparing the real product to be tested in the production line, the thermocouples are connected to a machine that will record the thermal cycles of each thermocouple during the Reflow soldering process. The recording of each thermocouple thermal cycle is initiated automatically, through a thermocouple that read the air temperature. The product to be tested and the machine to record the thermal cycles are then inserted in the Reflow oven with a Reflow thermal cycle appropriated for the product in study. After approximately 5 minutes, the product exits the Reflow oven and the test is completed.

The results are extracted from the machine that recorded the thermal cycles of each thermocouple directly to the computer. The results can be seen in PDF where the results are automatically treated according to the requirements predetermined or in Excel where the results are not treated. In this test, the Excel results were used to allow an analysis more detailed to the Reflow thermal cycle of each thermocouple. However, the Excel results cannot be used directly, necessitating to be treated by the user. It happens because the thermocouples do not enter the Reflow oven at same time, due its relative position in the product tested. In this way, it is necessary to eliminate the time difference between all thermocouples thermal cycle. This is a process that needs some experience from the user to identify correctly the time leg of each thermocouple in the product tested.

Finally, the treated Excel results can be presented in different forms, as graphics, which it facilitates the results analysis.

Chapter 4

Test Cases

In this chapter, the cases of study that originated the simulation models, the reasons for its study, the objectives of its realization, the simulation domains and its initial state, the properties of materials and other important variables, and the results expected, will be presented.

First, it is presented a summary of the work done by Costa (2014), since this thesis is a continuation of that work. In particular it is presented his last model, where it is simulated the melting of solder paste in the presence of a component, as this model will be used as starting point and at same time as the reference case of this thesis.

This model was tested and a problem with the deformation of solder paste at room temperature was found. To solve the problem two strategies are followed, since the first was not capable of solving the problem. In the second strategy, the impact of Mushy-zone parameter and surface tension are studied. This strategy allowed to solve the problem and to create a new model with a new Mushy-zone parameter and with a surface tension variable.

The new model is then improved to simulate a simplified Reflow thermal cycle taking into in consideration the melting and solidification of solder paste.

During the internship at Bosch Car Multimedia, other case of study was treated involving the thermal simulation of a real product and the confirmation of the simulation results with a practical test in the production line.

4.1 Reference Model

Since this thesis is a continuation of the work done by Costa [34], at this point, a summary of the work previously done will be presented.

Costa (2014) starts by replicate an example of the literature in order to validate his model and to understand the interaction of the different models used by ANSYS Fluent, such as the VOF model, the Solidification/Melting model, and the heat transfer model. This example was at same time the basis for other cases of study, where the material to be melted was changed. Starting with water, once it is a material with a behavior well known, the model could be validate. Then, Tin was used, once it is a material with properties near to the solder paste (about 95% of its constitution is Tin) used in the industry. Finally, it was used solder paste, SAC 405, since this is the material used in the Reflow soldering process, by Bosch Car Multimedia.

After the change of the processing material, other variables were studied such as the solder paste melting enthalpy, surface tension, and contact angles. The increase of melting enthalpy, it increases only the time needed to occur the transition between the solid and liquid state of solder paste, however it has the same qualitative behavior. The contact angle, between the solder paste and the pad, was obtained by experimental test in lab. To determine the surface tension of the solder paste, the experimental test was simulated in ANSYS Fluent, in the same conditions, where the unique variable unknown was the surface tension. In this way, it was possible by trial and error to find the correct surface tension of solder paste, comparing the geometry of solder paste after melting, in the simulation, with that obtained in the experimental test.

Finally, it is presented the reference case for this thesis and the last case of study in Costa's (2014) thesis. In this simulation, the main objective is to achieve a solder paste deformation equal or near the reality, in the presence of a copper pad and a component. The component is treated as a copper block, once the component connectors are in copper. In figure 4.1, the computational domain is presented.

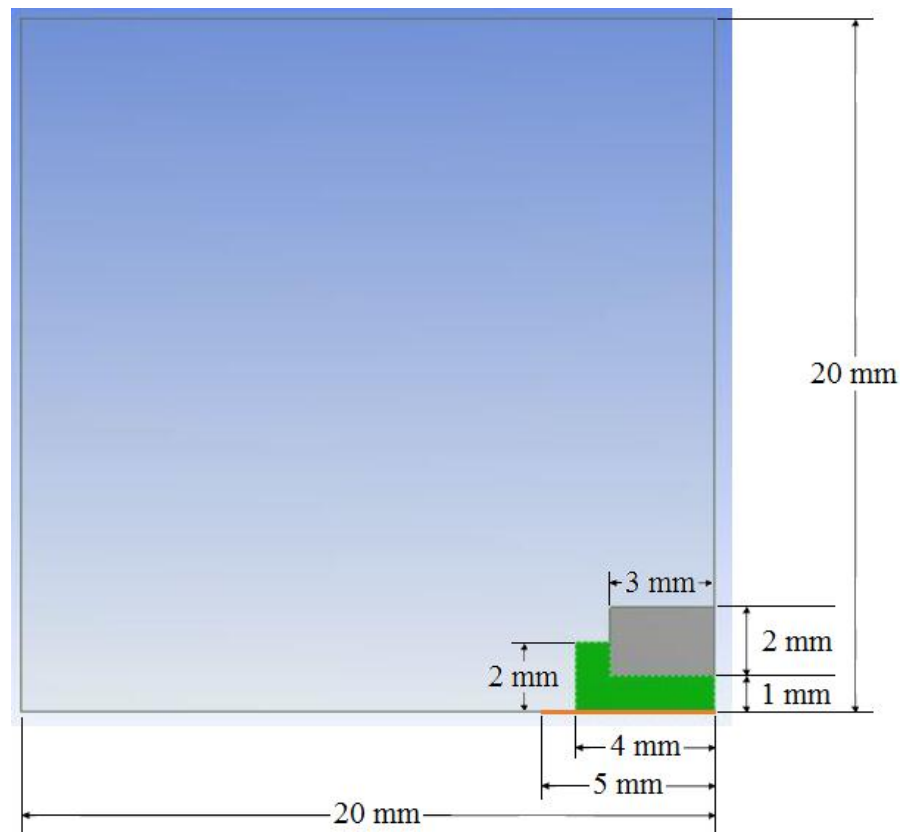


Figure 4.1 – Reference model simulation domain.

In figure 4.1, it is possible to observe the component in gray, the solder paste in green, and in the remaining simulation domain, the air, in blue. In order to represent the reality, in the best way possible, it was considered the component weight and the force exerted by the SMD component placement machine on the component on the solder paste. These two factors have a big influence in the solder paste geometry at the simulation initial state, by pressing the component onto the solder paste, slightly immersed, as it is shown in figure 4.1. It is also presented in the simulation domain, the copper pad in orange, and the PCB defined at left of the copper pad, in the remaining bottom line of the simulation domain.

The different materials properties used in this simulation are presented in table 4.1:

Table 4.1 – Material properties (Adapted from [34]).

Parameter	Symbol	Values	Units
<i>Air</i>			
Density	ρ_{ar}	1.225	[kg/m ³]
Specific heat	$c_{p,ar}$	1006.43	[J/(kg.K)]
Thermal	k_{ar}	0.0242	[W/(m.K)]

Parameter	Symbol	Values	Units
conductivity			
Viscosity	μ_{ar}	1.789×10^{-5}	[kg/(m.s)]
Copper			
Density	ρ_{cobre}	8978	[kg/m ³]
Thermal conductivity	k_{cobre}	387.6	[W/(m.K)]
Specific heat	$c_{p,cobre}$	381	[J/(kg.K)]
Alloy			
SAC405			
Density	ρ_{405}	$7640 - 9000 \times 10^{-4}T$	[kg/m ³]
Specific heat	$c_{p,405}$	236	[J/(kg.K)]
Thermal conductivity	k_{405}	62	[W/(m.K)]
Viscosity	μ_{405}	$0K - 490K \rightarrow 0.271$ $490K - 655K \rightarrow \text{Linear from } 0.271 \text{ to } 0.01148$ $655 - 1500K \rightarrow 0.01148$	[kg/(m.s)]
<i>Solidus</i>	T_s	490.15	[K]
<i>Liquidus</i>	T_l	498.15	[K]
Surface tension (defined for this case)	σ_{405}	0.75	[N/m]
Melting Enthalpy	L	59500	[J/kg]
PCB			
Density	ρ_{PCB}	1200	[kg/m ³]
Thermal conductivity	k_{PCB}	0.25	[W/(m.K)]
Specific heat	$c_{p,PCB}$	600	[J/(kg.K)]

The 2D simulation domain with 20 mm by 20 mm side, as it is shown in table 4.1, is constituted by four materials: a) air, b) copper, c) solder paste, and d) PCB. The heat source is the copper pad,

which is set at a constant temperature equal to 503 K, and the initial temperature is 300 K, for the entire domain. The gravity force is considered as well as the surface tension of 0.75 N/m and the adhesion. The contact angles are also taken into account, being defined by experimental tests. These tests resulted in a contact angle between the solder paste and the copper of 30° and between the solder paste and the PCB of 90°.

Other properties, such as the density and viscosity of solder paste, were defined as function of temperature, in order to take into account the changes in the properties of solder paste, during the heating process and phase change. These functions were however simplified and considered linear. It was defined too, the solder paste *Solidus* and *Liquidus* temperature, once it is an alloy and instead of having a constant melting temperature, as pure metals do, it has an interval of melting temperatures. During this temperature interval, the solder paste is in a mix of solid and liquid phase, named mushy-zone.

Once all parameters are defined, the simulation begins with the heat flux being transferred by conduction, from the copper pad to the solder paste and then to the component, and by natural convection, to the air. It is important to note that this simulation does not represent entirely the Reflow soldering process, where the heat source often comes from the air, in a process of heat transfer by forced convection. However, this simulation was developed with the objective of study the solder paste deformation, which it is not affected by the heat source; so this simplification was done in order to reduce the time of simulation, the problem complexity, and the computational memory needed.

4.2 Reference Model Test and Problem Found

After analyzing and understanding the reference model done by Costa (2014), that it is the start point for this thesis, it is time to test and to validate this model before trying to do something else.

With this objective in mind, and after looking for the solder paste deformation during the simulation, it is possible to see that the deformation occurs in places where the temperature is low and far of melting point. This may mean that the solder paste deformation occurs independently of temperature.

In order to check this possibility, a simulation equal to the reference case was done, with exception of heat source that was eliminated. This means that the simulation occurs without heat source and at room temperature. The main objective of this simulation is to check if there is solder

paste deformation at room temperature. If this happens, it is proven that there is a problem with the reference model, where the solder paste deformation is independently of temperature. Note that, it is expected that the solder paste deformation occurs only when its temperature is near of *Solidus* temperature, during the Mushy-zone, and at liquid phase. But, this is not expected at low temperatures and during the solid phase.

After to see the previous simulation results, it was confirmed that there is a deformation of solder paste independently of temperature. For this reason, four other simulations were realized, in order to verify the validity of solder paste geometry after its deformation. The four simulations are based in the reference model, however the heat source was eliminated and some changes were done to the simulation domain. First, a smaller copper pad with a normal and a high quantity of solder paste was considered. In the second, a bigger copper pad with a normal and a high quantity of solder paste was considered. The simulation domain for all simulations is represented in figure 4.2.

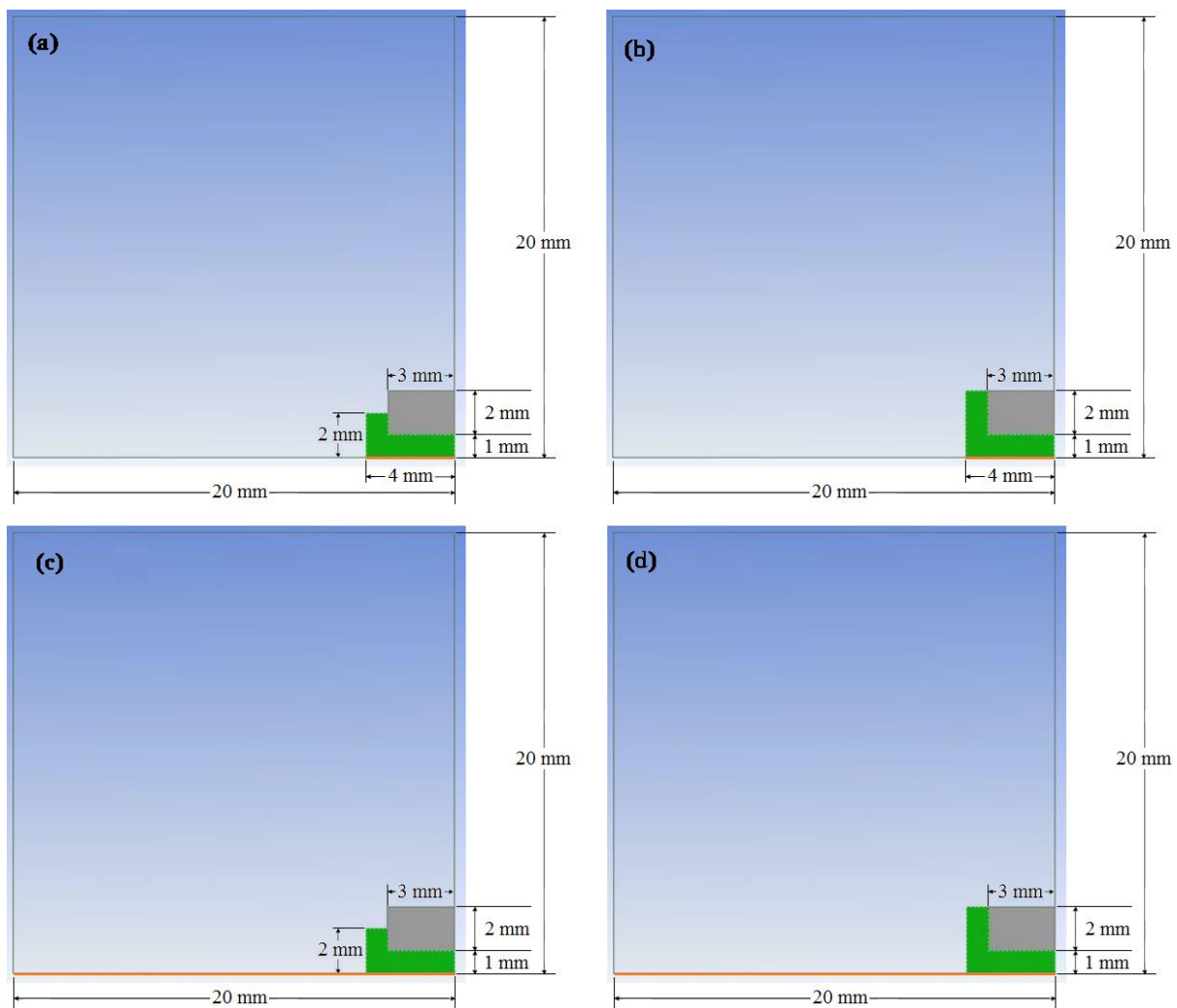


Figure 4.2 – Simulation domain with a small copper pad and a normal quantity of solder paste (a) and with a high quantity of solder paste (b). Simulation domain with a big copper pad and a normal quantity of solder paste (c) and with a high quantity of solder paste (d).

The objective of all simulations is to check if the solder paste deformation occurs according to reality. In the simulation (a) and (b), it is expected that the solder paste presents a resistance in wetting the PCB, so the solder paste, after deformation, should present a concavity turned outwards. Contrarily, in the simulation (c) and (d), it is expected that the solder paste has a good wetting, resulting in a solder paste concavity turned inwards. If the predicted for all simulations do not happen it means that there is other problem with the reference model.

4.3 Influence of some Variables in the Solder Paste Deformation

As it is possible to see in the next chapter, where it is shown the study cases results, the reference case presents a problem related with the solder paste deformation at room temperature. With the objective of to solve this problem, a strategy was defined that it passes by the analysis of some variables that may have some influence in the solder paste deformation.

The first variable analyzed was the solder paste density. Two simulations were realized in order to check the influence of this solder paste property in its deformation at room temperature. It was considered a density increase of 10 and 100 times, relatively to the reference case. Once the solder paste with a higher density has more weight per unity of volume, it is expected that the density increase speed up the solder paste deformation.

The second variable analyzed was the solder paste viscosity. To check its influence in the solder paste deformation, two simulations considering a viscosity increase of 10 and 100 times, relatively to the reference case were made. It is expected that the viscosity increase slow down the solder paste deformation at room temperature.

The third variable analyzed was the surface tension. Again, in order to understand the influence of this solder paste property in its deformation at room temperature, two simulations considering a surface tension increase of 10 and 100 times were made. Once the surface tension is a force that it maintains the solder paste cohesion, it is expected that the surface tension increase speed up the solder paste deformation.

The last variable analyzed was the gravity absence. This it is not a solder paste property as the previous, but the gravity is a force that it pulls the solder paste down, which may cause the deformation observed at room temperature. Thus, it is expected that the gravity absence slow down the solder paste deformation.

The first three variables were chosen, because they are the unique solder paste properties that could influence its deformation. However, three forces are exerted in the solder paste, gravity, surface tension, and adhesion. These forces may cause the deformation observed, the surface tension was already analyzed, the adhesion force cannot be changed in ANSYS Fluent, so only it is possible to analyze the effect of the gravity absence. It was for this reason that it was chosen.

After analyzing the previous variables, two more situations were defined to simulate. These situations pass by conjugate the results obtained from the previous variables, with others variables, as the contact angles. These simulations were realized with the objective of find a solution for the solder paste deformation at room temperature.

4.4 Influence of Mushy-zone Parameter in the Solder Paste Deformation

The first attempt to solve the problem with the solder paste deformation at room temperature it was not successful, as it is possible to see in the results chapter. Thus, it is necessary think in a new approach to solve the problem. However, the analysis of some variables showed that the surface tension is the unique variable that it has a significant impact in solder paste deformation, at room temperature. But, it is not enough.

By analyzing the models used by ANSYS fluent, specifically the Solidification/Melting model, it was found the Mushy-zone parameter that may solve the problem.

In the Solidification/Melting model, when a material solidifies the liquid phase has a velocity and this velocity decreases as the material solidifies. However, the fall of velocity it is not instantaneous. This means that there is some velocity in the solid phase near the interface with the liquid phase.

In the reference case, at room temperature, the Solidification/Melting model treats the air as a liquid and the solder paste as a solid. This means that there is an interface between liquid and solid phases, and the respective gradual fall of velocity between the phases.

The Mushy-zone parameter is a constant that it is part of the momentum equation in the Solidification/Melting model. This constant defines the amplitude of velocity damping, as the higher the value, the faster is the decrease of material velocity while solidifies [42].

With all this in mind, the Mushy-zone parameter increase seems to be a good approach, in order to stop the solder paste deformation, at room temperature. The Mushy-zone parameter, recommended by ANSYS Fluent, it is between 10^4 and 10^7 , and the default it is 10^5 . Note that all cases of study

previously analyzed were performed with a default Mushy-zone parameter of 10^5 . To test this theory, two simulations were accomplished, based in the reference model, first with a Mushy-zone parameter of 10^7 , and second with a Mushy-zone parameter of 10^8 .

Due the results obtained, it was considered more two simulations based in the previous simulations, but considering the surface tension of 0 N/m, due to the results obtained in the analysis at the influence of surface tension in the deformation of solder paste, at room temperature. These simulations were performed without heat source and at room temperature, with the objective of find a solution for the solder paste deformation at room temperature.

4.5 Solution and Validation

After the second attempt to solve the problem of solder paste deformation, at room temperature, it was finally found a solution. This solution passes by changing, relatively to the reference model, the Mushy-zone parameter from 10^5 to 10^8 , and the surface tension from 0.75 N/m to 0 N/m at the solid state of solder paste. However, the surface tension remains 0.75 N/m for temperatures higher than *Solidus* temperature, to achieve a solder paste behavior near to the reality for solid and liquid phase.

To describe the surface tension variation of solder paste as function of temperature, a piecewise-linear function was created, which is presented in figure 4.3. Since the solder paste cannot have for the same temperature two different surface tensions, it was created a surface tension linear variation near the *Solidus* temperature, from which the solder paste begins to melt.

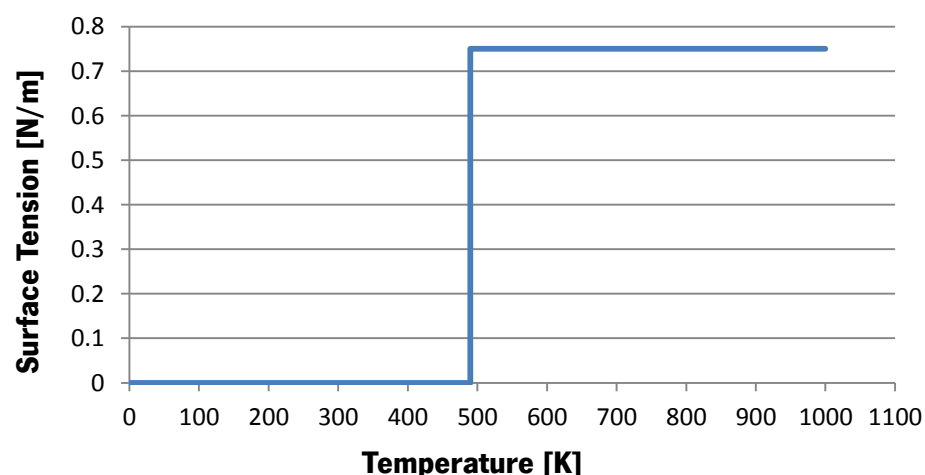


Figure 4.3 – Surface tension variation function of temperature.

The simulation with the new model was accomplished for all range of temperatures, from room temperature to 503 K. The solder paste deformation was then analyzed in order to confirm if its behavior is the correct at solid and liquid state.

4.6 Thermal Cycle

With the new model working well, during the heating of solder paste until liquid phase, and with the deformation problem of solder paste corrected, at room temperature, it is time to try simulate the complete thermal cycle of Reflow soldering process. This means heating the solder paste from room temperature until a temperature higher than *Liquidus* temperature; maintaining the temperature above *Liquidus* temperature until the solder paste melts completely, and then cooling down until room temperature.

The real thermal cycle of Reflow soldering process is more complex than the one presented below. As explained in Chapter 2, it is very important to define carefully and with precision the temperature and time of each phase of Reflow thermal cycle, in order to achieve a good soldering process.

However, the real thermal cycle is too long to be simulated, having a real duration of 350 s. This means that it is needed two or three weeks to simulate the real thermal cycle, needing about two hours of simulation for each second of real time.

In order to overtake this difficulty, the thermal cycle was simplified, allowing obtaining a model with a shorter time of simulation. This thermal cycle used in the present work is presented in figure 4.4.

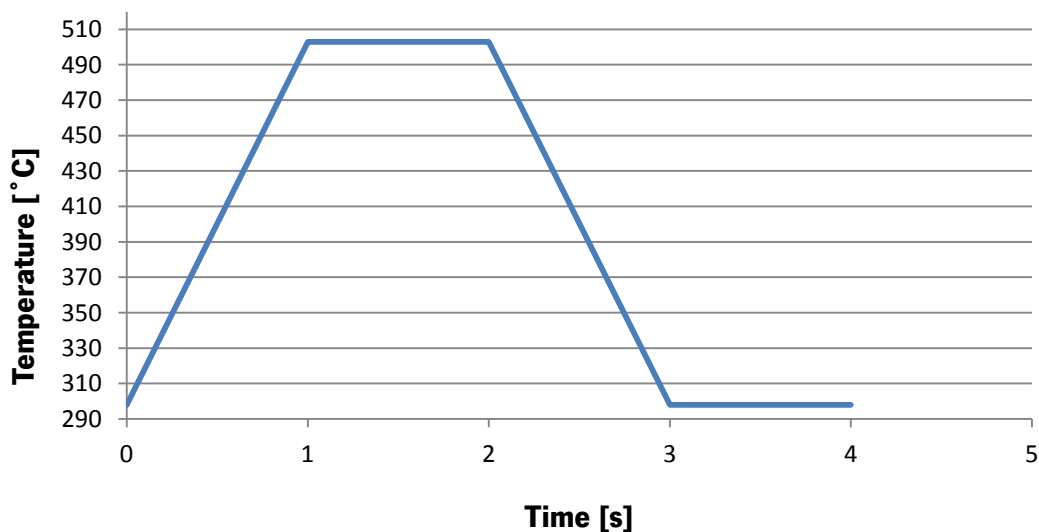


Figure 4.4 – Simplified Reflow thermal cycle, used in the simulation.

In order to create this thermal cycle, it was necessary to use a UDF. With this user defined function, it is now possible to simulate any Reflow thermal cycle simply changing the settings of time and temperature in the UDF, to correspond to the desired Reflow thermal cycle.

Although this thermal cycle is much simpler than the real, this was considered good enough to represent the real Reflow soldering process, with the objective of analyzing the solder paste deformation during the entire soldering process.

This thermal cycle was applied to the previous model copper pad, with a Mushy-zone parameter of 10^8 and a surface tension as a function of temperature.

4.7 Study Case at Bosch

During the internship at Bosch Car Multimedia, the work done had the main objective of to analyze the possibility of producing real products successfully and without using nitrogen (N_2) in the Reflow soldering process.

In order to accomplish this study, it was chosen a product to be produced with and without N_2 , in the Reflow soldering process. After its production, the products were analyzed to check if there are differences between both processes of production and its impact in the soldering process quality.

The product chosen suffered two soldering processes: the Reflow soldering process, and the Wave soldering process. Between the two soldering processes were even inserted radial components and SMD components, in the PCB face B. The product is also produced in *nutzens* of two products per *nutzen*.

During the analysis of data, provided by the automatic optical inspection (AOI), in the Reflow line, it was possible to verify an abnormal situation. In one specific component, it was observed a significant difference in the average number of AOI pseudo-errors, for both products of the same *nutzen*. They were produced about 60 *nutzens* of this product, with and without N_2 , resulting in the average of AOI pseudo-errors, for this specific component, as it presented in figure 4.5.

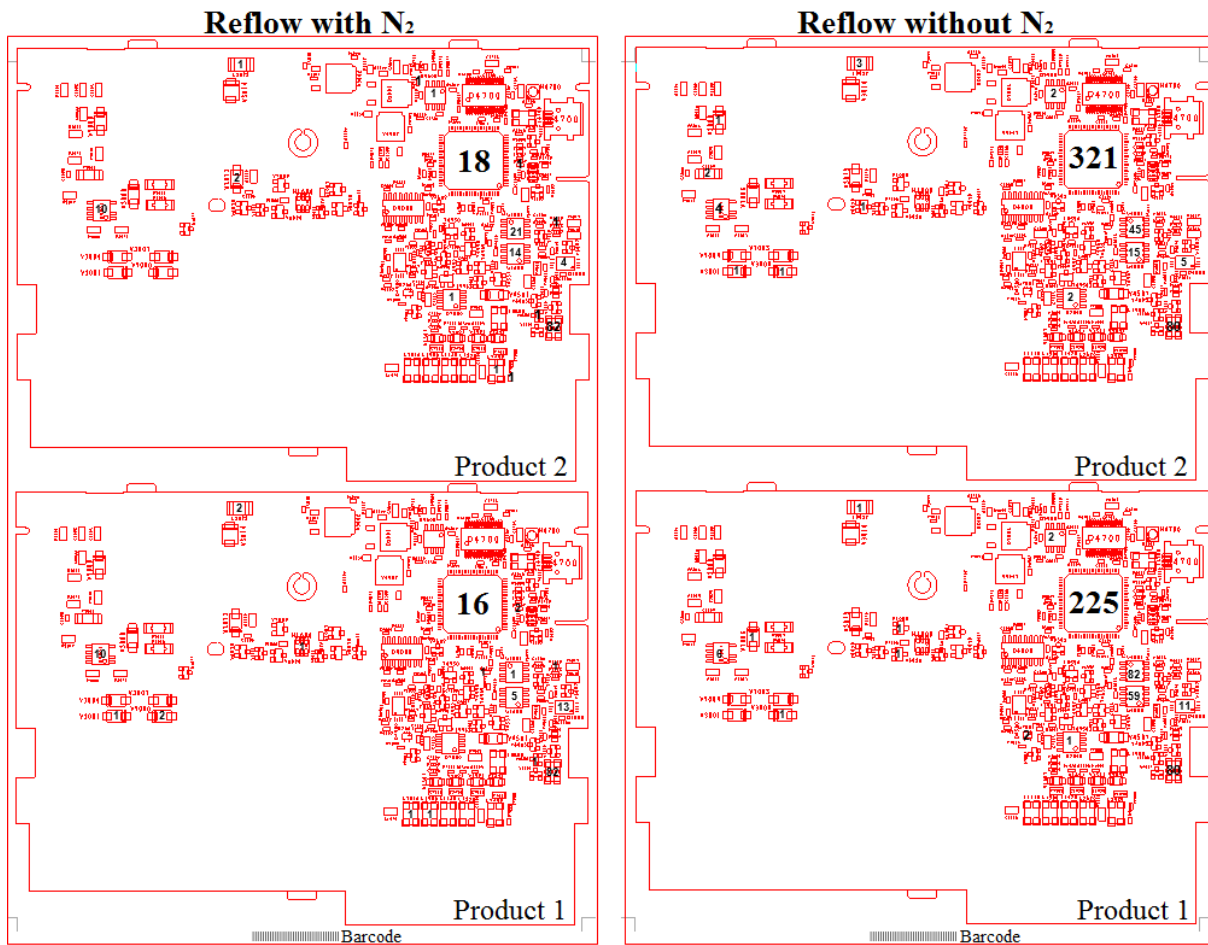


Figure 4.5 – Average of AOI pseudo-errors per component, in the Reflow soldering process with and without N_2 .

The difference in the average number of AOI pseudo-errors observed between the *nutzens* produced with N_2 and without N_2 is normal and expected, due the difference of atmosphere used during the Reflow soldering process. However, the difference observed between the two products of the same *nutzen*, principally in the *nutzens* produced without N_2 , it is difficult to explain, since the production process is the same.

Thus, a possible explanation emerged that may justify the difference in AOI pseudo-errors observed for the same *nutzen*. This explanation may be the difference of temperature between the two components, during the Reflow soldering process, due to their different locations relatively to the *nutzen*.

To confirm this assumption, a numerical simulation of the product produced was done. The computational program used was the 6SigmaET, because it is the program used at Bosch Car Multimedia to make this kind of simulations.

The product drawing is imported to the 6SigmaET directly from its *gerber* (technical drawing of the entire product), as it is presented in figure 4.6, for the product produced at Bosch. This drawing

was used by the 6SigmaET to simulate the real product during the Reflow soldering process, and as it is possible to observe all components are simulated as well as the PCB with the copper layers and the electrical circuits, with an impressive detail.

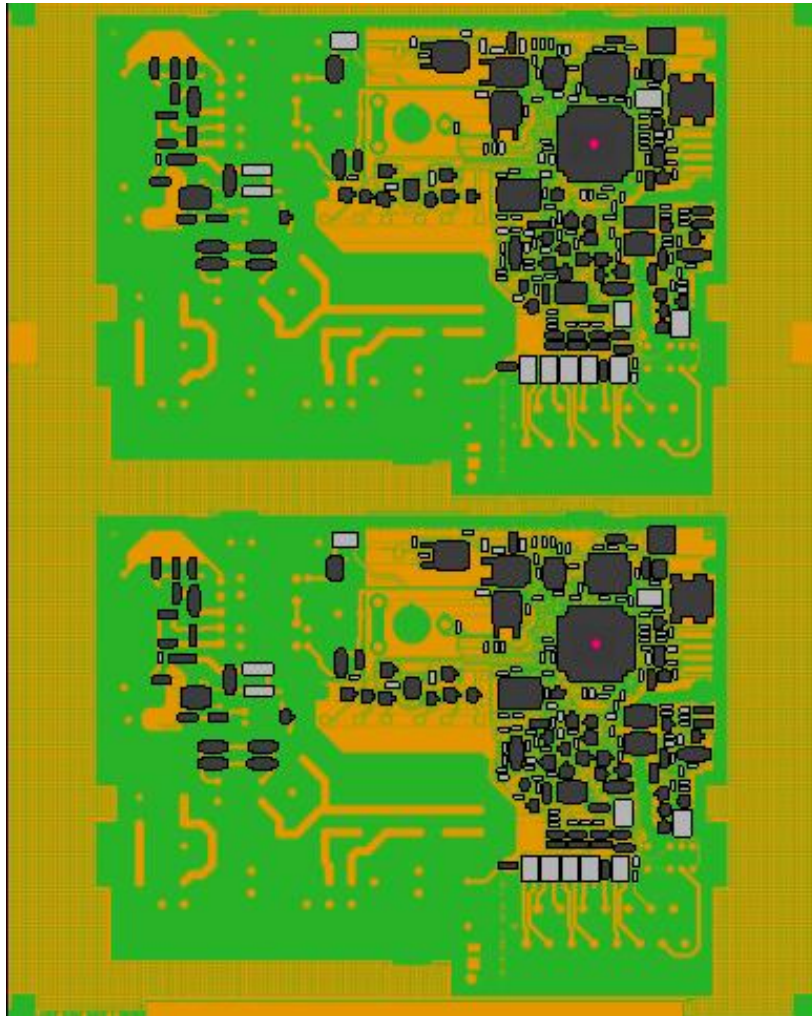


Figure 4.6 – Product to be simulated with the 6SigmaET.

Contrarily to the ANSYS Fluent, where until now the heating source is the copper pad and the heat passes to the product by conduction, in the 6SigmaET, a section of the Reflow oven is simulated and the air flow around the product, as it is presented in figure 4.7. This it allows to have a simulation model much closer to the reality, with the heat being transferred from the air to the product by forced convection, as it happens in the real process.

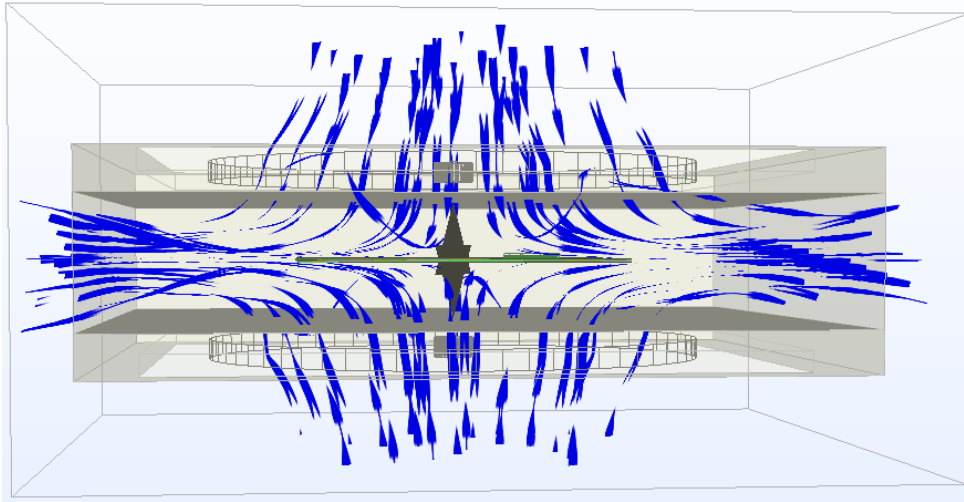


Figure 4.7 – Simulation domain of the program 6SigmaET.

In the real process of reflow, the product passes inside the Reflow oven and through different phases of heating and cooling. In the simulation process, with the computational program 6SigmaET, as there is only one section of the Reflow oven and the product stands still, it is changed the air temperature, in order to simulate each phase of the real process. The number of phases, the temperature, and the time of each phase, are defined by the real Reflow thermal cycle, and this it is simply inserted in the simulation model. In this simulation, the thermal cycle presented in figure 4.8 is used.

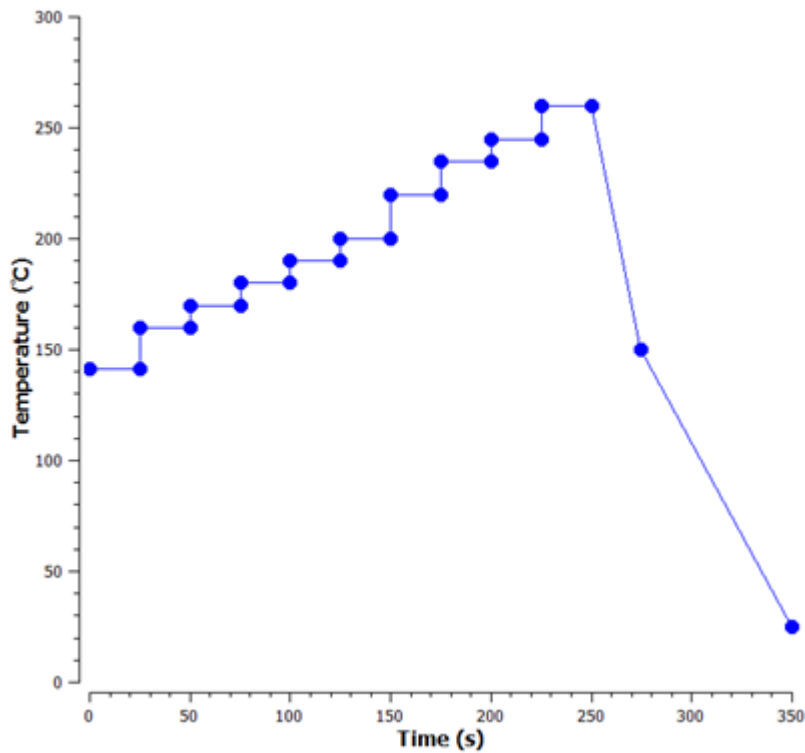


Figure 4.8 – Thermal cycle of the Reflow oven used to produce the product in analysis and perform the simulation.

In order to obtain the temperature of the components in analysis, a thermocouple in each component of the *nutzen*, was placed as it is represented by the red points in figure 4.6.

Experimental test in the production line

After the simulation and knowing the results, it was necessary to confirm them, since the temperature difference of between the components is small. This will allow at the same time to measure the simulation model accuracy.

This confirmation was done with a real product, where four thermocouples were installed to read the temperature in the real Reflow soldering process. It was installed a thermocouple in each component body, as in the simulation model, and an additional thermocouple in each component solder joint, since that it is the difference of temperature in these points that may justify the difference in the number of Reflow AOI pseudo-errors, for the same *nutzen*. The thermocouples layout in the product to be tested is presented in figure 4.9.

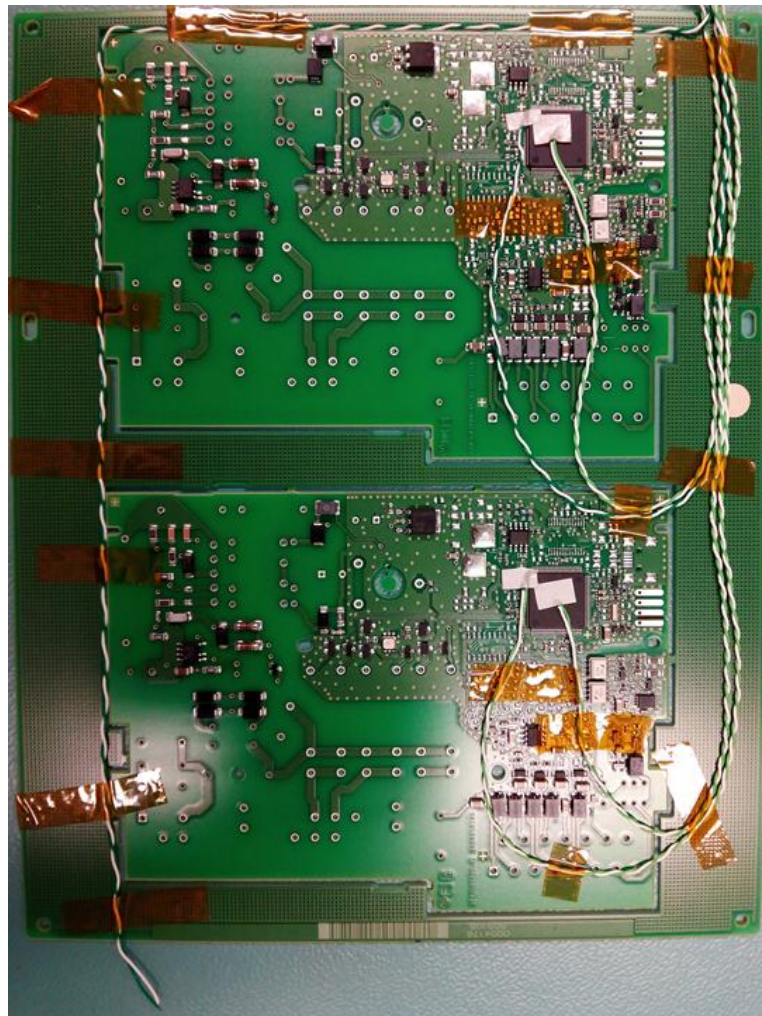


Figure 4.9 – Real product with thermocouples installed.

The product, shown in figure 4.9, is then inserted in the Reflow and the thermal cycle of each thermocouple installed recorded. However, the Reflow oven used to do this test was a different oven that the used to produce this product in first place. While the Reflow oven used to produce this product has 10 heating phases, the Reflow oven used to make this test has only 7 heating phases. In this way, the heating phases of both Reflow ovens need to be different and carefully defined, as well as the velocity of the production line, to ensure that the product has the same thermal cycle in both Reflow ovens and that it is in compliance with the Bosch Car Multimedia requirements. This change of Reflow oven happens because at the time of this test, this it was the only oven where the product in analysis was being produced.

As conclusion, it is possible to say that the two Reflow ovens are equivalent from the point of view of the product, and in this way, the Reflow oven used in this test does not will have influence in the results. The thermal cycle of the Reflow oven used in this test it is presented in figure 4.10, and the results are presented in the next chapter.

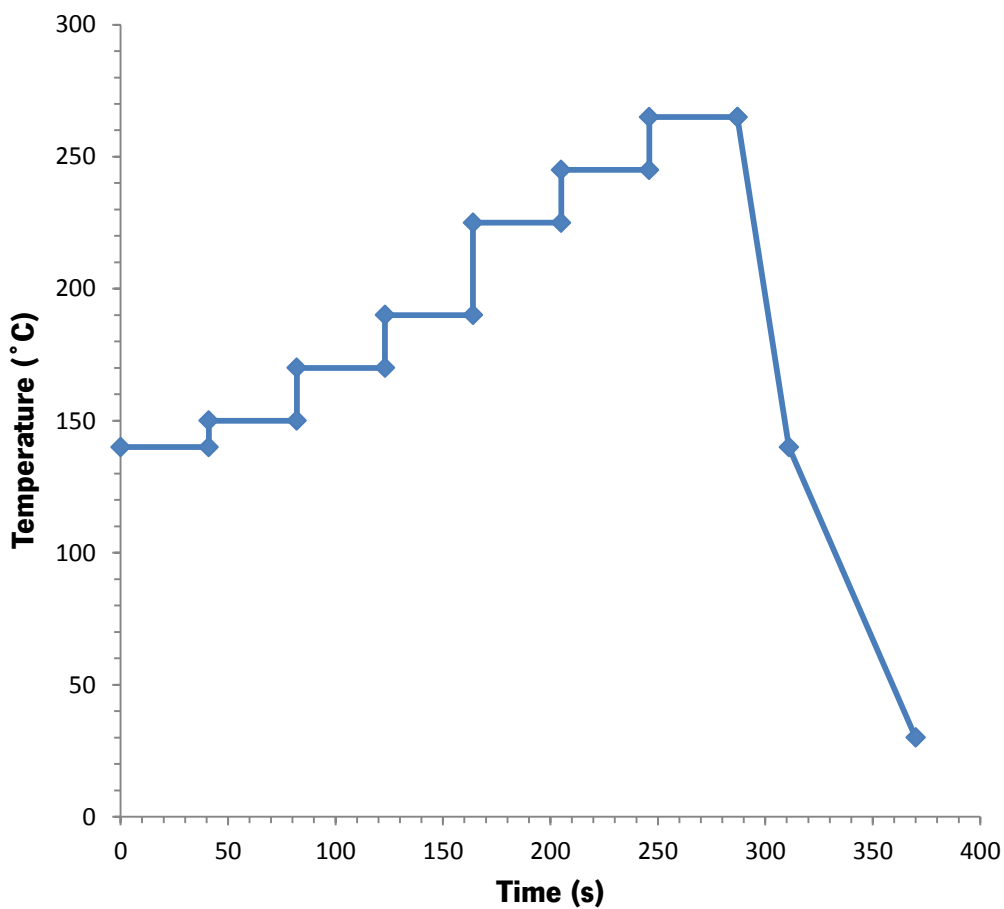


Figure 4.10 – Thermal cycle of the Reflow oven used to test the product in analysis.

Results and Discussion

During this chapter, the results obtained for all simulations realized will be presented and discussed the reasons that may be the explanation for these results.

First, the results achieved by Costa (2014) for its last model are presented, which will be used in this thesis as the reference model, where the melting of solder paste is simulated in the presence of a component. It is also introduced a new variable, Beta, which it has a great importance in the presentation of simulations results.

Next, the tests results done to the reference case are presented, which it allowed to find the problem with the deformation of solder paste at room temperature. The first strategy to solve the problem was not successful. In this way, a second strategy was followed in order to solve the problem, and this time, a solution was found.

The new model is then tested until the melting of solder paste and the results are compared with the reference case to prove that the problem is solved. This model is even improved to simulate a Reflow thermal cycle that includes the melting and solidification of solder paste and the results are analyzed with the objective to confirm that the solder paste has a deformation according to reality.

Relatively to the study case realized at Bosch Car Multimedia, the simulation results of a real product are presented as well as the experimental test results realized in the production line. Both results are then compared.

5.1 Reference Model

In this point it is presented the results of the last simulation model done by Costa (2014) with the objective of analyze the solder paste deformation in the presence of a component. This model is also the reference model and the start point for this thesis.

The initial state of this simulation is presented in figure 5.1. It is possible to identify the Beta variable that it represents the three possible phases that can be found in the simulation domain.

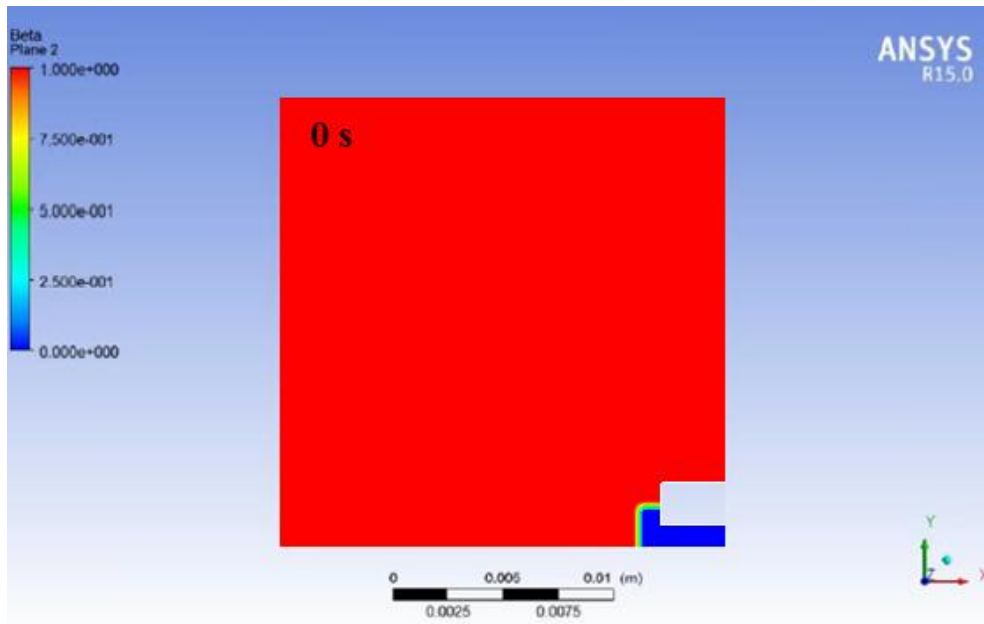


Figure 5.1 – Initial state of simulation.

Note that during the simulation, three phases will be present in the simulation domain, air, solder paste in solid state, and solder paste in liquid state. However, these three phases cannot be observed in the same image with the standard variables available in ANSYS Fluent. The VOF model introduces the primary phase volume fraction (α) that it distinguishes only the air of solder paste, independently of its phase. The Solidification/Melting model introduces the liquid fraction (β) that it distinguishes only the solder paste in solid state of the solder paste in liquid state and air, note that this variable cannot distinguish the solder paste in liquid state of the air.

However, a new variable was created to represent the three phases at same time, taking into account both variables mentioned previously. The new variable, named “Beta”, has the following formulation:

$$Beta = \frac{(\alpha + \beta)}{2} \quad (16)$$

The variable Beta can have any value between 0 and 1, and its value identifies the different phases present in the simulation domain. When Beta has the value of 0 it represents solder paste in solid state. Any value of Beta between 0 and 0.5, it represents solder paste in the Mushy-zone, in other words, it represents solder paste with a temperature between *Solidus* and *Liquidus* temperature. When Beta has the value of 0.5 it represents solder paste in liquid state. Any value of Beta between 0.5 and 1 it represents the control volumes in the interface between the solder paste and the air, where the control volumes contain air and solder paste in liquid state. Finally, when Beta has the value of 1 it represents the air.

In figure 5.2, it is possible to observe the deformation of solder paste in liquid state after the simulation. The solder paste wetting is good, as it is proven by the solder paste ascendant movement in the component left face.

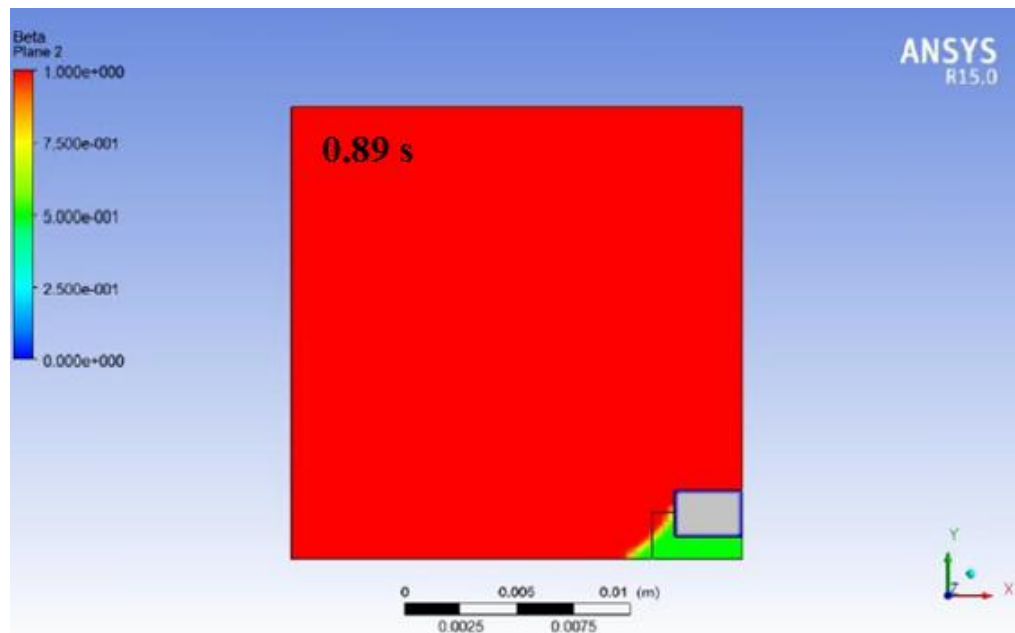


Figure 5.2 – Liquid solder paste deformation in the presence of a component (Adapted from [34]).

This happens due the three factors that combined result in the ascendant movement of solder paste. First the surface tension that maintains the solder paste cohesion. Second the solder paste achieves the interface between the copper pad and the PCB, which it is proven by the contact angle of 90° observed in the solder paste in this position. This fact creates a resistance to the solder paste spread, which contributes to the ascendant movement of solder paste in the component left face. Third the adhesion, between the solder paste and the component, which allows the climb of solder paste to the component and its permanence attached to it.

The temperature along the simulation domain, as it is presented in figure 5.3, represents the temperature variation inside the domain of simulation in the same instant of time that the figure 5.2.

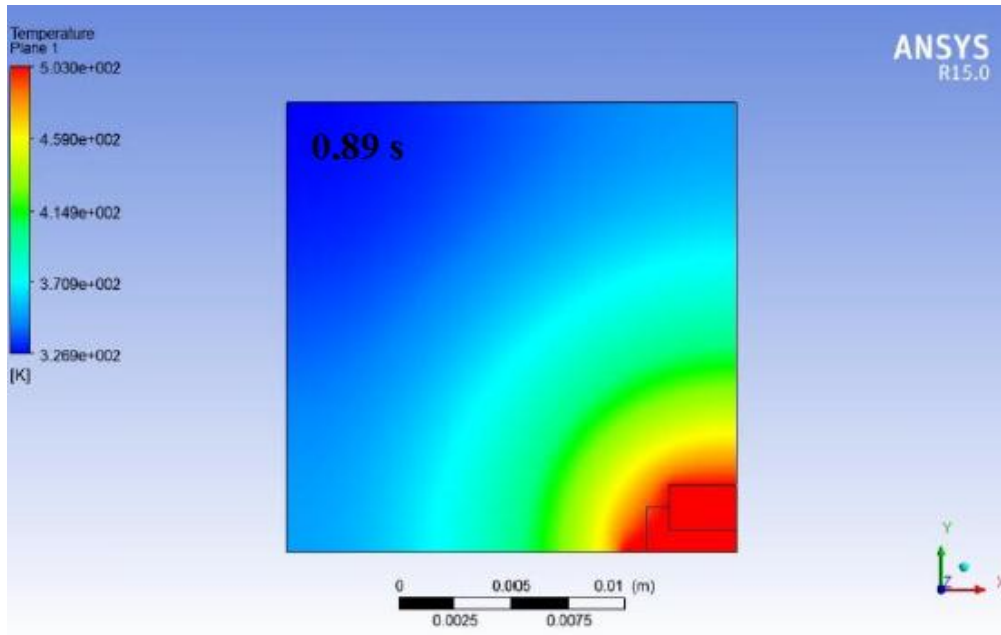


Figure 5.3 – Temperature variation in the simulation domain (Adapted from [34]).

5.2 Reference Model Test and Problem Found

Starting with the reference model and excluding the heat source, which it means run the simulation at room temperature, the result obtained is the presented in figure 5.4.

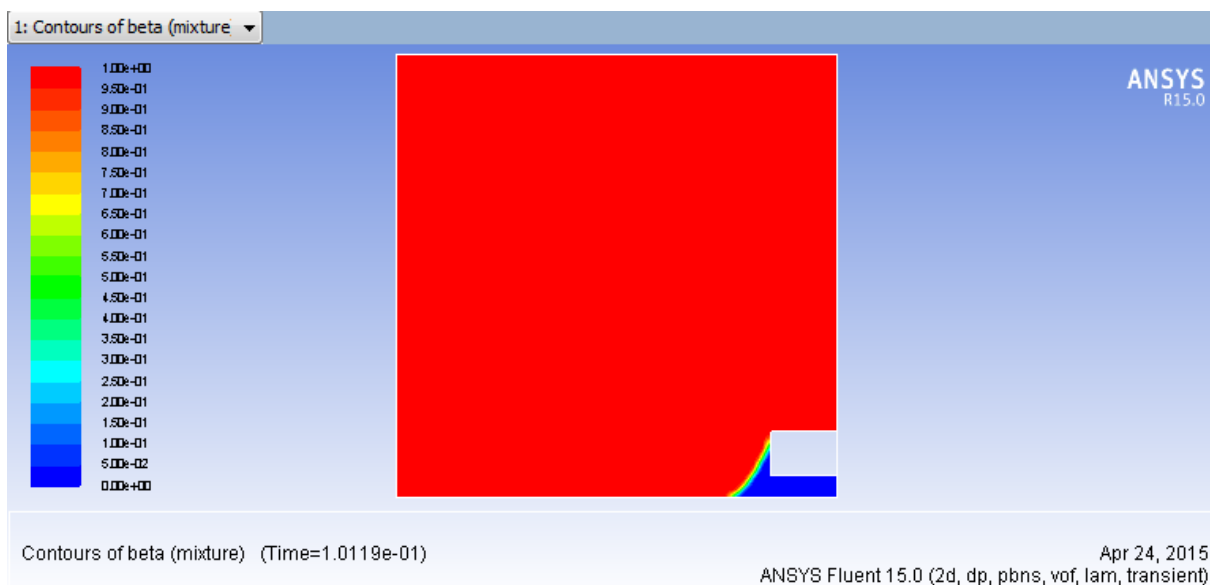


Figure 5.4 – Solder paste deformation at room temperature.

As it is possible to see in figure 5.4, the solder paste deformation happens even in solid state and at room temperature. This deformation is also fast, occurring in only 0.1 s of simulation. This

represents clearly a problem with the reference model, where contrarily to the expected the solder paste has a behavior independent of temperature.

After found this problem, it was defined more four situations to test the reference model, in order to check if the results provided by this model are according to reality. In other words, it was found a problem with the solder paste deformation at room temperature. However, it is necessary to verify if this deformation happens according to reality.

In the first situation, it was defined a short copper pad and a normal quantity of solder paste. The result of this simulation is presented in figure 5.5, and as it predicted in the previous chapter, it is possible to verify that the solder paste moves to above the PCB, since the contact angle is of 90° . It is also possible to affirm that the solder paste presents a resistance in wetting the PCB, since it reaches nearly the component top and it presents a curvature outwards, while in the reference model the curvature presented by the solder paste is inwards.

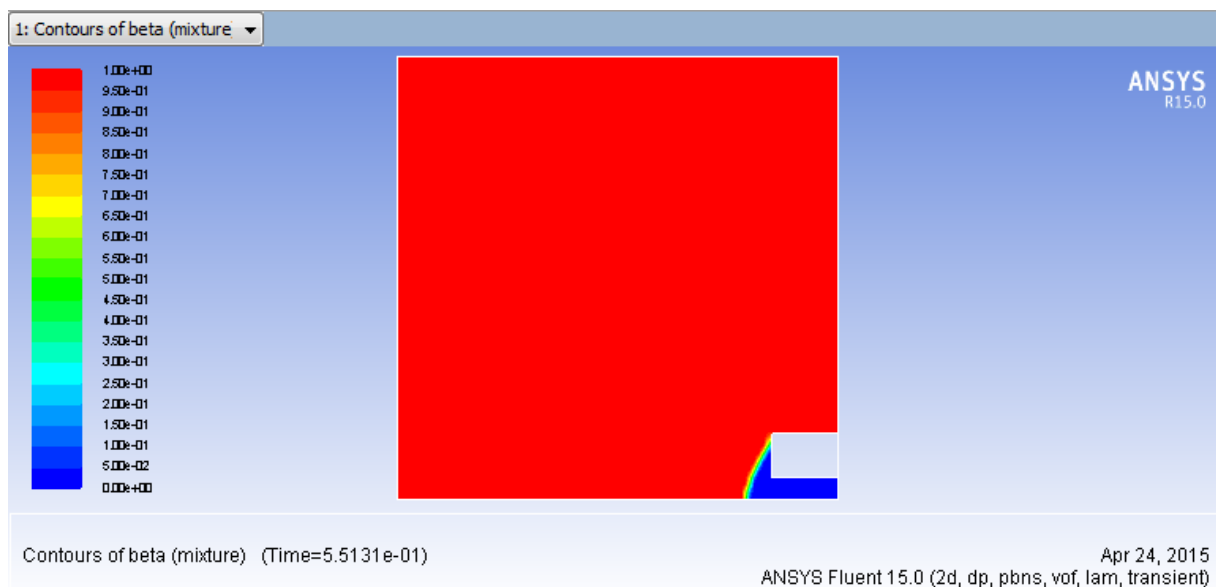


Figure 5.5 – Solder paste deformation with a shorter copper pad.

In the second situation, the amount of solder paste in the previous situation was increased. From the simulation result, as it is represented in figure 5.6, it is possible to observe that the solder paste moves a little more above the PCB, the solder paste reaches the component top, and the solder paste curvature outwards is now bigger than previously. This result confirms the resistance of solder paste in wetting the PCB.

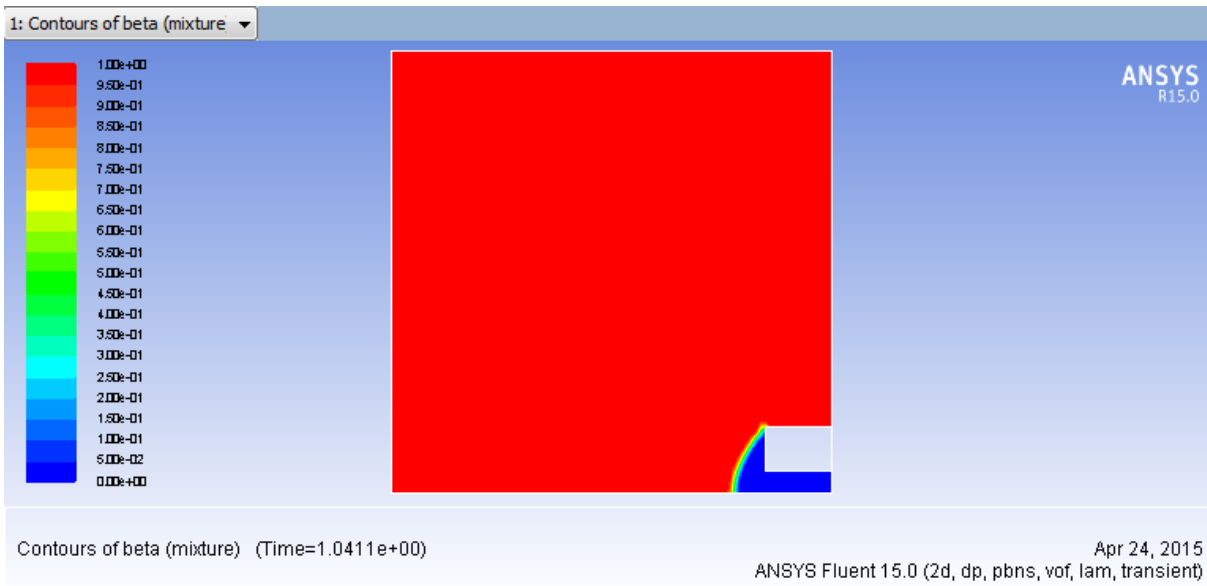


Figure 5.6 - Solder paste deformation with a shorter copper pad and with more solder paste.

In the third situation analyzed, the copper pad was increased and it has now the simulation domain bottom dimension. The solder paste content is the same that the used in the reference model. The result of this simulation is presented in the figure 5.7, where it is possible to see a solder paste deformation similar to the reference model. However, since in this case the solder paste does not have the restriction of copper pad end, the solder paste spreads more along the copper pad. At same time, due to the good spreading of solder paste, its concavity is turned inwards.

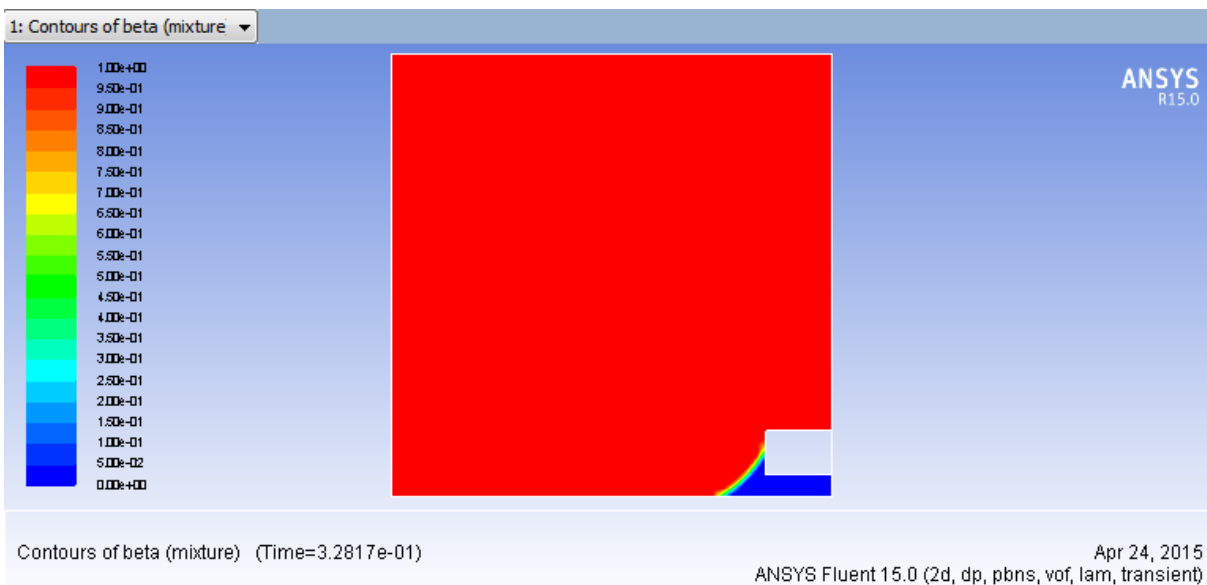


Figure 5.7 - Solder paste deformation with a bigger copper pad.

In the fourth situation, it was simply increased the amount of solder paste in relation to the previous situation. In the result of this simulation, as it is presented in figure 5.8, it is possible to

observe that due the increase of solder paste, it spreads more along the copper pad, comparing to the previous situation. The solder paste geometry, it is also similar to the previous situations, with the concavity turned inwards, due to the non-resistance to the solder paste spreading.

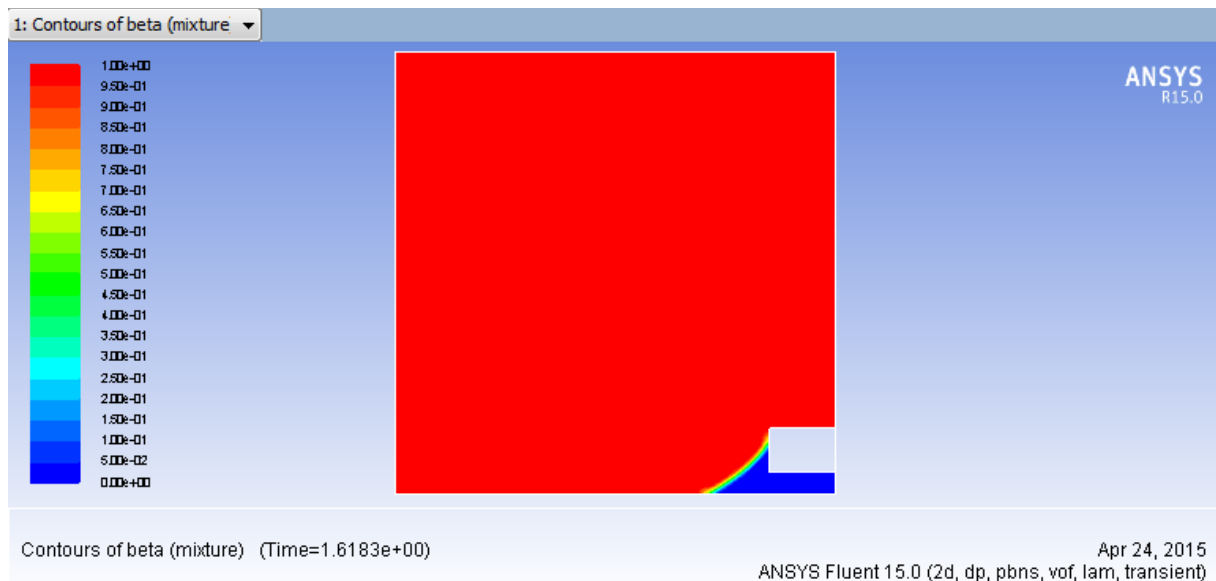


Figure 5.8 – Solder paste deformation with a bigger copper pad and with more solder paste.

After all the tests done to the reference model, it is possible to conclude that independently the solder paste deformation at room temperature, this deformation occurs according to reality, as it is proven by the last four situations of test, where the solder paste deformation occurred according to the predicted in Chapter 4. In this way, it is only necessary to correct the solder paste deformation at room temperature, since it is the unique problem found in the reference model.

5.3 Influence of some Variables in the Solder Paste Deformation

As mentioned in Chapter 4, the strategy defined to solve the problem with the solder paste deformation at room temperature, it passes by analyzing the effect of some variables that may have some influence in solder paste deformation at room temperature.

The first variable analyzed is the solder paste density. Considering the results shown in figure 5.9, it is possible to affirm that with the increased density, the solder paste has a slightly faster deformation at room temperature than in the reference model. In the simulation (b), with a density increase of 100 times, it is also possible to see the effects of solder paste weight that it overcomes the surface tension, adhesion and the resistance created by the PCB to the solder paste spreading, resulting in a deformation of solder paste that does not correspond to reality.

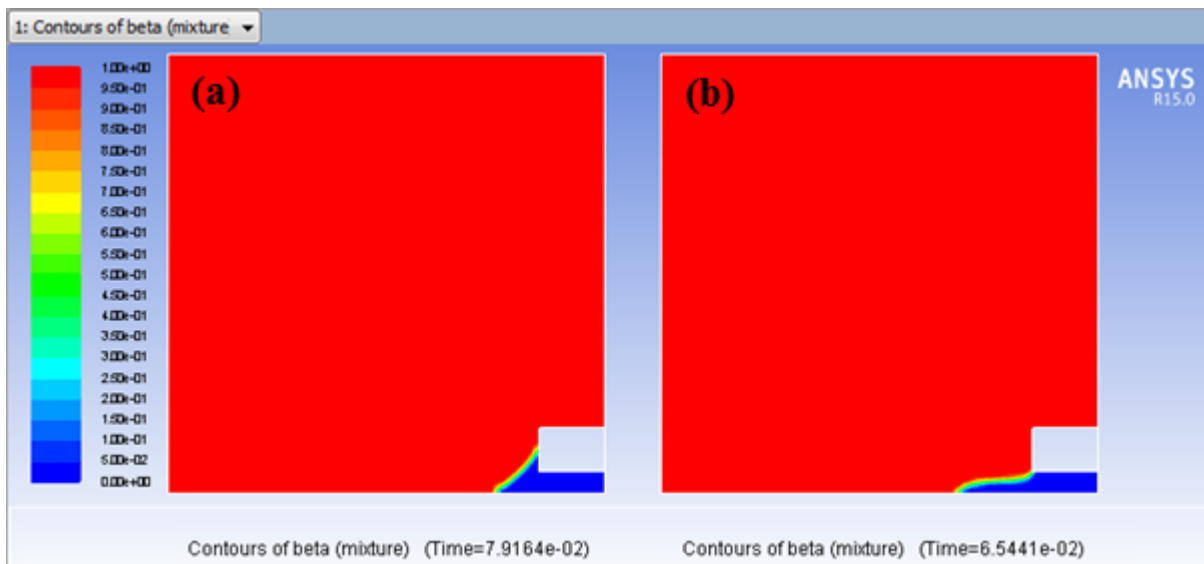


Figure 5.9 – Density increase of 10 times (a) and 100 times (b), relatively to the reference model.

Next, the solder paste viscosity was analyzed, and the results presented in figure 5.10. It is possible to see that with the increased solder paste viscosity, the time needed to occur the deformation of solder paste at room temperature increases considerably. However, in the situation (b), with an increased viscosity of 100 times, a instability in the concavity of solder paste is observed that does not happen in reality.

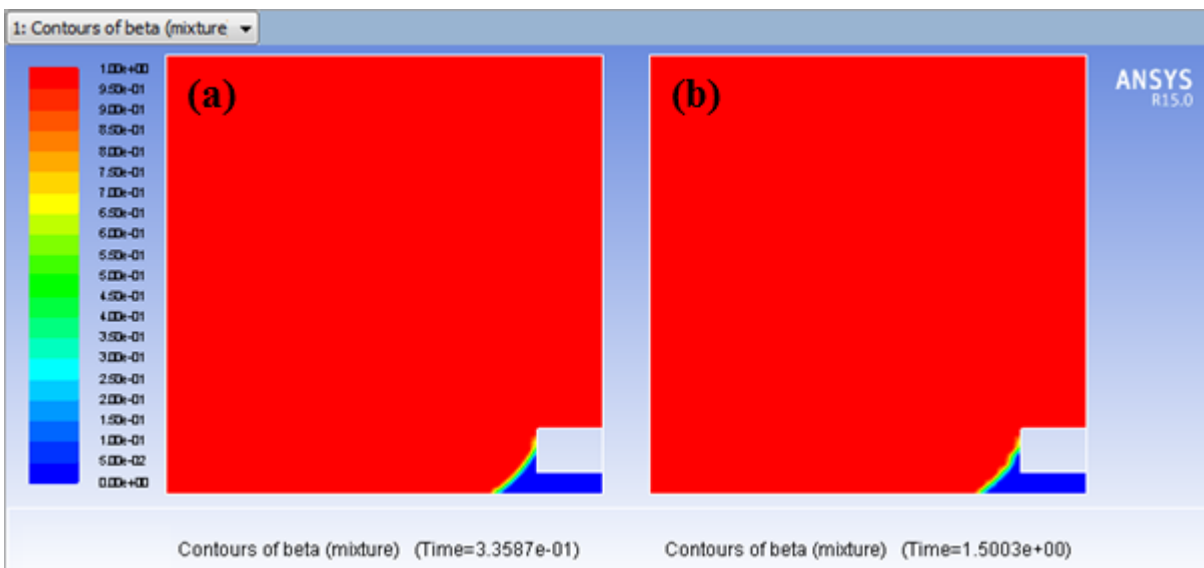


Figure 5.10 - Viscosity increase of 10 times (a) and 100 times (b), relatively to the reference model.

In figure 5.11, the results for the solder paste surface tension study are presented. Through the results presented, it is possible to affirm that due to the increase of the surface tension value, the time needed for the solder paste deformation at room temperature is now significantly less than in the reference model. This variable has in this way an important influence in the deformation of solder paste

at room temperature. This variable presents yet the advantage, unlike the previous variables, which does not influence the solder paste geometry relatively to the reference model. This it is very important because, as it was previously seen, the deformation of solder paste in the reference model happens according to reality. So, the solution to the solder paste deformation at room temperature needs to take into account that cannot change the solder paste geometry. Until now the surface tension seems to be the unique variable that may do that.

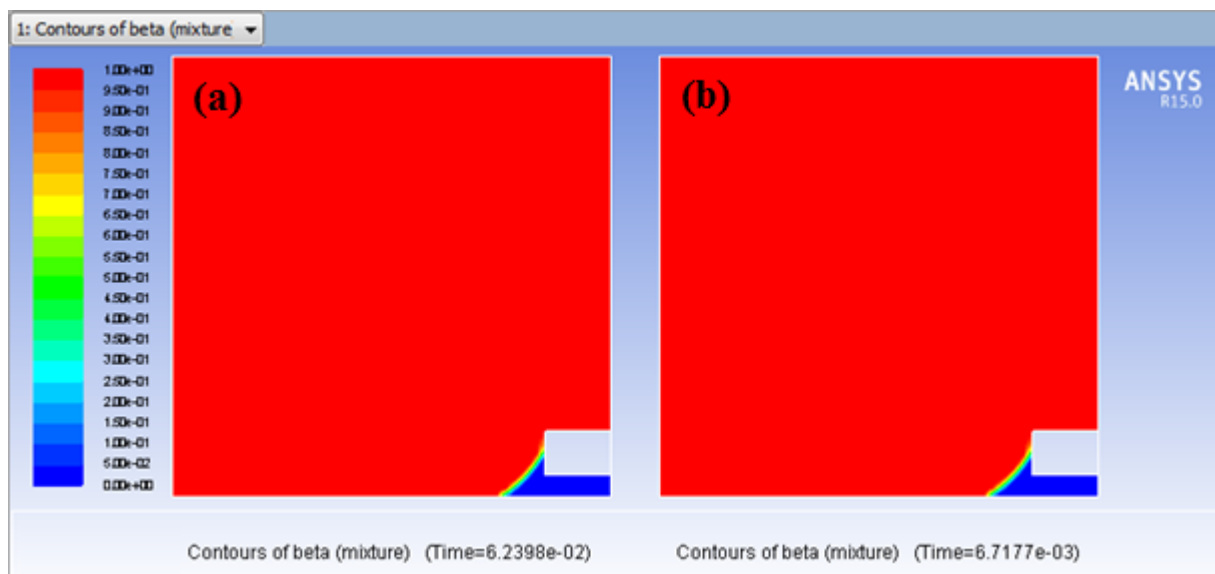


Figure 5.11 – Surface tension increase of 10 times (a) and 100 times (b), relatively to the reference model.

The gravity absence is the last situation of test. The result presented in figure 5.12, it shows that the gravity absence has a little influence in the time needed for the deformation of solder paste at room temperature. Due the absence of gravity force, it is also observed a lifting of solder paste in the component left face.

After analyzing the four situations, which initially it was thought that could stop the deformation of solder paste at room temperature, but without changing its geometry after deformation, comparing to the reference model. It became clear that the only variable able to do it, it is the solder paste surface tension. Until now, contrarily to the density and the viscosity that they are function of temperature, the surface tension is defined as a constant. However, this is not a good simplification, since all materials have a different surface tension depending of its temperature and principally of its phase.

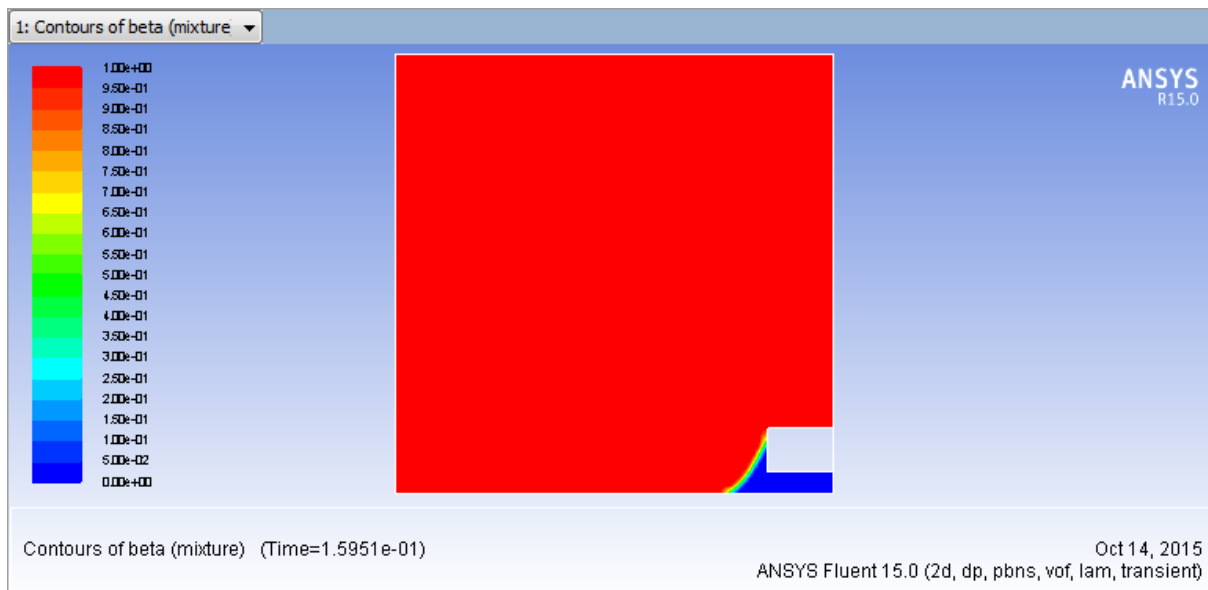


Figure 5.12 – Gravity absence.

5.3.1 Problem Correction First Attempt

With the results analysis of the previous variables in mind, a new situation to simulate, with the objective of try to stop the deformation of solder paste at room temperature was defined. In all simulations realized previously, it was clear that the solder paste deformation starts in the contact angles and then it propagates along the solder paste interface with the air.

In this way, it was realized a simulation with the solder paste surface tension equal to 0 N/m, at room temperature, and with the contact angles of 90°. The result of this simulation is presented in figure 5.13. As it is possible to see, this solution does not prevent the deformation of solder paste at room temperature. The surface tension has the function of to maintain the solder paste cohesion, when it is too high, the solder paste deforms quickly, and its geometry becomes similar to the shape of a sphere. However, when it is very small, just as in this simulation where the surface tension is 0 N/m, the solder paste longer has any force that it maintains its cohesion. For this reason, the solder paste deforms occupying the simulation domain bottom.

The deformation observed in figure 5.13 can be only explained by the existence of gravity, since it is the only force in the domain that pulls the solder paste down.

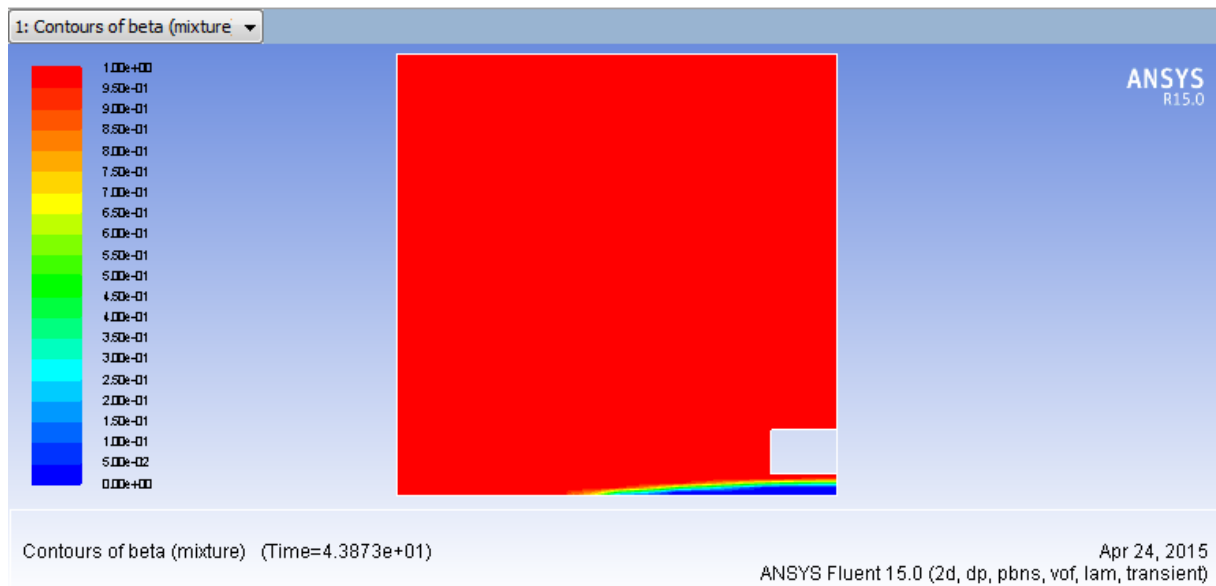


Figure 5.13 – Surface tension equal to 0 N/m and contact angles equal to 90°.

To confirm this assumption, it was realized a new simulation, based in the previous, where the effect of gravity was deactivated. The result presented in figure 5.14, confirms the predicted previously. As it is possible to see for 1 s of simulation there is not deformation of solder paste at room temperature. This simulation can be in this way considered a solution for the problem of solder paste deformation at room temperature, found in the reference model.

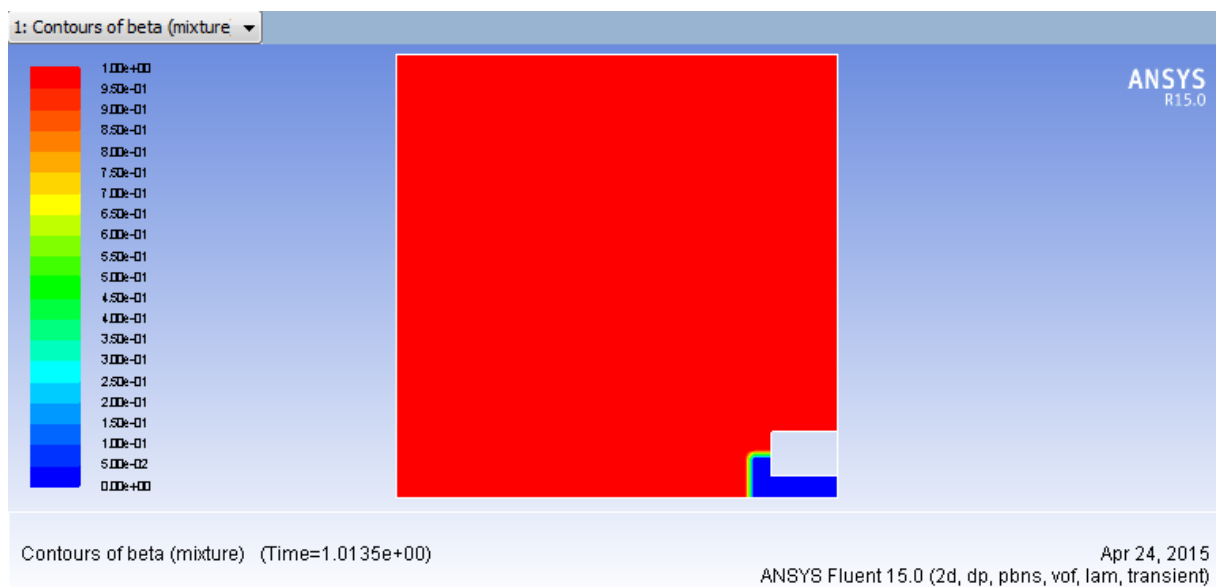


Figure 5.14 - Surface tension equal to 0 N/m, contact angles equal to 90° and gravity absence.

It can be concluded that there is not deformation of solder paste in solid state when it is conjugated in the same simulation, at room temperature, three factors. First, a solder paste surface tension of 0 N/m. Second, the contact angles need to be defined with the same value of the angles

presented by the solder paste in the initial state of the simulation, in this case 90° . Third the gravity needs to be deactivated.

However, it is necessary to change the value of these three variables, between the solid and the liquid state of solder paste, to achieve a model that represents the reality in all situations. But, in the ANSYS Fluent the gravity cannot be activated and deactivated in the same simulation. It means that it is necessary to find a new solution that does not pass by the change of gravity to solve the problem with the deformation of solder paste at room temperature.

5.4 Influence of Mushy-zone Parameter in the Solder Paste Deformation

The second strategy to solve the problem with the deformation of solder paste at room temperature, it passes by to analyze the influence of Mushy-zone parameter.

To do that, two simulations based in the reference model were performed, in the first it was used a Mushy-zone parameter of 10^7 while in the second it was used a Mushy-zone parameter of 10^8 .

The result of these two simulations is presented in figure 5.15. Where it is possible to see that for the simulation (a), after 10 s of simulation, the deformation of solder paste is near to the observed in the reference model, where the deformation happens in only 0.1 s. For the simulation (b) this fact is even more evident. After 10 s of simulation, it is clear that the deformation of solder paste is now significantly less than the observed for the reference model. It shows the enormous impact of the Mushy-zone parameter in the deformation of solder paste at room temperature.

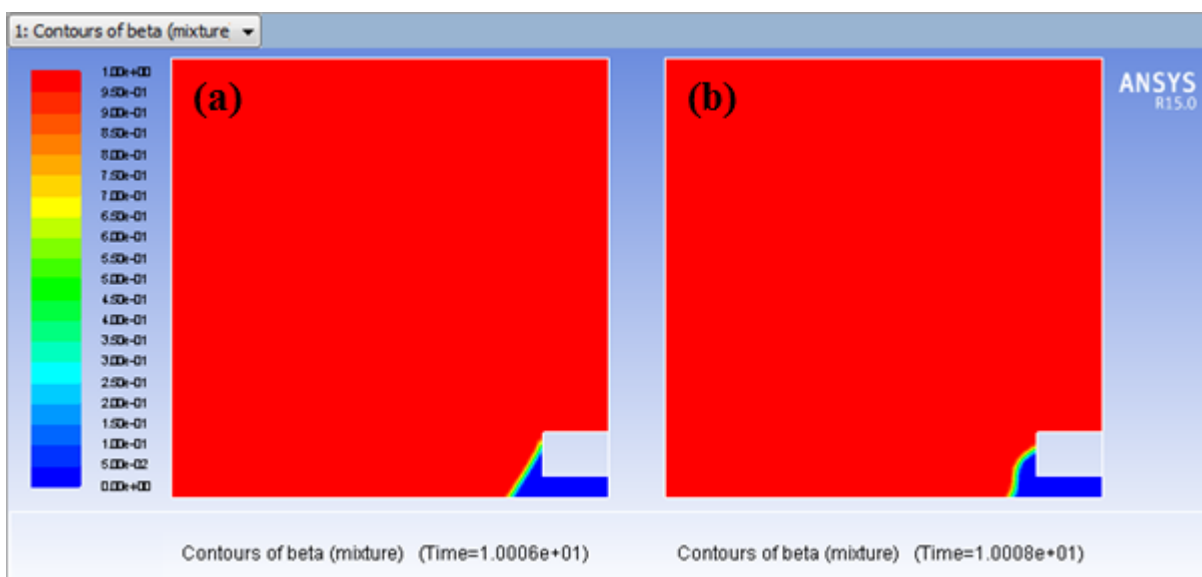


Figure 5.15 - Mushy-zone parameter of 10^7 (a) and 10^8 (b).

5.4.1 Problem Correction Second Attempt

Even with the good results achieved in the Mushy-zone parameter study, it is clear that it is not enough change only the Mushy-zone parameter, to stop the deformation of solder paste.

In this way, two other simulations were realized, based in the previous simulations, where the surface tension was considered for both simulations of 0 N/m, due the good results obtained in the study of the influence of this variable in the deformation of solder paste at room temperature.

In figure 5.16, it is possible to see the results of these two simulations. In the simulation (a) for a Mushy-zone parameter of 10^7 and without surface tension, the deformation of solder paste starts around the 5 s of simulation and it presents a little deformation in its left face with 31 s of simulation, at room temperature. However, in the simulation (b) for a Mushy-zone parameter of 10^8 and without surface tension, there is not deformation of solder paste at room temperature, until 30 s of simulation. Comparing the results of these two simulations with the previous two simulations, it is possible to prove one more time the importance of surface tension in the deformation of solder paste at room temperature.

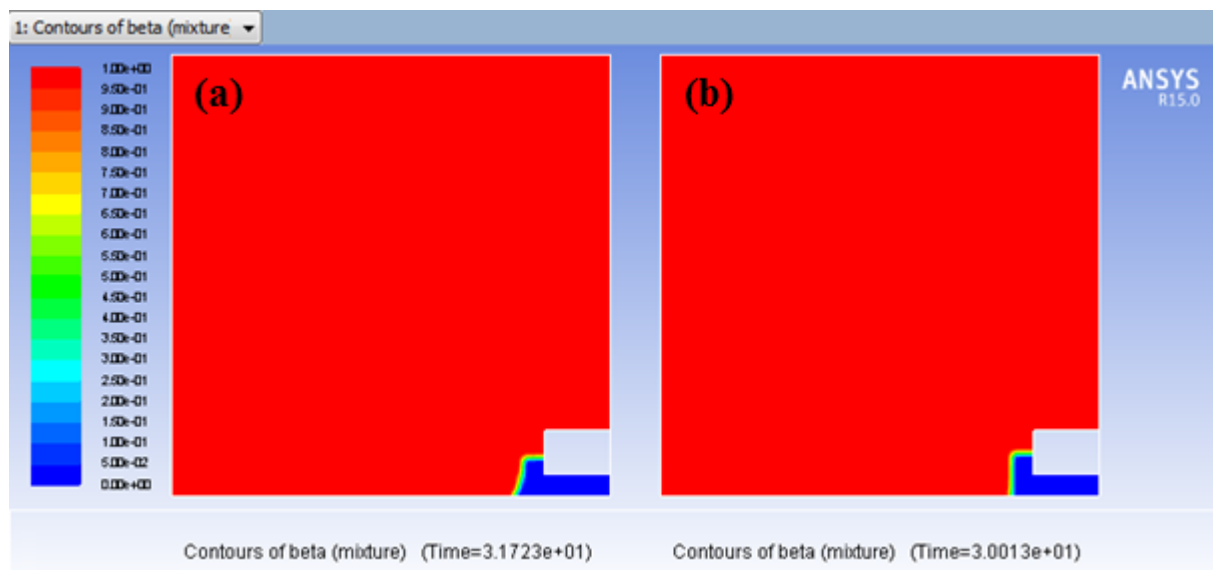


Figure 5.16 – Mushy-zone parameter of 10^7 (a) and 10^8 (b), and surface tension of 0 N/m.

Note that the solution cannot stop the deformation of solder paste completely and indefinitely. As explained in Chapter 4, the solder paste near the interface with the air has a velocity, even in solid state, and this velocity can be only reduced increasing the Mushy-zone parameter, but cannot be eliminated completely. In this way, the solid solder paste near the interface with the air will have always a velocity, and consequently movement, however small.

With this in mind, it was considered that the simulation (b) in figure 5.16, accomplished with a Mushy-zone parameter of 10^8 and a surface tension of 0 N/m, it is a solution good enough for the present study realized in this thesis. Since this solution do not present any visible deformation of solder paste at room temperature until 30 s of simulation, when the simulations present in this thesis do not exceed 3 s.

5.5 Solution and Validation

After found a solution for the deformation of solder paste at room temperature, it was created a new model to simulate the melting of solder paste, as it happens in the reference model, but in the new model the solution found for the deformation of solder paste in solid state was taken into account.

Contrarily to the reference model, it is now considered a Mushy-zone parameter of 10^8 and a solder paste surface tension variable and function of temperature. Its value is now of 0 N/m for temperatures below *Solidus* temperature and of 0.75 N/m for temperatures above *Solidus* temperature. The heating source is as in the reference model the copper pad and it has a constant temperature of 503 K.

In figure 5.17, the result of this simulation, for 0.5 s of simulation is presented, where it is possible to see the heat coming from the copper pad, and the solder paste starting to melt.

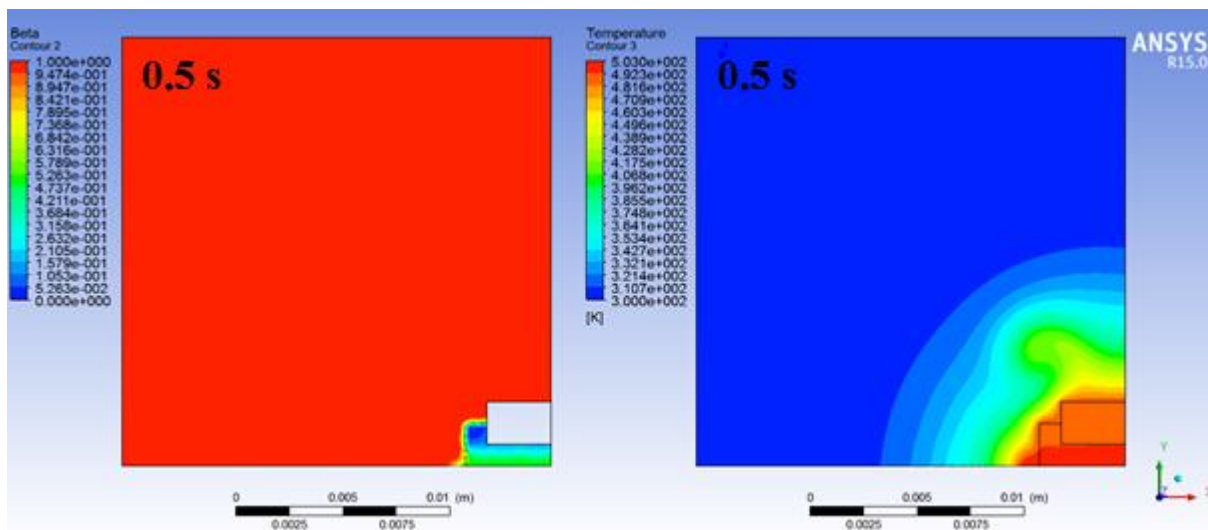


Figure 5.17 – Solder paste deformation and temperature after 0.5 s of simulation.

Remember that for the reference model, the deformation of solder paste is complete with only 0.1 s of simulation. Comparatively, now for 0.5 s of simulation, the solder paste presents only a little

deformation in the bottom left side, where the solder paste is already in liquid state. At same time, in the solder paste top, as it is in solid state, there is not any deformation.

In figure 5.18, for 0.76 s of simulation, it is possible to see a higher deformation of solder paste when compared with the previous simulation. The deformation of solder paste is now visible along the entire interface between the solder paste and the air. However, it is more significant near to the copper pad and near to the component left face, due to the definition of the contact angles of 30° and to the adhesion forces. It is also possible to see that the solder paste is already in liquid phase or in the Mushy-zone, where the movement of solder paste is allowed.

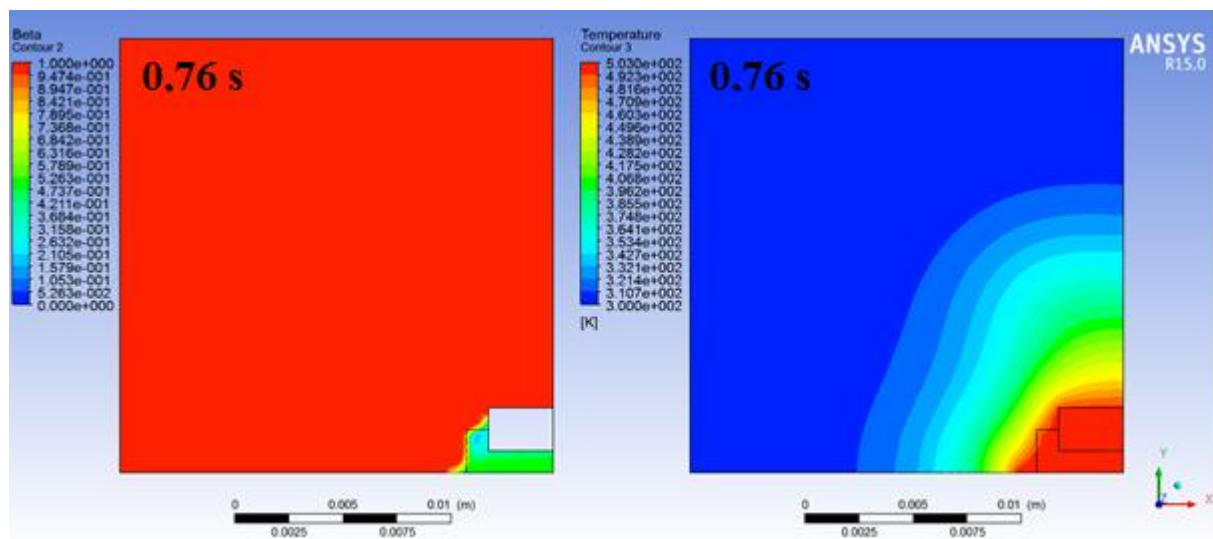


Figure 5.18 – Solder paste deformation and temperature after 0.76 s of simulation.

The final result of this simulation is shown in figure 5.19, where the solder paste is already totally melted and deformed, after 1.2 s of simulation. All the solder paste achieves the liquid state with around 1 s of simulation, but its deformation continues until achieve the shape observed in figure 5.19. Comparing the shape of solder paste achieved with this simulation and with the reference model, it is clear that there is not any significant difference. This result proves that the solution found for the deformation of solder paste at room temperature does not affect the deformation of solder paste in liquid state.

As a conclusion, it is possible to say that the new model is a success, allowing to obtain results in accordance with reality for the deformation of solder paste during all process of simulation, where the solder paste can be in solid or liquid state.

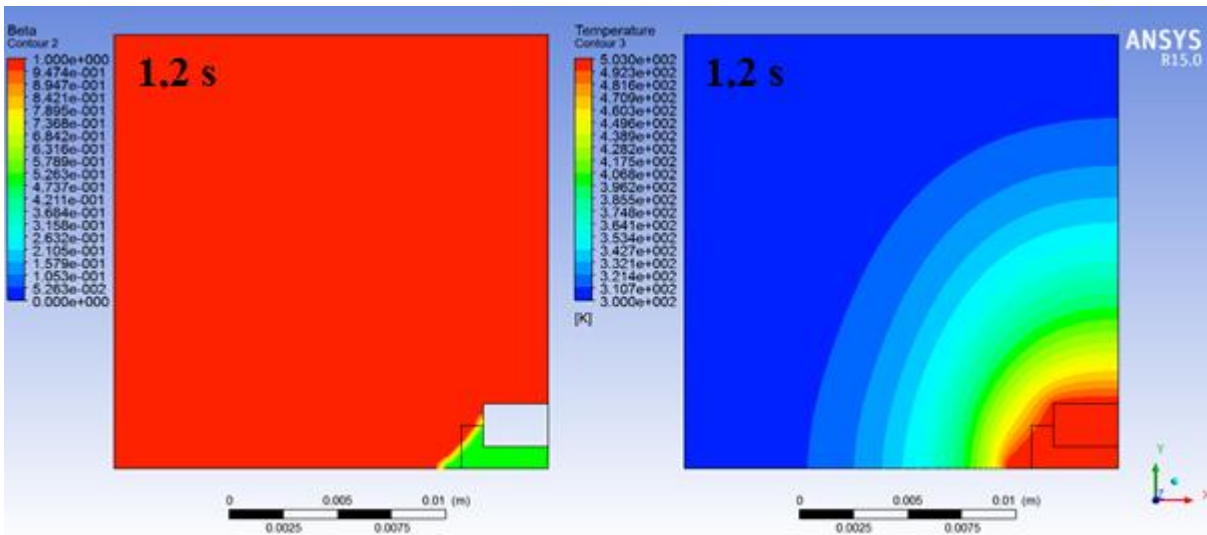


Figure 5.19 - Solder paste deformation and temperature after 1.2 s of simulation.

5.6 Thermal Cycle of Solder Paste

After the correction of the problem found in the reference model and its validation, during the melting process of solder paste, it is time to simulate a thermal cycle of solder paste that includes its melting and solidification. To do that, a new model was created based in the previous model, where the constant temperature of copper pad was changed for a simplified Reflow thermal cycle, as presented in Chapter 4.

The initial state of this simulation, as it is presented in figure 5.20, is equal to the presented by the previous model and by the reference model. Where, it is possible to see the solder paste at solid state and the entire domain of simulation at room temperature.

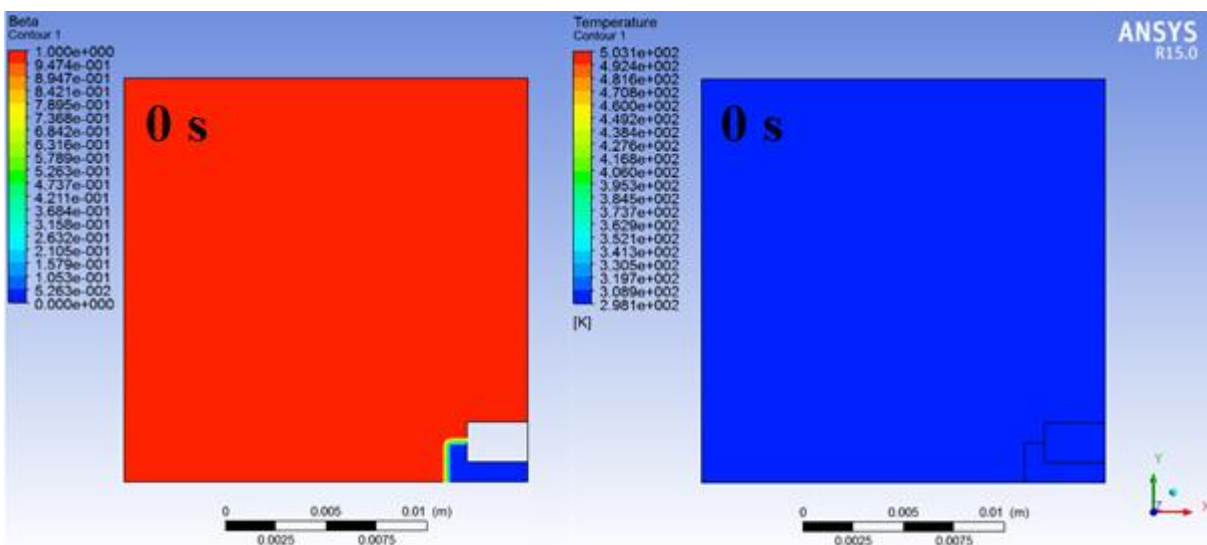


Figure 5.20 – Simplified Reflow thermal cycle, initial state.

From the initial state until 1 s of simulation, the temperature of the copper pad increases linearly from room temperature to 503 K. After this period, the temperature is maintained constant for 1 s, to give time the solder paste to melt completely.

In figure 5.21, after 1.4 s of simulation, it is already possible to see part of solder paste in liquid state, due to the increase of temperature. It is also possible to see the beginning of its deformation, near the copper pad and the component left side, due to the contact angles of 30° , and to the adhesion forces established between the solder paste and the copper which made the pad and the component.

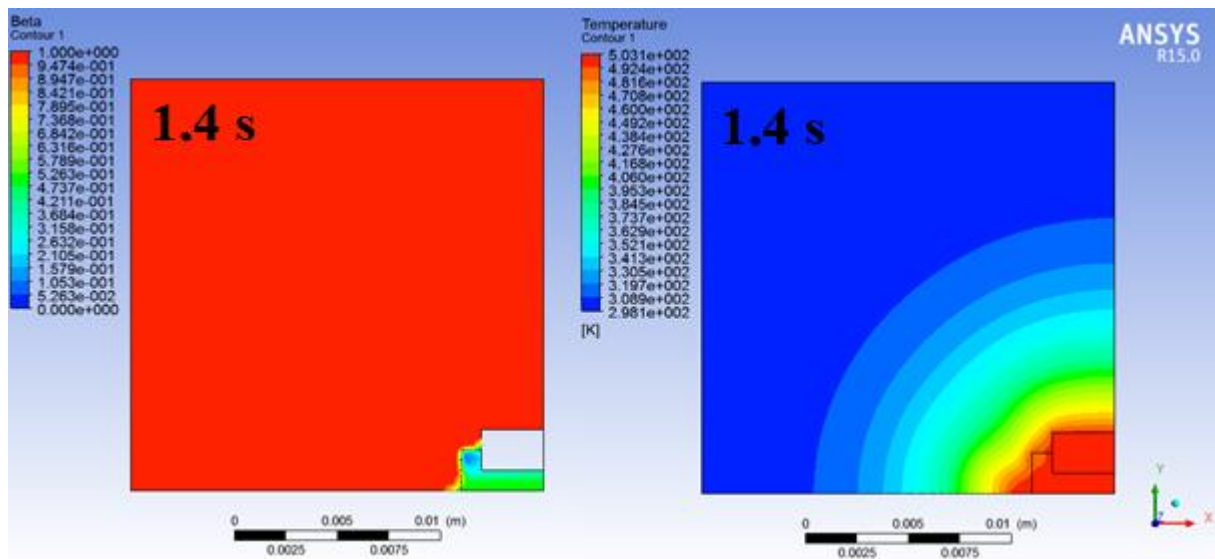


Figure 5.21 - Simplified Reflow thermal cycle, at 1.4 s of simulation.

For 1.5 s of simulation, in figure 5.22, the quantity of solder paste in liquid state increased, comparing to the previous result, resulting in the increase of the solder paste deformation.

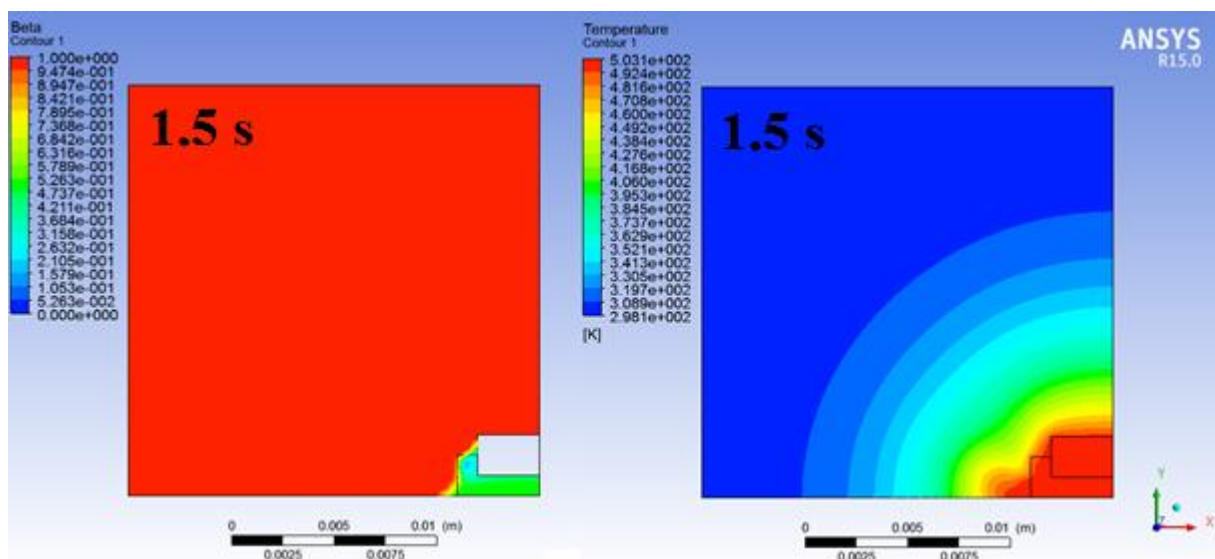


Figure 5.22 - Simplified Reflow thermal cycle, at 1.5 s of simulation.

As it presented in Chapter 2 about the Reflow soldering process, the definition of a Reflow thermal cycle is crucial for the success of the soldering process. The definition of a peak temperature high enough to melt the solder paste in all points of the PCB is very important, due the difference of temperature that may there is in the product during the soldering process. But, it is also important to define carefully the time above the *Liquidus* temperature of solder paste, to allow the solder paste to have time enough to melt in all points of soldering existing in the product.

In this simulation, there is only a single point of solder paste, but as it is possible to see there is a difference of temperature inside this point of solder paste. This shows that it is not enough to define a peak temperature higher than the *Liquidus* temperature of solder paste to melt it, it is necessary at same time to define with precision the time above *Liquidus* temperature, to be sure that the solder paste melts completely.

In figure 5.23, it is presented the solder paste totally melted after 1.73 s of simulation. However, the peak temperature happened with 1 s of simulation, and as it is possible to see, the solder paste needs more 0.73 s of simulation, at peak temperature, to melt completely. This result shows the importance of the time above *Liquidus* temperature in the success of Reflow soldering process.

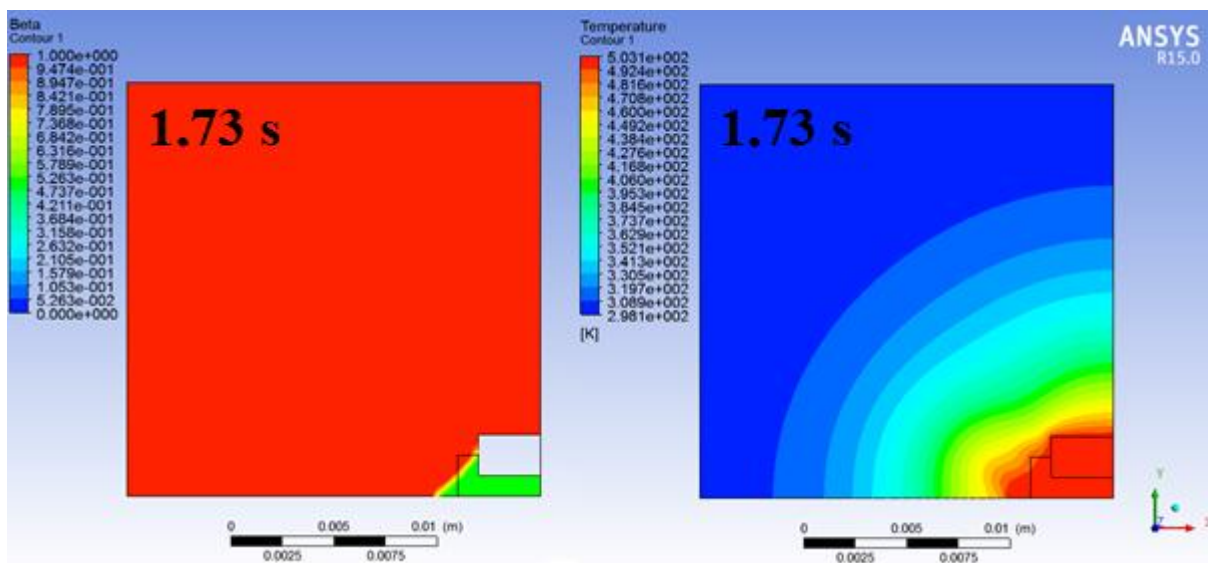


Figure 5.23 - Simplified Reflow thermal cycle, at 1.73 s of simulation.

Furthermore, Figure 5.23 allows to conclude that the geometry of solder paste in liquid state is not affected for this thermal cycle, comparing to the previous model, because its geometry is the same for both models. This makes sense, because for the solder paste has a different geometry, it must have also different properties. However, because the peak temperature is the same for both models, the solder paste at liquid state has the same properties, resulting in the same behavior.

The temperature of copper pad is maintained constant until 2 s of simulation, after this period the temperature starts cool down linearly from the 503 K until the room temperature, which it is achieved within 3 s of simulation.

At 2.16 s of simulation, as it is presented in figure 5.24, the temperature of solder paste near the copper pad is already lower than the solder paste *Solidus* temperature. This happens because the loss of heat from the solder paste to the copper pad by conduction it is higher than the loss of heat from solder paste to the air by natural convection. In this way, the solder paste starts to solidify from bottom to top.

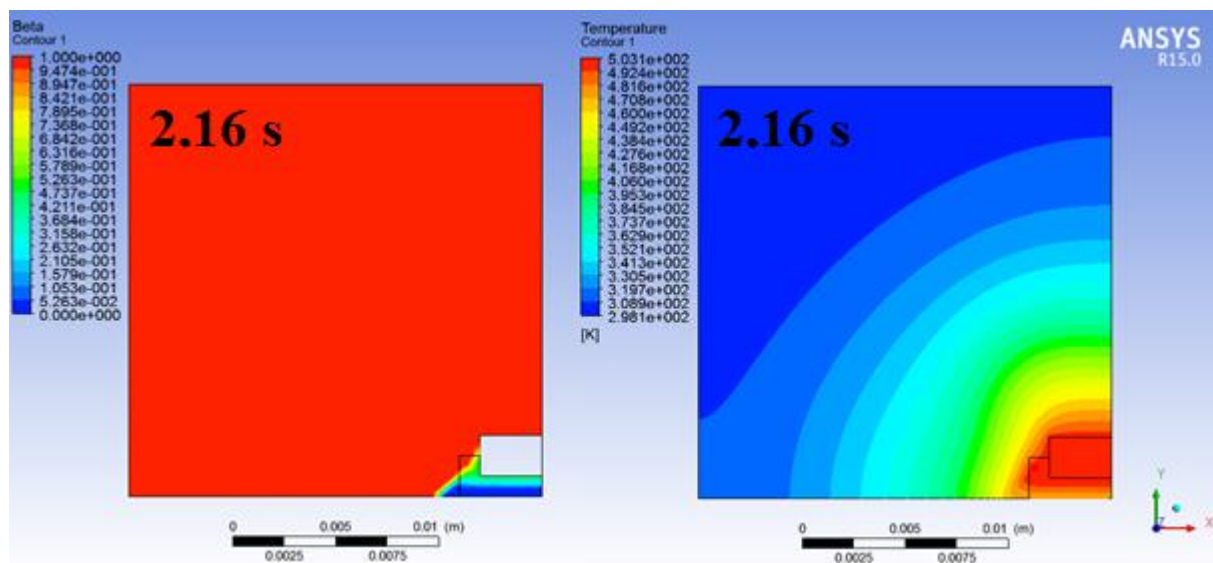


Figure 5.24 - Simplified Reflow thermal cycle, at 2.16 s of simulation.

In figure 5.25, after 3 s of simulation, it is possible to see all the solder paste already in solid state and with a temperature near to the room temperature. It is also possible to see that there is not any change of solder paste geometry in solid state comparing to its geometry in liquid state. This result shows that the model is working well and it respects the reality, since it is expected that the solder paste with its solidification stays unable of moving.

Looking with attention to the thermal cycle used in this simulation, it is possible to see that it is symmetric. So, it is normal to think that the time needed to heat the solder paste should be the same needed to cool down it. However looking to the results of these simulations, it is possible to see that it is not in this way. The time needed to heat all the solder paste from room temperature to peak temperature is about 1.73 s, but the time needed to cool down the solder paste again to room temperature is a little more than 1 s.

This event has also a simple explanation. During the heating process of solder paste, the heat comes from the copper pad to the solder paste, but some of this heat is also lost for the component and for the air. During the cool down of solder paste, the heat is lost for the copper pad and for the air, but at same time, the solder paste receives some heat from the component. However, the loss of heat during the heating process is higher than the gain of heat during the cooling phase, resulting in the differences observed in the times of heating and cooling.

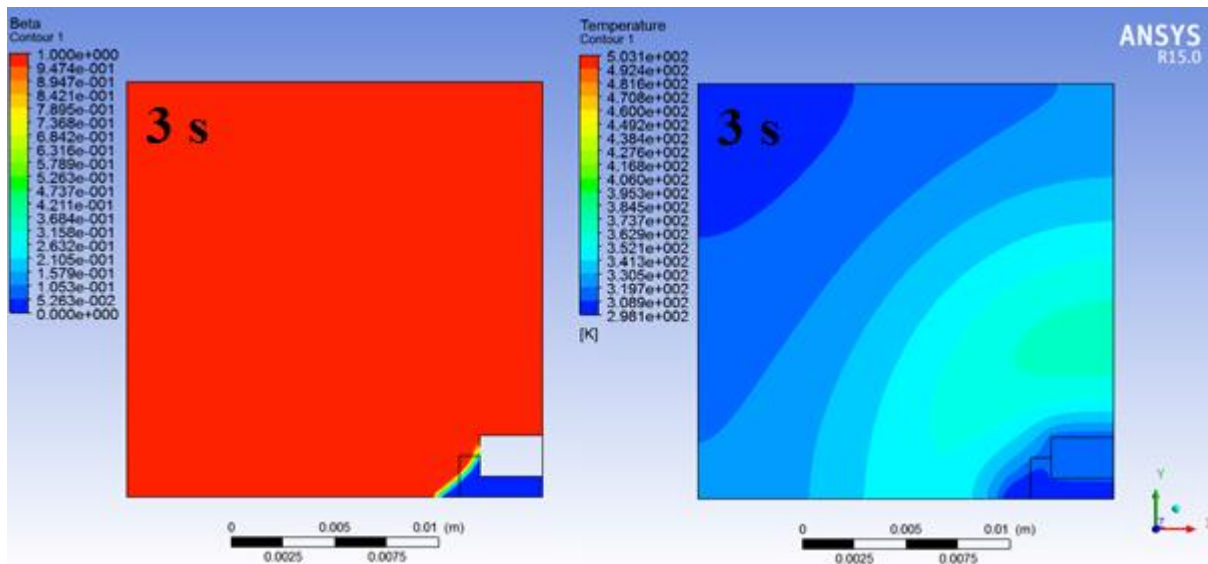


Figure 5.25 - Simplified Reflow thermal cycle, at 3 s of simulation.

5.7 Study Case at Bosch

At Bosch Car Multimedia, in order to understand the difference of Reflow AOI pseudo-errors, between two components of two equal products of the same *nutzen*, it was performed a Reflow thermal simulation of the *nutzen* containing the products in analysis. This simulation will allow check if there is a difference of temperature, between the two components, which may explain the difference of AOI pseudo-errors. The thermal cycle used in this simulation, as it is presented in Chapter 4, is similar to the real process.

In figure 5.26, it is presented the simulation state after 100 s. At this moment, it is already possible to see a temperature difference of 20 °C, between the hottest and the coldest *nutzen* point. It is also possible to see that there is a difference of temperature, between the component 1 and the component 2, of about 3 °C. Where the component 2 placed in the last product to enter in the Reflow oven, it has a higher temperature than the component 1 placed in the first product to enter in the Reflow oven.

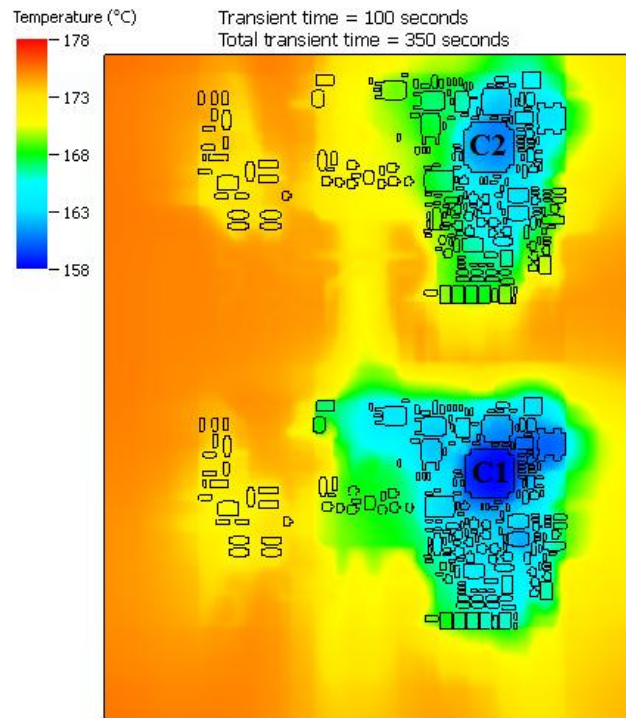


Figure 5.26 – Product 5106, Reflow thermal simulation, after 100 s of simulation.

For 200 s of simulation, figure 5.27, the max temperature difference observed in the *nutzen* is now of 18 °C. The difference of temperature between the two components in analysis is now smaller than in the previous result, of about 2 °C. However, the component 2 continues to have a higher temperature than the component 1.

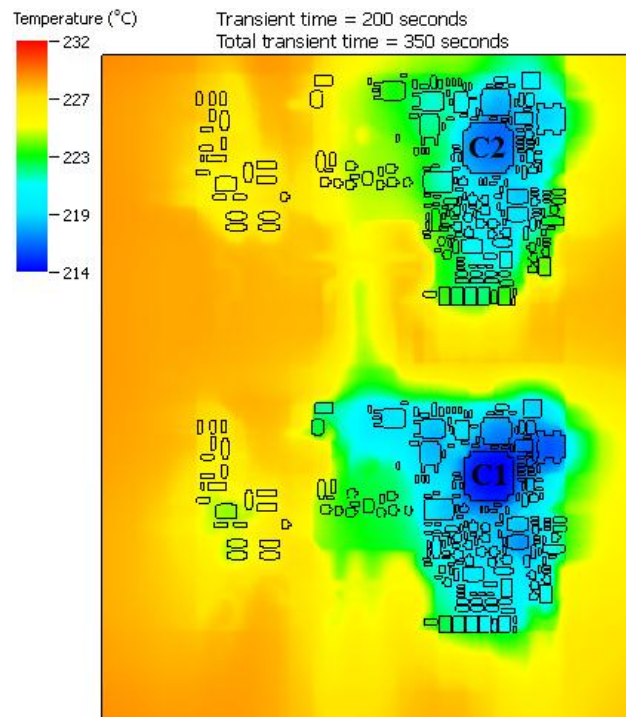


Figure 5.27 - Product 5106, Reflow thermal simulation, after 200 s of simulation.

After 250 s of simulation, figure 5.28, the peak temperature is achieved and at this moment starts the cooling phase. It is possible to conclude from simulation that all the solder paste, present in the real product, has a temperature enough to melt, since the minimum temperature in the *nutzen* is higher than the solder paste *Liquidus* temperature. However, once the solder paste is not simulated, it is impossible to predict if the time above *liquidus* is enough to melt all the solder paste in the *nutzen*. The max temperature difference in the *nutzen*, is now even smaller than in the previous two situations, of about 15 °C. The temperature difference between both components remained in 2 °C. The component 2 remained also hotter than the component 1.

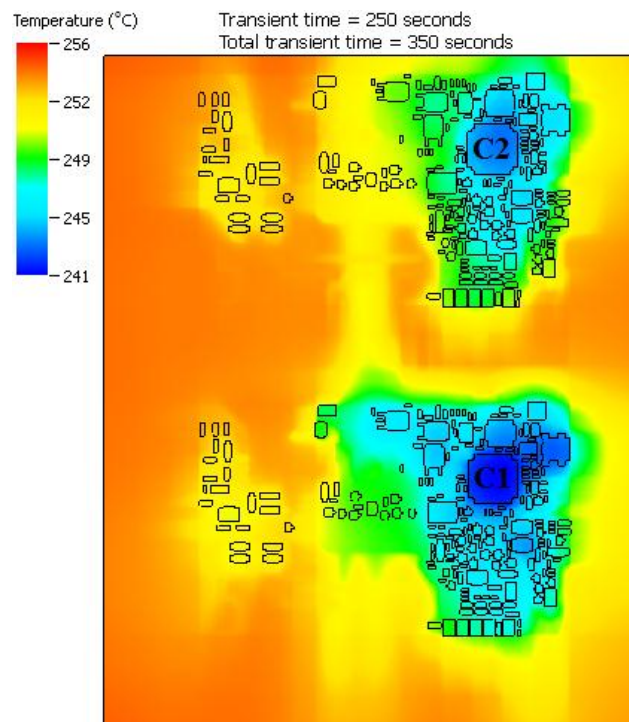


Figure 5.28 - Product 5106, Reflow thermal simulation, after 250 s of simulation.

After the cooling phase, figure 5.29, the simulation of Reflow soldering process ends. The max temperature difference observed in the *nutzen* is now higher than in previous situations, of about 34 °C. The difference of temperature between the components in analysis is also higher than in the previous situations, being now of 3 °C. However a big change has occurred, since the component 2 is no longer the hottest. The component 1 is now, contrarily to what happened in the heating phase, the component with a higher temperature comparing to the component 2.

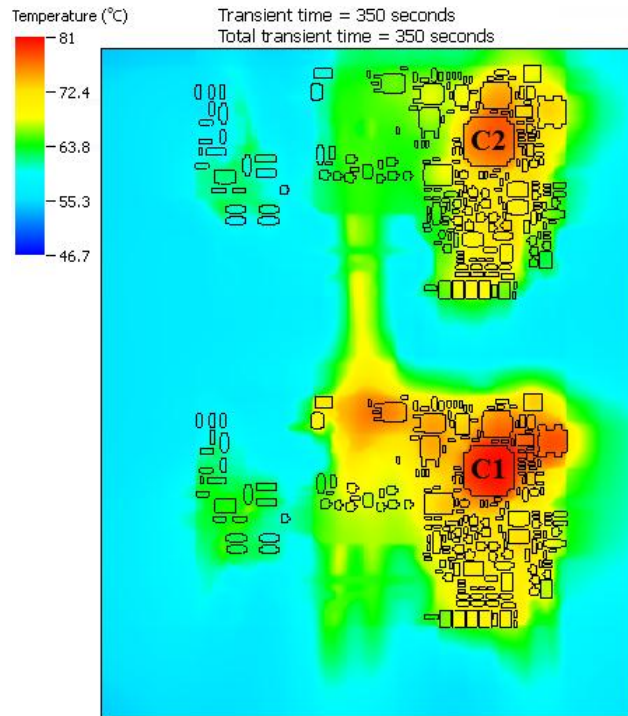


Figure 5.29 - Product 5106, Reflow thermal simulation, after 350 s of simulation.

Because the main objective of this simulation is check if there is a difference of temperature between the two QFP components in analysis, a thermocouple is placed in each component, in order to obtain the specific thermal cycle of each component during the Reflow soldering process simulation. The results are presented in figure 5.30.

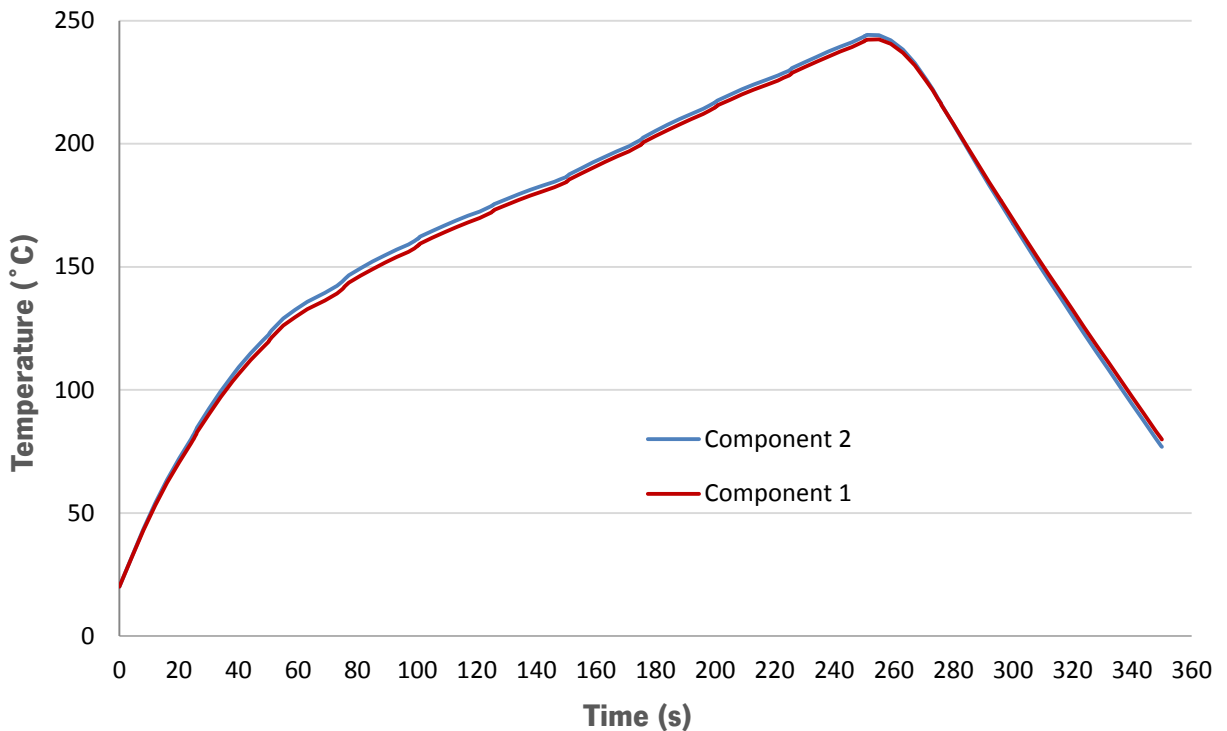


Figure 5.30 – QFP components thermal cycle.

As it is presented in figure 5.30, the thermal cycle of both components is very similar, but it is at same time clear that the component 2 has a higher temperature during the heating phase and the component 1 has a higher temperature during the cooling phase.

To see in more detail the temperature difference between the two components, it was subtracted the component 1 temperature to the component 2 temperature, during the entire thermal cycle. In figure 5.31, it is possible to see this difference of temperature. As seen previously, the temperature difference between the two components, increases rapidly until to achieve about 3 °C. After this point, the temperature difference starts decrease slowly until to achieve the 2 °C, remaining constant until the end of the heating phase. During the entire heating phase the component 2 has a higher temperature than the component 1, which means that the component 2 heats up faster than the component 1. This fact cannot be explained by the properties of both components because they are equal. However, its relative position in the *nutzen* is not equal, which may be the explanation for the temperature differences found. During the cooling phase, the difference of temperature between both components decreases rapidly, until the temperature of both to be the same. After this point, the temperature difference between both components increases again until the 3 °C, but now it is the component 1 that it has a higher temperature than the component 2. This result shows that during the cooling phase, the component 2 cools down faster than the component 1.

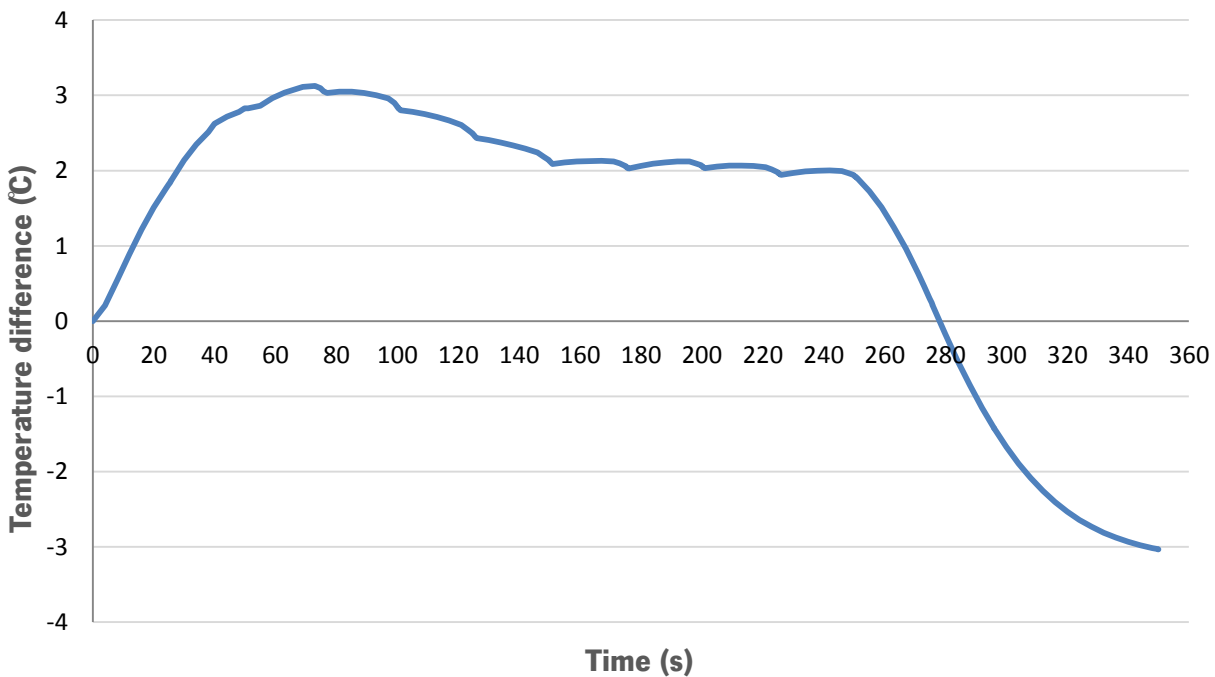


Figure 5.31 – Temperature difference between the QFP components (C2 - C1).

As conclusion, it is possible to affirm that the temperature difference between both components in study really exists. However, it is impossible be sure if this temperature difference is enough to justify the differences of Reflow AOI pseudo-errors observed in figure 4.5, for the same *nutzen*. It is also difficult to explain the reason for the existence of this difference of temperature between both components. The most likely explanation seems to be the position of each component in the *nutzen*. The component 1 is placed near the *nutzen* center, and due that there is more thermal mass around this component, which it contributes to a larger heat dissipation during the heating phase and the opposite during the cooling phase. On the other hand, the component 2 is placed near the *nutzen* rear side, where the less thermal mass around the component may explain its faster heating and cooling.

Other possible explanation may be the difference of air velocity near the components, which it has influence in the heat transferred by forced convection. In figure 4.7, it is presented the simulation domain used by the program 6SigmaET, where it is possible to see that the quantity and velocity of the air in the *nutzen* center is smaller than in its front and rear. As consequence, the component 1 near the *nutzen* center will have less air passing by it and with lower speed, which it has a great impact in the quantity of heat transferred between the air and the component by forced convection. However, the component 2 due its position will have more air passing by it and with more speed, which it increases the quantity of heat transferred between the air and the component by forced convection. This allows the component 2 heating and cooling faster than the component 1. However, these are only qualitative explanations, due the difficulty of quantify this assumptions.

Experimental test in the production line

After making the thermal simulation and analyze the results, it was decided check if in reality the temperature difference between both components is the same that the predicted by the simulation. The practical test was carried out in the production Reflow line with a real product, where four thermocouples were placed in the components and in its solder joint. The thermal cycle used in the Reflow oven was the presented in Chapter 4.

The results of this test are presented in figure 5.32 and 5.33. As observed, the temperature of each compered is very similar during all Reflow thermal cycle. However, there are some differences between all thermal cycles.

Looking first to the components, it is possible to see that the component 2 has a higher temperature than the component 1, during the entire heating phase. The component 2 has a higher

peak temperature of 250 °C. The component 2 has also a higher cooling rate than the component 1, up to 150 °C. To see in more detail the temperature difference between the two components and solder joints, it was subtracted the component 1 temperature to the component 2 temperature and the solder joint 1 temperature to the solder joint 2 temperature, during the entire thermal cycle, as it is presented in figure 5.33.

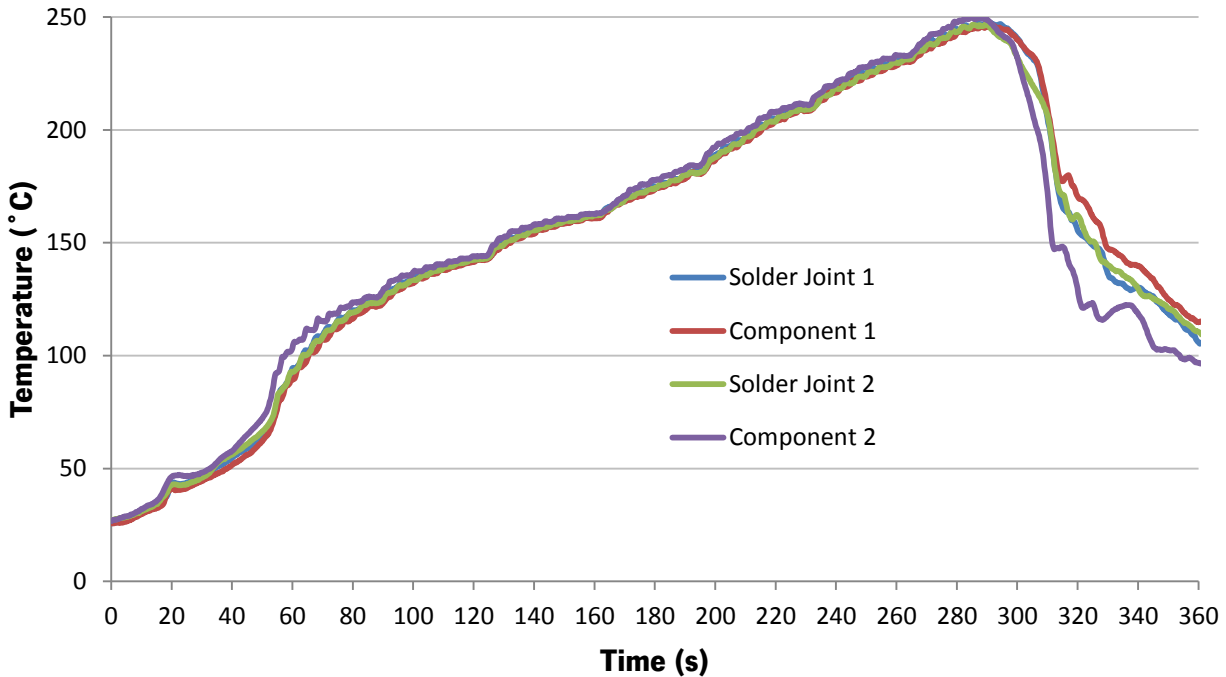


Figure 5.32 – Real Reflow thermal cycle of the QFP components and solder joints.

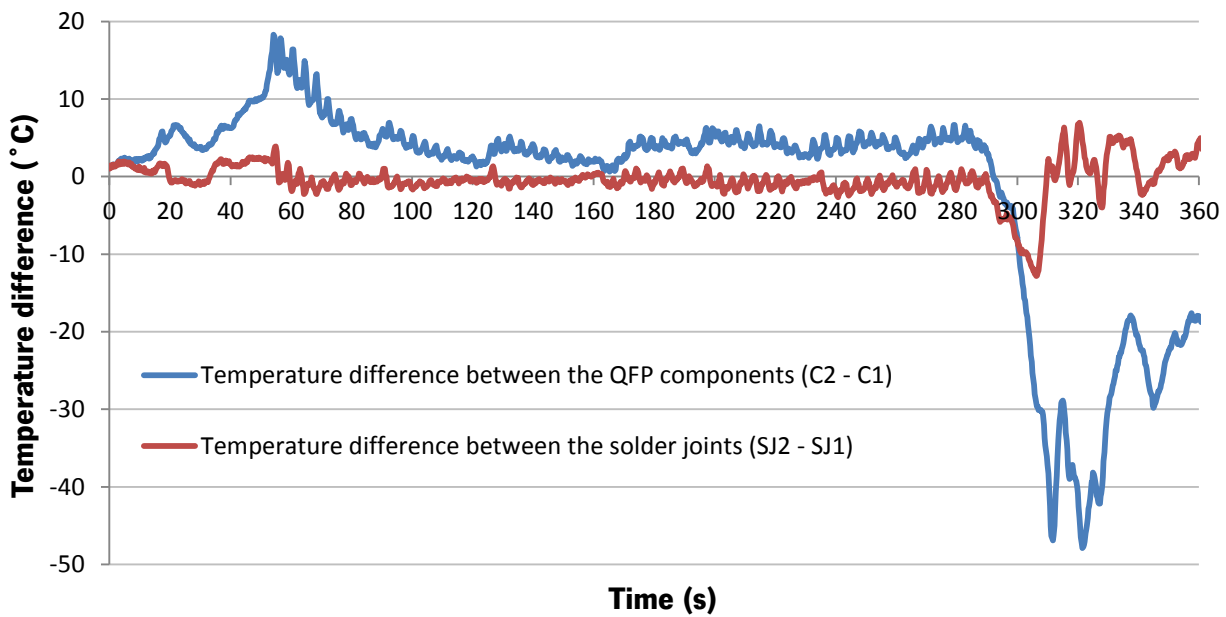


Figure 5.33 – Real temperature difference between the QFP components and solder joints.

In figure 5.33, the temperature differences between the QFP components and its respective solder joints are also presented. For the QFP components, it is possible to observe that there is a temperature difference between both components. During the heating process is also possible see the influence of the different Reflow oven heating phases in the difference of temperature between the components.

In the Reflow oven, when the *nutzen* enter in a new heating phase the difference of temperature between the components increase faster for positive values, between 1 °C and 17 °C. This means that the component 2 heats faster than the component 1, when both components enter in the same phase where the temperature is constant. During the same Reflow oven heating phase, the difference of temperature decreases a little bit, but the component 2 remains the hottest component during all heating process.

During the initial cooling phase is also clear that the component 2 has a higher cooling rate that the component 1, achieving a temperature difference of 45 °C. Since the difference of temperature between both components is negative during the entire cooling phase, this means that the temperature of component 1 is higher than the temperature of component 2.

These results seem to confirm that the component 2 heats and cools faster than the component 1, as it observed in the simulation. It is even possible to see that the component 2 is the hottest at peak temperature and that the temperature difference between both components at this moment it is of 5 °C, more than double that it predicted by the simulation.

However, the temperature difference between the solder joint of both components it is other variable that may originate the difference observed in the Reflow AOI pseudo-errors, for the same *nutzen*. It was for this reason that the thermocouples were placed in the solder joint of each component. The same it was not possible in the simulation, because the solder paste is not simulated.

Looking now to the solder joint of each component, it is possible to see in figure 5.32 that the solder joint of component 1 has a temperature approximately equal to the solder joint of component 2, during the entire heating phase. The peak temperature of both solder joints is about of 248 °C. During the cooling phase, it is possible to observe that the solder joint of component 2 has a lower temperature comparing to the solder joint of component 1, until to achieve the temperature of 208 °C.

Looking with more detail for these temperature differences, in figure 5.33, it is clear that the difference of temperature between both solder joints is near 0 °C, during the entire heating phase. During the initial cooling phase is evident that the solder joint of component 2 cools faster than the

solder joint of component 1, achieving a difference of temperature of 12 °C near the *Solidus* temperature of solder paste. Since the difference of temperature at this moment is negative, this means that the temperature of the solder joint of component 2 is lower than the temperature of the solder joint of component 1.

Analyzing these results, it is easy conclude that if there is any difference in the temperature of both solder joints that justifies the difference in the Reflow AOI pseudo-errors for the same *nutzen*, this temperature difference is in the cooling phase. This temperature difference is particularly important when the solder paste is not in solid state, because it is in this phase that the solder paste has movement. Other variable very important is the time that the solder paste stays above its *Solidus* temperature. In this case, the solder joint of component 1 remains above *Solidus* temperature of solder paste during 71.5 s and the solder joint of component 2 during 67 s. This result shows that the solder joint of component 1 remains more 4.5 s above the *Solidus* temperature of solder paste than the solder joint of component 2, which may have a great influence in the wetting of solder paste.

As example, they are presented in figure 5.34 two cross section cuts of the QFP component's pins, where the unique difference in its production it is the use or not of N₂, during the Reflow soldering process. This example shows that in the product produced with N₂ the solder paste has a better wetting, reaching the top of the component's pins. On the other hand, it is possible to observe that in the product produced without N₂ the solder paste has a poor wetting, as it is proven by the geometry of solder paste that it does not achieve the top of the component's pins.

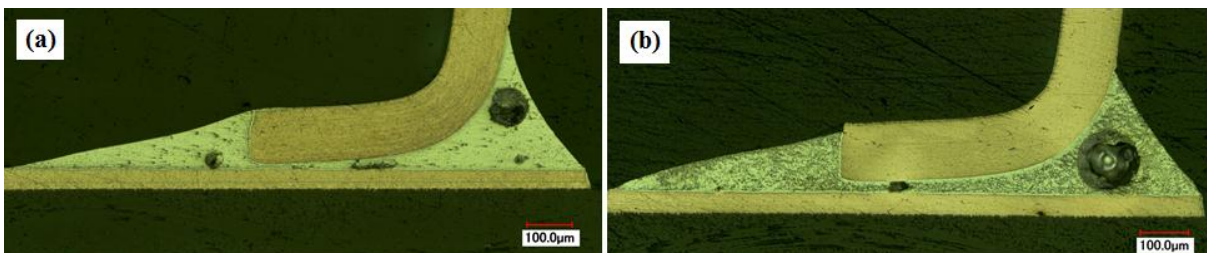


Figure 5.34 – Sectional cuts of the QFP component's pins, in a product produced with N₂ in the Reflow soldering process (a), and in a product produced without N₂ in the Reflow soldering process (b).

This difference in the wetting of solder paste happens due to the difference of atmosphere used in the Reflow oven. An atmosphere of N₂ is considered a non-oxidant atmosphere, and for this reason the oxidation of component's pins is minimized during the heating phase of Reflow thermal cycle, which improves the solder paste wetting. However, when it is used an atmosphere without N₂, for example atmospheric air, which it is considered an oxidant atmosphere, the result is the aggravation of oxidation

of the component's pins during the heating phase of Reflow thermal cycle. The result of this higher oxidation of the component's pins is the poor wetting of solder paste, as it observed in figure 5.34 (b).

This explanation for the difference observed, in figure 5.34, for the wetting of solder paste, it is also the justification for the difference of the Reflow AOI pseudo-errors, found in figure 4.5 between the two *nutzens*, where the first it is produced with N_2 and the second without N_2 .

Beyond the atmosphere used in the Reflow oven, other variable that can aggravate the oxidation is the temperature, where higher temperatures create more oxidation of the component's pins during the heating phase of Reflow thermal cycle.

Looking for the difference of temperature between the QFP components, it is clear that the component 2 has a higher temperature than the component 1, during the entire heating phase of Reflow thermal cycle. This will aggravate the oxidation of component's 2 pins comparing to the component 1. Resulting in a poor wetting of solder paste of component 2, and for consequence, in a higher number of Reflow AOI pseudo-errors, even for a product produced with the same atmosphere in the Reflow oven. This may be part of the justification for the difference in the Reflow AOI pseudo-errors shown in figure 4.5 for the same *nutzen*, where the conditions of production are the same.

Other variable that may influence the wetting of solder paste is the time that it remains at liquid state. Normally, the wetting of solder paste increases with the increase of time that it remains at liquid state.

As shown previously, the difference of temperature between the solder joints of both components is very small in the heating phase. However, during the cooling phase, from the peak temperature until the *Solidus* temperature of solder paste, this difference of temperature increases significantly. This means that the solder joint of component 2 cools faster than the solder joint of component 1. For this reason, the solder joint of component 2 remains less 4.5 s at liquid state than the solder joint of component 1. Resulting in a poor wetting of solder paste in the solder joint of component 2, which it has as consequence the increase of Reflow AOI pseudo-errors shown in figure 4.5 for the same *nutzen*, where the conditions of production are the same.

As conclusion, it is possible to say that the higher temperature of component 2 during the heating phase of Reflow thermal cycle, ally with the faster cooling of the solder joint of component 2, they are the reasons for the poor wetting of the solder paste of component 2. This results in an increase of Reflow AOI pseudo-errors for this component, when it is considered the same *nutzen*.

Conclusions and Future Work

6.1 Conclusions

In this work a numerical simulation model for the deformation of solder paste used by the industry in the Reflow soldering process of electronic products was developed. This enables to simulate any Reflow thermal cycle with this model and evaluate its influence in the deformation of solder paste, inclusively in its melting and solidification.

During the course of this work it was even possible to verify the importance of cooper pad dimension and of solder paste amount in the deformation and final geometry of solder paste. Other properties of solder paste that may have some influence in its deformation were also analyzed, such as density, viscosity and surface tension. It was concluded that the surface tension is the solder paste property with the greatest impact in its deformation.

The analysis of the solder paste melting simulation model enabled to conclude that the solder paste at solid state has movement near the interface with the air, resulting in a deformation of solder paste at room temperature. This problem is due to the Solidification/Melting model and can be mitigated, through the change of Mushy-zone parameter and surface tension, although it cannot be entirely eliminated.

The solution found for the deformation of solder paste at room temperature, it was then used to correct the solder paste melting simulation model. Where it is possible to conclude that the solution was

a successful, allowing stop the deformation of solder paste at solid state and at same time do not committing the deformation of solder paste at liquid state in accordance to reality.

It was also developed a simulation model of solder paste melting and solidification, through the use of a simplified Reflow thermal cycle. With this model was concluded that the final geometry of solder paste cannot be changed with different thermal cycles if its peak temperature is the same, since the solder paste properties are defined as function of temperature. However, different thermal cycles with different rates of heating and cooling will influence the velocity of the solder paste deformation. It could also be concluded from this model that the solidification process of solder paste does not affect the geometry of solder paste, once its geometry after the solidification it is equal to the geometry of solder paste at liquid state.

Relatively to the work done during the internship at Bosch Car Multimedia, it was possible to found the justification for the difference in the Reflow AOI pseudo-errors, between the two QFP components of two products of the same *nutzen* (structure with two or more equal products). The results of the simulation and of the real test in the production line, show that the QFP component 2 has a higher temperature than the QFP component 1 during the heating phase, which it increases the oxidation of the component's 2 pins. On the other hand, the solder joint of component 2 cools faster than the solder joint of component 1, resulting in less time at liquid state of solder joint of component 2. These two factors combined have a significant impact in the wetting of solder paste, resulting in a poor wetting of the solder paste of component 2 comparing with the component 1. As consequence of the poor wetting of solder paste, its geometry is affected, being detected by the Reflow AOI resulting in an increase of Reflow AOI pseudo-errors.

This work allowed also check the accuracy of the computational program 6SigmaET, through the comparison of the results obtained in the simulation model with the practical test in the production line. The results show that the temperature difference between the two QFP components is under predicted by the simulation model than in the reality, where the difference of temperature is more irregular and higher. The temperature difference between the two QFP components it is also higher in reality than predicted by the simulation model. However, the temperatures predicted by the simulation model are only a few degrees different of reality, so it can be concluded that it is a program accurate enough for the application.

6.2 Future Work

To continue the simulation model development of the Reflow soldering process, in order to achieve a model as close as possible to the reality, some future work are suggested.

First the contact angles of solder paste with the copper pad and component, which until the moment they are considered constants, may be considered as function of temperature using a UDF (User Defined Function), allowing a better prediction of the deformation of solder paste.

The copper pad and the electronic component can be also upgraded. In a real PCB, above the copper pads it is deposited a surface finish, which may be also included in the simulation model. The electronic component that in the simulation it is considered as a copper block, should be considered as a mix of different materials, as it happens in reality. The component should have also a metallization above its copper connectors. All this changes will improve the deformation of solder paste and at same time make the simulation model much more close to the real Reflow soldering process.

Another very important future work passes by change the heat source. At the moment, the heat source is the copper pad and the heat is transferred to the solder paste by conduction. However, in the real Reflow soldering process, the heat source is the air and the heat is transferred to the product to be soldered by forced convection. This change will allow the creation of a simulation model almost equal to the real Reflow soldering process.

Finally it should be possible to simulate more complex products with more components and soldering points, in 2D or 3D, until achieve the main objective of to simulate the electronic products used in the industry.

After all this, the simulation model will be ready to be used in the development of electronic products and in the prediction of production errors, specifically in the Reflow soldering process.

References

- [1] "DIRECTIVA 2002/95/CE do Parlamento Europeu e do Conselho de 27 de Janeiro de 2003 relativa à restrição do uso de determinadas substâncias perigosas em equipamentos elétricos e eletrónicos".
- [2] C.-S. Lau, M. Abdullah and F. C. Ani, "Three-dimensional thermal investigations at board level in a reflow oven using thermal-coupling method," in *Soldering & Surface Mount Technology*, 2012, pp. 167-182.
- [3] I. Balázs and B. István, "Numerical study of the gas flow velocity space in convection reflow oven," Budapest, 2013.
- [4] K. A. Brakke, "The Surface Evolver," in *Experimental Mathematics*, vol. 1, 1992, pp. 141-165.
- [5] K. A. Brakke, *Surface Evolver Manual*, 2.26 ed., Selinsgrove, PA, 2005.
- [6] C. Ya-Yun, C. Hung-Ju, K. Jer-Haur and H. Weng-Sing, "The Simulation of Shape Evolution of Solder Joints during Reflow Process," in *Materials Transactions*, 2006, pp. 1186-1192.
- [7] Y. Hao, T. Mattila and J. K. Kivilahti, "Thermal simulation of the solidification of lead-free solder interconnections," in *IEEE Transactions on Components and Packaging Technologies*, vol. 29, 2006, pp. 475-485.
- [8] H. Yu and J. Kivilahti, "CFD modelling of the flow field inside a reflow oven," in *Soldering & Surface Mount Technology*, vol. 14, 2002, pp. 38-44.
- [9] D. Whalley, "A simplified model of the reflow soldering process," in *8th Intersociety Conference on Thermal and Thermomechanical Phenomena in Electronic Systems*, San Diego, California, 2002.
- [10] F. Sarvar and P. P. Conway, "Effective Modelling of the Reflow Soldering Process: Basis, Construction and Operation of a Process Model," in *IEEE Transactions on Components, Packaging and Manufacturing Technology Part C: Manufacture*, vol. 21, 1998, pp. 126-133.

- [11] C. Srivalli, M. Abdullah and C. Khor, "Numerical investigations on the effects of different cooling periods in reflow-soldering process," in *Heat Mass Transfer*, 2015.
- [12] J. Costa, D. Soares, S. F. Teixeira, F. Cerqueira, F. Macedo, N. Rodrigues, L. Ribas and J. C. Teixeira, "Modeling the Reflow Soldering Process in PCB's," ASME, 2015.
- [13] R. Strauss, D. Ing. and FIM, *SMT Soldering Handbook*, Oxford: Newnes, 1994-1998.
- [14] B. C. M. COCs, "Internal documents and guidelines of Bosch Car Multimedia," Braga, 2014.
- [15] R. Strauss, D. Ing. and FIM, "Reflowsoldering," in *SMT Soldering Handbook*, Oxford, Newnes, 1994-1998, p. Chapter 5.
- [16] Profiling Guru, "Profiling BGA Webinar," [Online]. Available: <http://profilingguru.com/reflow/profiling-bga-webinar/>. [Accessed 16 09 2015].
- [17] R. Strauss, D. Ing. and FIM, "Wavesoldering," in *SMT Soldering Handbook*, Oxford, Newnes, 1994-1998, p. Chapter 4.
- [18] R. S. Khandpur, "Basics of Printed Circuit Boards," in *Printed Circuit Boards - Design, Fabrication, Assembly and Testing*, USA, Tata McGraw-Hill, 2005, p. Chapter 1.
- [19] R. S. Khandpur, "Multi-layer Boards," in *Printed Circuit Board - Design, Fabrication, and Assembly*, USA, McGraw-Hill, 2006, p. Chapter 11.
- [20] Altium, "Engineering Innovation for PCB Design," [Online]. Available: http://techdocs.altium.com/sites/default/files/wiki_attachments/209845/Pcb_Obj-Via_Via_LayerStackup.png. [Accessed 22 09 2015].
- [21] R. Schueller, D. Ph., W. Ables, J. Fitch and D. Ph., "A Case Study For Transitioning Class A Server Motherboards To Lead-Free," Texas, 2008.
- [22] J. Clyde F. Coombs, "Printed Circuit Board Surface Finishes," in *Printed Circuits Handbook*, USA, McGraw-Hill, 2008, p. Chapter 32.

- [23] G. Subbarayan, "A Systematic Approach Selection of Best PB-Free Printed Circuit Board (PCB) Surface Finish," New York, 2007.
- [24] K. J. Puttlitz and K. A. Stalter, "Overview of Lead-Free Solder Issues Including Selection," in *Handbook of Lead-Free Solder Technology for Microelectronic Assemblies*, New York, Marcel Dekker, 2004, p. Chapter 1.
- [25] B. Trumble, "Get The Lead Out," IEEE Spectrum, 1998.
- [26] D. Wojciechowski, M. Chan and F. Martone, in *Microelectronics Reliability*, vol. 41, ELSEVIER, 2001, pp. 1829-1839.
- [27] J. W. Evans, "Solder Alloys," in *A Guide to Lead-free Solders*, USA, Springer, 2005, pp. 7-8.
- [28] M. Schwartz, "Fluxes," in *Soldering - Understanding the Basics*, USA, ASM International, 2014, p. Chapter 4.
- [29] J. Clyde F. Coombs, "Solder Fluxes," in *Printed Circuits Handbook*, USA, McGraw-Hill, 2008, p. Chapter 46.
- [30] J. Clyde F. Coombs, "Assembly Processes," in *Printed Circuits Handbook*, USA, McGraw-Hill, 2008, p. Chapter 40.
- [31] iNEMI, "iNEMI Recommendations on Lead-Free for Components Used in High-Reliability Products," iNEMI, 2006.
- [32] N.-C. LEE, "Reflow," in *Reflow Soldering Processes and Troubleshooting SMT, BGA, CSP and Flip Chip Technologies*, USA, Newnes, 2002, pp. 77-81.
- [33] J. Clyde F. Coombs, "Soldering Techniques," in *Printed Circuits Handbook*, USA, McGraw-Hill, 2008, p. Chapter 47.
- [34] J. Costa, "Estudo numérico da fusão da solda no processo de soldadura por reflow," Guimarães, 2014.

- [35] Altera Corporation, "Reflow Soldering Guidelines for Surface-Mount Devices," Altera Corporation, 1999.
- [36] LEDNEWS.ORG, "Guideline for SMD LED soldering," [Online]. Available: <http://www.lednews.org/guideline-smd-led-soldering/>. [Accessed 11 6 2015].
- [37] H. Ma and J. C. Suhling, "A review of mechanical properties of lead-free solders for electronic packaging," Springer, USA, 2009.
- [38] F. Pan, T.-C. Chou, F. Bath, D. Willie and B. F. Toleno, "Effects of reflow profile and thermal conditioning on intermetallic compound thickness for SnAgCu soldered joints," USA, 2009.
- [39] A. Inc., "Multiphase Flows," in *ANSYS Fluent Theory Guide*, USA, ANSYS Inc., 2013, p. Chapter 17.
- [40] A. Inc., "The Euler-Lagrange Approach," in *ANSYS Fluent Theory Guide*, USA, ANSYS Inc., 2013, p. 373.
- [41] V. R. Voller and C. Prakash, "A Fixed-Grid Numerical Modeling Methodology for Convection-Diffusion Mushy Region Phase-Change Problems," in *International Journal of Heat and Mass Transfer*, vol. 30, ELSEVIER, 1987, pp. 1709-1720.
- [42] A. Inc., "Solidification and Melting," in *ANSYS Fluent Theory Guide*, USA, ANSYS Inc., 2013, p. Chapter 18.
- [43] C. R. Swaminathan and V. R. Voller, "A general enthalpy method for modeling solidification processes," in *Metallurgical and Materials Transactions*, vol. 23, Springer, 1992, pp. 651-664.
- [44] R. Eymard, T. Gallouet and R. Herbin, "Finite Volume Methods," Marseille, 2003.
- [45] S. V. Patanker, "Discretization Methods," in *Numerical Heat Transfer and Fluid Flow*, USA, McGraw-Hill, 1980, p. Chapter 3.

- [46] J. H. Ferziger and M. Peric, "Finite Volume Methods," in *Computational Methods for Fluid Dynamics*, Berlin, Springer, 2002, p. Chapter 4.
- [47] Future Facilities, "6SigmaET," [Online]. Available: <http://www.6sigmaet.info/aboutus.php>. [Accessed 10 9 2015].
- [48] Future Facilities, "6SigmaET," [Online]. Available: <http://www.6sigmaet.info/software/overview.php>. [Accessed 10 9 2015].
- [49] V. Semin, L. U. Future Facilities Ltd., M. Bardsley, O. Rosten and C. Aldham, "Application of a multilevel unstructured staggered solver to thermal electronic simulations," in *Thermal Measurement, Modeling & Management Symposium (SEMI-THERM), 2015 31st*, San Jose, CA, IEEE, 2015.